

Response to interactive comment of anonymous referee #1

By Hedy M. Aardema in agreement with co-authors.

5 **Reviewer:** *The manuscript by Aardema and co-authors investigates high resolution in situ measurements of phytoplankton photosynthetic activity and abundance in the Dutch North Sea. The main topic of this study is relevant and provides useful information, particularly when considering monitoring requirements and in defining sampling/monitoring strategies. This study is also a very good example of integrated sampling and outputs from different instruments (i.e. fRRF, flow cytometer, FerryBox).*

10 **Response:** We really appreciate the elaborate and helpful comments on the manuscript. Based on this detailed and insightful review we rewrote and restructured the manuscript extensively.

General comments

15 **Reviewer:** *The introduction is focused on primary productivity (PP) but the main part of the paper investigates the photophysiological variables and phytoplankton groups with limited mention of productivity. I would suggest emphasizing more the estimates of PP throughout the ms.*

20 **Response:** Although the primary productivity is a very interesting parameter to calculate, the aim of the paper is to give a broader view of the phytoplankton community. Therefore, we shortened the part on primary productivity in the introduction, but did give it more attention in the results and discussion sections.

25 **Reviewer:** *Collinearity between variables: flow cytometer (FCM) phytoplankton groups were considered in the analysis even if showing collinearity (VIF>6). Statistical principles should be applied consistently across the analysis and to all the variables. If not, this should be explained clearly.*

30 **Response:** This is a good point. We reran the PCA and spatial clustering with the VIF>6 variables excluded. The Multiple Linear Regression was removed from the manuscript, because of the lack of information derived from it together with the abundance of literature already addressing the predictors of primary productivity.

35 **Reviewer:** *Spatial autocorrelation: transect data with high frequency sampling is likely to be spatially autocorrelated – has this been considered? If spatial autocorrelation is not considered to be a problem in this dataset, please explain why. Alternatively, presence of spatial autocorrelation could be investigated with the use of variograms.*

Response: As the reviewer expected, most parameters were spatially autocorrelated. We tested the spatial autocorrelation with Moran's I. This is indeed a problem for the multiple linear regression, but as mentioned previously, we removed this analysis from the manuscript. For the spectral classification clustering and PCA analysis, spatial parameters (latitude, longitude) were not included in the analysis. Without time and space in the calculation we only consider features of the data, so spatial autocorrelation does not influence the results (Demsar et al., 2013, Rousseeuw et al., 2015). Because the similarity between neighbouring points is of interest, we plotted of the spectral clusters on maps to visualize the spatial heterogeneity present.

Reviewer: Diurnal changes in some of the photophysiological variables: the authors clearly show that the diurnal cycle affect the clustering of observations (e.g. Page 25), so the clusters identified were not only based on changes in phytoplankton community but also in sampling activity (i.e. day vs night). As stated in the ms, it is difficult to separate the temporal from spatial variability; however, the effect of spatial variability could be investigated, for example, using measurements collected around specific time of day or night (e.g. 12:00±4 hours) and rerunning the cluster analysis on this sub-dataset and comparing the outcome with the current clusters. In this way it would also be possible to test the suggestion in line 30-31 (page 27) that spatial patterns are more important than temporal.

Response: We performed the suggested analysis for the month of August by clustering only the measurements that fall into the 12±4 h timeframe (see Fig. R1b). In this timeframe the southern coastal zone is distinct from the rest of the Dutch North Sea and corresponds to cluster 10 in the analysis of the complete dataset (Fig. R1a), so this cluster is defined by spatial variability. Cluster 12 and 13 are grouped together in the 12±4h timeframe as cluster 1. Cluster 11 is only encountered outside the 12±4h timeframe, so is a temporal rather than a spatial cluster. We included Fig R1 in the supplementary material and included the following text in the manuscript: “The third cluster corresponds to only night time sampling periods and is defined by low E_k and low $1/\tau$, suggesting that this cluster is a temporal cluster instead of a spatial cluster. To test this we repeated the analysis for the month of August but only including the measurements that fall into the 8 hour timeframe around noon (12:00±4h; see supplementary material Fig. S2). Cluster 11 is not recognized as cluster within the 12±4h timeframe, so seems indeed controlled by temporal rather than spatial variability.”

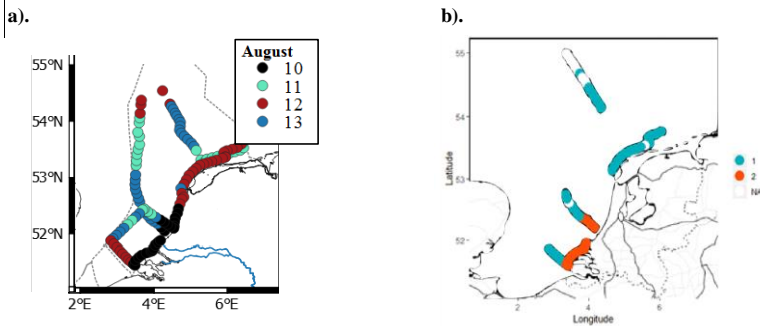


Fig. R1: Maps of clusters as defined by spectral clustering of the whole dataset (left) and only the measurements at 8h around noon (8:00h to 16:00h). Based on the FCM-based five described phytoplankton groups (Table 2) and non-collinear FRRF-parameters on photophysiology (F_v/F_m , $1/\tau$, [RCII], σ_{PSII} , α , E_k).

Specific comments

Reviewer: Title – phytoplankton photosynthesis does not provide a clear idea of the content of the paper that covers different photophysiological variables aswell as measurements of PP. I would suggest to being more specific.

Response: We prefer to stay with the chosen title. The main purpose of this study was to provide an example of high-resolution methods that could serve in a phytoplankton monitoring program. Based on the results of these methods further calculation can provide an estimate of the PP or can serve in identification of distinct biogeographical regions, of which we gave examples.

Reviewer: *Data analysis: it would be useful if the authors could explain why clusters, stepwise regressions and PCA have been used as chosen statistical analysis and what they are you aiming to explain with these techniques?*

Response: The main aim of the data analysis was to aid in the interpretation and visualization of the multitude of parameters derived with the high-resolution measurements. The PCA reduces the amount of parameters (or dimensions) and gives an impression on the relationship between parameters. The cluster analysis was chosen to test for spatial heterogeneity; when clusters would contain measurements randomly distributed over the study area, no spatial heterogeneity is present. When clustering shows spatial structure, it is. The stepwise regression was at first used to identify drivers for primary productivity, but will be removed after realization that the dataset of this study does not add to existing knowledge on this topic.

Reviewer: *Data analysis: Biomass vs chl a – repeatedly in the ms the authors refer to ‘biomass’, as synonymous of chl a (from validate fluorescence). Although chl a is often used as a proxy for phytoplankton biomass, they are not the same and this should clearly be stated at the start of the ms. Confusion arises from figures and tables referring to ‘abundance’, ‘fluorescence’, ‘chl a’, while the text refers to ‘biomass’; please check for consistency. In addition, the implications of a variable Chl-a : C ratio should also be considered and discussed. If the main interest is on biomass the authors could consider calculating it from the FCM measurements (for example, see DOI: 10.1016/j.dsr2.2006.05.004).*

Response: The authors are aware of this issue and tried to address this problem in the results section ‘3.2 phytoplankton parameters’. Obviously, we failed to consistently address the issue in the rest of the manuscript. To improve this, the term biomass was deleted in the manuscript. Although this is a very interesting parameter, and we are working on a method to calculate biomass based on scattering measured by the FCM. We already found good agreement between our biovolume and images obtained by the Image in Flow of the FCM (unpublished). However, this relationship seems to be taxon specific, which we want to study more in depth and is beyond the scope of the current study. The method to calculate biomass of Tarran et al. (2006) assumes all cells have a spherical shape and a constant C content per biovolume. Because this is an oversimplification, we prefer to use cell counts and fluorescence in the current paper. We did include our view on biomass calculation from flowcytometer data in the discussion.

Reviewer: *UHMM and cluster identification – it is not clear whether the clusters between the different months (Figure 5) are the same or not – in other words, is cluster 1 in April characterized (defined) by the same variables as cluster 1 in May? If not, then it may be better to separate the clusters e.g. with different numbers and/or colours in the figures.*

Response: we adjusted the figure as suggested.

Reviewer: *Discussion of results: results of the analysis of the photophysiological variables and of PP appear discussed separately. Outcomes from these two parts of the study should be brought (and discussed) together, where possible.*

Response: In the result section, primary productivity and Photophysiology are now both under an own header.

Reviewer: *Conclusions – I would suggest to highlight the importance of this study for monitoring program. Also, a bit more considerations on combining low and high resolution measurements would be useful.*

Response: We rewrote the conclusions accordingly:

“A good monitoring program monitors the presence of nuisance phytoplankton, the carrying capacity of the ecosystem and changes in biogeochemical cycling. The objective of this study was to evaluate the use of FRR fluorometry and flowcytometry for monitoring purposes. The four conducted cruises spread over 5 months offered a wide variety of environmental conditions and phytoplankton community states, which the utilized methods were able to visualize.

Inclusion of high-resolution methods in monitoring programs allows for analysis of finer scale events. Furthermore, it allows for analysis of living phytoplankton and is thereby able to measure rates and avoid effects of preservation and storage of samples. Another advantage is that high-resolution methods allows for easier comparison between countries, once common protocols have been established. Nevertheless, low resolution methods remain a necessity for more detailed taxonomic analysis, information on vertical heterogeneity, to calibrate and to correct for blanks. Data analysis might be the biggest bottleneck of the implementation of these high-resolution methods. The cluster analysis of flowcytometric data has high potential for improvement to increase the informative value of the method. Especially identification of phytoplankton clusters with a functional quality, such as nitrogen fixers, calcifiers or DMS-producers, would be helpful for interpretation of ecosystem dynamics and biogeochemical fluxes. Regarding the FRRf, the main challenge is converting electron transport rate to gross primary productivity in carbon units. Further research in these topics would benefit implementation of these methods into monitoring protocols. Furthermore, it is important to account for diurnal patterns in monitoring set-up to be able to distinguish between diurnal and spatial variability. Possibly the diurnal variability could be modelled, but more studies with a Langragian based approach would be needed for a better understanding of the impact of diurnal variability in the data. Overall, the in this study presented high-resolution measurement set-up has large potential to improve phytoplankton monitoring in supplement to existing low-resolution monitoring programs.”

Reviewer: *Supplementary information – need to be linked (and referred to) in the main text of the ms, otherwise it may be difficult for the reader to know that this info is available.*

Response: Done.

Technical corrections

Reviewer: *Page 1: 23-26 – rewording is needed*

Response: Rephrased to: “One of the major concerns when using these methods for monitoring purposes is the presence of a diurnal cycle concurrent to the spatial variation, especially in photophysiological parameters. This concurrent presence of spatial and temporal patterns needs to be taken into account when designing a monitoring program. Nevertheless, the richness of additional information provided by high-resolution methods, such as the FCM and FRRf, can supplement low-resolution monitoring to attain a better understanding of the phytoplankton community.”

Reviewer: *Page 1 30 -keywords, consider adding primary productivity*

Response: Added.

Reviewer: *Page 2: 10-12 – this sentence would fit better at the start of the paragraph. It also requires references*

Response: Moved to beginning of the paragraph.

Reviewer: *Page 3: 5 – ‘a sum’: consider replacing with ‘a combination’*

Response: Done.

Reviewer: *Page 3: 23 – ‘pigment ratio’ slightly incorrect as the ratio considered is of fluorescence*

Response: Agreed and adopted.

Reviewer: *Page 3: 24-25 – Aims – this statement about key driver of PP is very general and can be misinterpreted as the ms focuses on only 4 months during the growing season of a particular year. Time frame of this study should be specified*

Response: reformulated

Reviewer: Page 4: 3-5 – not clear, needs rewording

Response: Rephrased to: “The Dutch North Sea is a shallow tidal shelf sea in the southern part of the North Sea. The main water flow is Northward flowing Atlantic water that enters the North Sea in the south through the Channel. The Atlantic water flowing around Scotland enters the North Sea and meets the Channel water and the freshwater from the rivers forming the Frisian Front.”

Reviewer: Page 5: 1- would be useful to have the exact dates of the surveys.

Response: Added.

Reviewer: Page 5: 6 – more details on the temporal frequency indicated as ‘low resolution’ should be provided (e.g. how many samples per station? How many a day? How many depths?)

Response: Added.

Reviewer: Page 5: 27-32 – please provide more details of the methods or a published reference (for people not being able to access the internal protocols).

Response: Added.

Reviewer: Page 6: 16 & 18 – acronyms (e.g. NPQ and F0’) should be explained when used the first time

Response: Added.

Reviewer: Page 8: 12-13 – formula 8 is missing

Response: It was removed. We changed formula 9 to formula 8.

Reviewer: Page 8: 17 – need rewording

Response: Rephrased as: “Volumetric P_{\max} and α were derived by fitting JV_{PII} in $\mu\text{mol photons m}^{-3} \text{ h}^{-1}$ to equation 1 (the exponential model of Webb et al., 1974) and used to integrate productivity over depth. The light availability in the water column was estimated as [...] with $E(z)$ being the irradiance at depth z , E_{surface} the incoming surface irradiance and K_d the light extinction coefficient.”

Reviewer: Page 8: 20-21 – it is not clear how surface irradiance was calculated; please reword this section

Response: We adjusted the text to the following explanation: “To avoid effects of changing incident surface irradiance (E_{surface}) on the spatial pattern and to be able to compare GPP between regions we used monthly average surface irradiances (E_{surface}) in our calculations of primary productivity. From 2010-2016 irradiance (400-700 nm) was measured at the roof of the NIOZ building in Yerseke using a LI-190 quantum PAR sensor and hourly averages stored using a LI1000 datalogger. E_{surface} was then calculated by averaging all irradiance data from the years 2010-2016 for the respective month.”

Reviewer: Page 9: 17 – was the clustering carried out by the FCM software or was it done by expert judgment manually? Also, was data cleaned from potential presence of air bubbles etc? Please provide details on these points.

Response: The chosen cluster criteria were based on expert judgement. The clustering was done by the software Easyclus 1.26 (ThomasRuttenProjects) according to these criteria. Noise, air bubbles and other potential outliers were removed after the clustering.

Reviewer: Page 10: 2 – outliers –specify which analysis you are referring to (e.g. outliers from the fRRF?)

Response: All data, rephrased in manuscript.

Reviewer: Page 10: 5 – provide a reference for the value of 0.65

Response: Added; Kolber, Z. and P. G. Falkowski. 1993. Use of active fluorescence to estimate phytoplankton photosynthesis in situ. *Limnology and Oceanography*. 38:1646-1665.

Reviewer: Page 10: 12 – please specify which are the photophysiological variables considered

Response: We added the following sentences to the data analysis section: “Phytoplankton parameters were first tested for collinearity and predictors with a variance inflation factor (VIF) over 6 were removed (Zuur et al., 2009). This left for the cluster analysis FCM-parameters Pico-red, Nano-red, Micro-red and *Synechococcus* and the FRRf-parameters σ_{PSII} , F_v/F_m , a_{LIII} , $1/\tau$, E_k ”

Reviewer: Page 10: 13 – acronyms (VIF) should be defined here

Response: Added.

Reviewer: Page 11: 20 – ‘nitrate’: should this be ‘DIN’?

Response: Yes.

Reviewer: Page 11: 27-28 – please explain the evidence for P and Si-limitation (i.e. discuss the ratios vs expected limiting ratios in literature). Also, please specify the value of Redfield Ratio and reference.

Response: We removed the nutrient ratios from the results. The paper only reports the nutrient values as additional background information to understand phytoplankton dynamics. A detailed analysis of concentration vs ratio is past the subject of this paper, but in the discussion nutrient limitation is now discussed.

Reviewer: Table 3 legend – ‘not completely comparable’: this expression doesn’t have a clear statistical meaning. Please specify briefly in the legend which month had a different sampling route and station so for the reader to understand in which month the study area is not fully covered.

Response: True. We removed the term ‘not completely comparable’ from the legend and added a short explanation of the differences between months. Also, we moved the table to the supplementary information and replaced it with the nutrient concentration table.

Reviewer: Figure 2 provide equations of linear regressions with R2 and significance

Response: The R² and significance are now added to the legend. The linear regressions are irrelevant because the unit of the x-axis is in relative fluorescence units (RFU) and instruments will require separate calibration.

Reviewer: Page 14: 27 – ‘suggesting physiological stress’, please provide reference

Response: Suggett et al., 2009.

Reviewer: Page 16: 9 – it is not clear to which phytoplankton group the % are referring to.

Response: The nanophytoplankton. Rephrased.

Reviewer: Page 16: 14 – please specify which are ‘these regions’

Response: Rephrased.

Reviewer: Page 16: 15-16 – this paragraph should be moved to the discussion so to allow the concept to be developed further. Page 16: 17 – please explain why low sigmaPSII may reflect Rhine River waters.

Response: Moved to discussion.

Reviewer: Page 17 – Figure 4 – I appreciate the different scaling was necessary to ‘visualize the spatial heterogeneity’ however it makes very hard the comparison between figures. In fact, the reader needs to keep checking the legend, which is printed in very small characters difficult to see. I would suggest reconsidering the use of a uniform scale (at least for some of the variables, if possible).

Response: We adjusted the figure to a uniform scaling.

Reviewer: Page 18: 17 – there is limited or no comments on the results of some of the photophysiological variables such as alpha, Pmax, effective absorption cross section.

Response: We expanded the result section on the Photophysiology.

Reviewer: Page 18: 25 – ‘sake of completeness’. See general comment about collinearity, please explain why statistical principle of $VIF > 6$ was not applied consistently to all variables

Response: We agree that this might not have been the best choice, we preferred to include all the phytoplankton groups. As mentioned before, we now deleted the collinear variables with $VIF > 6$.

Reviewer: Page 18: 28-29 – table should be provided (for example in the additional info) showing the contribution of each variable to the PC1 and PC2 for the 4 months, and total variance explained.

Response: We added this table to the manuscript, in combination with figure 6:

	April		May		June		August	
	PC1	PC2	PC1	PC2	PC1	PC2	PC1	PC2
Sigma	0.8	28.8	0.1	36.7	0.0	9.3	12.1	9.9
F_v/F_m	13.7	0.6	0.8	14.5	27.6	0.1	0.0	17.5
a_{LIII}	18.7	3.4	17.5	6.7	20.9	8.7	21.0	3.3
[RCII]	17.1	6.6	20.4	1.6	28.0	2.6	25.8	0.0
$1/\tau$	9.8	22.7	4.4	7.5	0.4	1.7	0.2	20.6
E_k	3.9	13.8	0.7	26.3	3.7	3.9	0.7	16.8
Pico-red	4.2	15.1	18.5	0.4	6.1	26.9	0.3	11.8
Nano-red	16.9	0.0	21.1	0.6	2.9	16.9	15.3	3.1
Micro-red	10.5	4.5	16.4	1.4	6.3	2.9	22.9	0.4
<i>Synechococcus</i>	4.3	4.4	0.0	4.3	4.2	27.0	1.8	16.7
Variance explained	45.6 %	19.3 %	42.5 %	18.9 %	29.1 %	18.7 %	33.9 %	25.7 %

Reviewer: Page 19: 1 – alpha is defined as Light utilisation efficiency (Table 1) but then in the text is referred to as ‘affinity’. please check for consistency.

Response: Changed in table. The value for alpha is the slope of the FLC, and is a measure for photosynthetic affinity for incoming light.

Reviewer: Page 21: 8-13 – consider whether to move this text in additional info (or to remove it?). It breaks the flow of the results and the addition of clusters ‘manually’ appears to not be meaningful and/or significant (as it doesn’t adopt the same statistical robust principle).

Response: It is true that it does not adopt the same statistical robust principle. However, there is spatial heterogeneity in the flowcytometer data, that are not visualized with the UHMM and this is what we wanted to explore. We do agree that the manual increase of amount of clusters might not be the best way to go forward with this, so we deleted this section from the manuscript.

5 **Reviewer:** Page 22: 6 – ‘abiotic’ and ‘salinity’ misspelled. Page 22: 9 – as for previous PCA, please provide variables used and information on their contribution towards variance explained.

Response: this paragraph and figure were removed from the manuscript because the PCA does not provide useful insights or new information on the phytoplankton community or Dutch North Sea.

10 **Reviewer:** Page 23: 6-7 – this paragraph is not clear particularly what is meant with ‘opposite’

Response: rephrased.

Figure 7 legend – Size of the open circles is a bit confusing and misleading as the reader may assume the size of the bubble refers to the amount of PP. Consider simplifying the figures and only plot productivity

15 **Response:** The figure was simplified as suggested.

Reviewer: Page 24: 15 – please indicate how much of the variability in PP is explained by the stepwise regression (e.g. R2?).

Response: because information on the nutrient availability was only available on a low-resolution spatial scale, the information provided by high resolution methods are not effectively used. To study the drivers of primary productivity another study design should have been chosen. Therefore, this analysis was deleted from the manuscript.

20

Reviewer: Page 25: 4 – reword please.

Response: rephrased

25 **Reviewer:** Page 26: 2-5 – require rewording particularly the need to clarify and be more specific on the work done in this study.

Response: removed from manuscript.

Reviewer: Page 26: 5 – this sentence may be misleading. The authors calculated PP along the sampling transects but did not provide an estimate for the wider Dutch North Sea as it may appear here.

30

Response: removed from manuscript.

Reviewer: Page 26: 8 & 11 – timing of the bloom is discussed in this section however it would not be possible to define the start of the bloom based on a 4-day sampling per month. Continuous observations throughout the year by an instrument buoy or remote sensing would allow to ‘contextualise’ the measurements within the growing season (i.e. determine when sampling was carried out within the phytoplankton growing season).

35

Response: Agreed and removed from manuscript.

Reviewer: Page 26: 24-25 – please reword

40

Response: rephrased

Reviewer: Page 27: 8-9 – repetition of method; should be deleted.

Response: Rephrased.

45 **Reviewer:** Page 29: Figure 10 legend, possibly just my issue, I don’t see the similarity between the two figures.

Response: We do see a basic similarity, with the separation between the different water masses being reflected in our results. However, the similarity might not be striking enough to include the figure and therefore we leave it out of the manuscript.

Reviewer: *Page 30: 13 – ‘low resolution’: should this be ‘high-resolution’?*

Response: no, we meant to say low-resolution. We rephrased to make it easier to follow: “Extra low-resolution sampling points in clearly deviating areas would be useful, because only low-resolution offer the level of detail which is required to identify toxic, keystone or invasive species.”

References

Demšar, U., Harris, P., Brunson, C., Fotheringham, A. S., & McLoone, S. (2013). Principal Component Analysis on Spatial Data: An Overview. *Annals of the Association of American Geographers*, 103(1), 106–128. <https://doi.org/10.1080/00045608.2012.689236>

Rousseuw, K., Poisson Caillault, E., Lefebvre, A., & Hamad, D. (2015). Achimer Hybrid hidden Markov model for marine environment monitoring. *IEEE JOURNAL OF SELECTED TOPICS IN APPLIED EARTH OBSERVATIONS AND REMOTE SENSING*, 8(1), 204–213. <https://doi.org/http://dx.doi.org/10.1109/JSTARS.2014.2341219>

Suggett, D. J., C. M. Moore, A. E. Hickman, and R. J. Geider. (2009b). Interpretation of fast repetition rate (FRR) fluorescence: signatures of phytoplankton community structure versus physiological state. *Marine Ecology-Progress Series* **376**:1-19.

Response to interactive comment of anonymous referee #2

By Hedy M. Aardema in agreement with co-authors.

5 **Reviewer:** *This paper analyses spatial and temporal patterns in cruise data with 3 high-resolution monitoring methods: FRRF, Flow-cytometry and Ferrybox. Correlations between the observed variables are also analysed. The large dataset, including many phytoplankton and environmental variables observed together enables the authors to understand the patterns in the various phytoplankton variables. The results could guide the optimal application of such novel monitoring methods in operational monitoring for a.o. MSFD.*

10 **Response:** We thank the reviewer for the helpful and critical comments. We rewrote and restructured the manuscript extensively based on these comments. We are happy to hear that the reviewer sees the potential of our applied methods.

General comments

15 **Reviewer:** *The paper lacks a clearly stated research question or hypothesis to be tested. Therefore, it is unclear what is the purpose of the various analyses performed and what we can learn from the results. Based on the conclusion that this type of "high-resolution is a very useful supplement to current monitoring", I would expect a hypothesis such as "combined high-resolution monitoring of many phytoplankton variables along with environmental variables allows us to quantify seasonal and meso-scale patterns in phytoplankton biomass, species composition and primary production. The concurrent measurement of different phytoplankton variables allows us to understand the effect of phytoplankton species composition and physiological adaptation processes on the observed patterns in phytoplankton biomass and production". Then the analysis should show how the variables should be combined to provide the most reliable estimates of phytoplankton biomass and primary production.*

20 **Response:** Because of the exploratory nature of our research, a hypothesis was not defined. The addition of the suggested sentences does help in making the manuscript easier to follow. We therefore adopted part of the sentences and added of the following sentences to the introduction: "The aim of this study is to test the suitability of these two high-resolution methods to be developed as novel phytoplankton monitoring method. The two high-resolution methods, a flowcytometer and a FRR fluorometer, were deployed concurrently on four 4-day cruises in April, May, June and August to meet a wide range of environmental conditions and phytoplankton community states. These measurements allow for quantification of seasonal and mesoscale spatial patterns in phytoplankton abundance, photophysiology and gross primary production. In this paper we provide an overview of the acquired results, use a spectral cluster analysis to visualize spatial heterogeneity and evaluate the potential of these methods to optimize current monitoring programs."

25 **Reviewer:** *There are many observed variables, which are not consistently named in the text, figures and tables. Therefore, it is easy to get lost in the description of patterns for all individual variables. A clear definition of variables that is consistently used throughout the text would help the reader to understand the storyline. Some of the variables observed by the FRRF seem to be very similar. Which of the variables should be used as indicator and which are redundant to answer the research questions?*

30 **Response:** We corrected the inconsistent naming. The variables of the FRRf might seem similar under some conditions. However, because these variables vary depending on community composition and environmental conditions, they might deviate when conditions change (Sugget et al., 2009; Kromkamp and Forster, 2003). Therefore, care must be taken into choosing the parameters. For the current study the main interest is on monitoring the phytoplankton community, therefore we are interested in parameters that are informative on physiological adaptation or characteristic for phytoplankton taxons. Additionally, we focus on high resolution measurements, so limit the parameters to the ones attainable at high-resolution.

Based on these considerations we decided to include the current parameters, which give us a broad overview of the photophysiological status of the phytoplankton community.

Reviewer: *In the conclusions section a recommendation on next steps would be much appreciated: what would be required to use the high-resolution methods in scope to provide reliable estimates of phytoplankton biomass, production and species composition for long term monitoring? In the introduction and conclusion the species composition is defined in functional types such as nitrogen fixers, calcifiers or DMS-producers, but these do not correspond to the phytoplankton clusters used in this paper.*

Response: the conclusions were rewritten:

“A good monitoring program monitors the presence of functional types of phytoplankton, including the harmful taxons, the carrying capacity of the ecosystem and changes in biogeochemical cycling. The objective of this study was to evaluate the use of FRR fluorometry and flowcytometry for such monitoring purposes. The four conducted cruises spread over 5 months offered a wide variety of environmental conditions and phytoplankton community states, which the utilized methods were able to visualize. Inclusion of high-resolution methods in monitoring programs allows for analysis of finer scale events. Furthermore, it allows for analysis of living phytoplankton and is thereby able to measure rates and avoid effects of preservation and storage of samples. Another advantage is that high-resolution methods allows for easier comparison between countries, once common protocols have been established. Nevertheless, low resolution methods remain a necessity for more detailed taxonomic analysis, information on vertical heterogeneity, to calibrate and to correct for blanks. Data analysis might be the biggest bottleneck of the implementation of these high-resolution methods. The cluster analysis of flowcytometric data has high potential for improvement to increase the informative value of the method. Especially identification of phytoplankton clusters with a functional quality, such as nitrogen fixers, calcifiers or DMS-producers, would be helpful for interpretation of ecosystem dynamics and biogeochemical fluxes. Regarding the FRRf, the main challenge is converting electron transport rate to gross primary productivity in carbon units. Further research in these topics would benefit implementation of these methods into monitoring protocols. Furthermore, it is important to account for diurnal patterns in monitoring set-up to be able to distinguish between diurnal and spatial variability. Possibly the diurnal variability could be modelled, but more studies with a Langragian based approach would be needed for a better understanding of the impact of diurnal variability in the data. Overall, the in this study presented high-resolution measurement set-up has large potential to improve phytoplankton monitoring in supplement to existing low-resolution monitoring programs.”

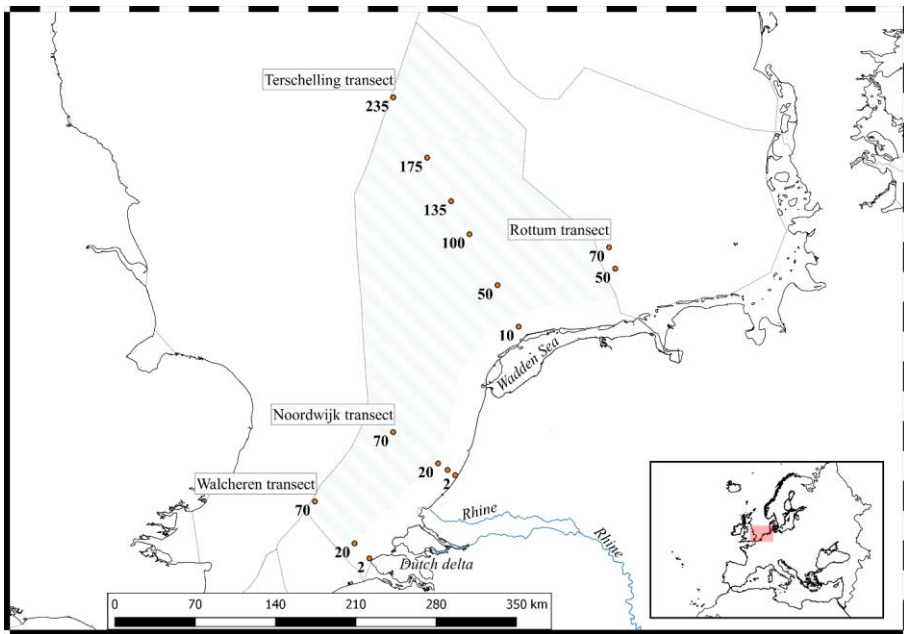
Specific comments

Reviewer: *Sentences are often long: consider breaking up in multiple sentences to improve readability.*

Response: We apologize for the difficulties and hope to have improved the readability in the new manuscript.

Reviewer: *Figure 1: please show only the stations (with names/ abbreviations) used in this study (see table S1) and the areas used in the text (such as Dogger Bank, Wadden, Den Helder, Rhine outflow) so the description of spatial patterns can also be understood by people that are not Dutch.*

Response: We updated the figure to the following:



Reviewer: Section 2.2: please refer to international protocols/methods rather than internal protocols.

Response: We added a more detailed description to the method section.

5

Reviewer: Table 1: it would help to have an additional column stating the interpretation / meaning of this variable, such as total biomass, nutrient stress, maximum growth rate, efficiency of light uptake etc. Then later in the text you can use these 'meaningful' names instead of codes, to facilitate understanding of observed patterns. Also a figure illustrating the meaning of the different variables (alfa, Ek, F', Fm' etc.) could prevent getting lost in all abbreviations.

10

Response: Unfortunately, the meaning of the different variables is usually not straightforward and dependent on multiple predictors (species, nutrient concentration, light availability etc.; Suggestt et al., 2009). Nonetheless, we tried to make the table more information easier to understand.

15

Reviewer: Equation 9: why did you use monthly averaged irradiance if you are looking at high-resolution patterns. Why did you not use irradiances measured during the cruise?

Response: Unfortunately, we were unable to collect reliable irradiance data for all cruises. Clearly, it is preferable to have irradiance (PAR) continuously measured in parallel to the FRRF measurements when aiming to monitor current primary productivity.

20

Reviewer: Table 2: Since you use both Length_FWS and O/R ratio as criteria to distinguish the phytoplankton groups, it would be logical to include a column for O/R ratio with the applied criteria.

Response: Good idea, we added the O/R-ratio to the table.

5 **Reviewer:** *It is not entirely clear whether pico-red includes pico-Synecho or not. On page 14, line 30 it says: “Both groups of picophytoplankton (Synechococcus and total)”, whereas table 2 and figure 3 suggest the two groups are exclusive.*

Response: Pico-red and Pico-synecho are two different groups, as correctly understood from table 2 and figure 3. We rephrased the sentence to: “Both groups of picophytoplankton (Synechococcus and Pico-red)”, and scanned the manuscript for other mixing up.

10 **Reviewer:** *Section 2.4: please state with every type of analysis what is the purpose / research questions for that analysis. For example: what are you trying to predict from what and why?*

Response: We added the following the sentences to section 2.4: “To find regions with similar phytoplankton communities, data was spectrally clustered using the uHMM R package (Poisson-caillault and Ternynck, 2016) in the statistical software R (version 3.4.1, R Core Team, 2017).” and “Principal Component Analyses (PCA) were performed to find which variables contributed most to the cluster results.”

15 **Reviewer:** *Section 3.1: I don't see the value of comparing averages over whole transects (with large spatial variability, which is the subject of this paper), that are not even the same, between months. The only thing you see is seasonal patterns that are well-known from other studies and that can be summarized in section 2.1 in a description of the study area. Most of this section describes the data in table S1. I would replace table 3 with table S1 and remove table S2. N/P ratios address that same question as table S1, but with an indicator that is controversial.*

20 **Response:** For the authors the table helped to visualize the seasonal patterns, but we agree on the comment that this table does not add to the already existing knowledge on seasonal patterns. We therefore adopted the suggestion to replace the table with the table S1 from the supplementary material.

25 **Reviewer:** *The text in this section (and subsequent sections) is sometimes hard to follow as it is not clearly structured in time and space and variable. We go back and forth in time. Section 3.2 describes first figure 2, then figure 3 and then again figure 2 and then figure 3. I suggest to make one section about phytoplankton biomass (figure 2) and then one section on species composition (figure 3).*

Response: Rewritten

30 **Reviewer:** *Page 16, line 14: the southern coastal stations are more strongly affected by the Rhine outflow than the Scheldt outflows (see for example: Lacroix, G., Ruddick, K., Ozer, J., & Lancelot, C. (2004). Modelling the impact of the Scheldt and Rhine/Meuse plumes on the salinity distribution in Belgian waters (southern North Sea). Journal of Sea Research, 52(3), 149-163.).*

Response: We reformulated to Rhine and Scheldt river outflow.

35 **Reviewer:** *Figure 4: Please use consistent legends for the same variable between different months, with the same colour scheme and symbols (squares vs. circles) and with blue indicating low values and red indicating high values, so the high values stand out, more than the low values. Also captions in the table per line (red fluorescence, O/R ratio etc.) and per column (april, may etc.) would help to easier understand the figure.*

Response: We remade the figures, see manuscript.

40 **Reviewer:** *Section 3.5: I don't see the added value of this analysis. What does it tell us?*

Response: Agreed. We aimed to get a better understanding of the drivers of primary productivity in the Dutch North Sea. However, we realize now that the dataset is not very well suited for this and we therefore removed the analysis.

45 **Reviewer:** *Page 24: I suggest to mention in the table all the variables that were included in the analysis and note coefficients or 'ns' for not significant and the p values per explanatory variable. Then readers don't need to reconstruct the overview from the text. Actually, the significance test is likely not valid due to strong spatial autocorrelation in the data.*

Response: The Multiple Linear Regression was removed from the manuscript, because of the lack of information derived from it together with the abundance of literature already addressing the predictors of primary productivity.

Reviewer: *Discussion: Here I would expect to get some advice: How to best estimate phytoplankton biomass from these data? Should we use total red fluorescence (best R2) or F0 (least affected by NPQ)? Is there a way to combine both (with other available variables) to get an even better estimate?*

Response: We added the following paragraph to the discussion:

“Biomass might be one of the most important parameters to understand phytoplankton dynamics, but its direct measurement is not possible using high-resolution methods. Chlorophyll a concentration is often used as an estimate for biomass, although the Carbon:Chl a ratio is dependent on abiotic conditions and species-specific phenotypic plasticity (Flynn, 1991, 2005; Geider et al., 1997; Alvarez-Fernandez and Riegman, 2014; Halsey and Jones, 2015). Red fluorescence gave a good estimate of chlorophyll a concentration, both using the FRRf (adjusted R²= 0.66) and FCM (adjusted R²=0.90). Both the FRRf and the flowcytometer estimate the chlorophyll a concentration based upon the fluorescence in the red spectrum after excitation in the blue spectrum. There are some slight differences in the optics, the FRRf excites with a 450 nm LED and measures the fluorescence at 682 ± 30 nm, while the FCM excites at 488 nm and filters the red fluorescence over a longpass 650 nm filter towards the red fluorescence detector. The smaller detection range of the FRRf detector is optimized around the maximum emission of PSII and limits contamination by PSI (Franck et al., 2002; Oxborough et al., 2012). The second difference is the fluorescent state of the photosystems, the strong laser of the flowcytometer can only measure the maximum fluorescence (F_m), which is a parameter more prone to quenching than the minimum fluorescence measured by the FRRf. Yet, the biggest difference concerns the method; where the flowcytometer measures the fluorescence per particle, the FRRf does only a bulk measurement. In a bulk measurement other particles in solution scatter the excitation and emission photons, plus the emitted fluorescence of the phytoplankton is subject to reabsorption, especially at higher biomass densities. The latter seems to have the most impact on chlorophyll a concentrations, as the fit of the flowcytometer derived red fluorescence is a better than the FRRf minimum fluorescence. Other studies that use the FCM to estimate chlorophyll a concentrations also showed good relationships, but find better fits using the bulk measurements using a fluorimeter (Thyssen et al., 2015; Marrec et al., 2018). The conversion to biomass may also be done from cell abundances. Some studies use the oversimplified assumption that all cells have a spherical shape and a constant C content per biovolume (Tarran et al., 2006). With the scanning flowcytometer it is also possible to estimate biovolume based on scattering properties of the cell, but this relationship appears to be taxon specific (Rijkeboer, pers. comm.). This relationship will be further explored by comparing the calculated biovolume based on the Image in Flow pictures and the flowcytometric properties of these phytoplankters.”

Reviewer: *Can we trust GPP from FRRF as a reliable estimate of primary production or is more work needed to achieve that goal? If so, what needs to be done?*

Response: We added the following paragraph to the discussion:

“The reliability of variable fluorescence as estimate of gross primary productivity is depending on many cell processes from the photon absorbance to carbon assimilation. The variable fluorescence reflects the first step of photosynthesis; the efficiency of which photons are captured and electrons produced and transferred. However, to interpret gross primary productivity in an ecological or biogeochemical meaningful way, the FRR units of electrons per unit time need to be converted to carbon units. Gross photosynthesis correlates well with photosynthetic oxygen evolution (Suggett et al., 2003), and multiple studies have shown good correlation between 14C-derived estimates of primary productivity and FRRf-derived estimates using a constant conversion factor (Melrose et al., 2006; Kromkamp et al., 2008). However, in reality this parameter is not a constant, as along the pathway from electron to carbon atom electrons are consumed by other cell processes (Flameling and Kromkamp, 1998; Halsey and Jones, 2015; Schuback et al., 2016). Therefore, a reliable GPP estimate in carbon units from FRR fluorometry requires more research and estimates provide relative rather than qualitative values. Despite its limitations the fact that the method can measure in situ, with relatively little phytoplankton manipulation before measurement, makes the method promising. Calibration with other methods, such as concurrent C14 of C13 incubations, could help to better understand the processes from electron excitation to carbon fixation. However, it should be recognized that these types of measurements come with their own problems, and measure something in between net and gross primary productivity depending on the incubation time and growth rate of the phytoplankton (Halsey and Jones, 2015). So it remains a question which method is measuring the ‘real’ primary productivity. Attempts to calculate primary productivity from flowcytometer data have also been made, which is actually based on the diurnal cycle in cell size caused by cell division (Marrec et al., 2018). Despite the limitations of GPP estimates by variable fluorescence, our results clearly show large spatial variability in gross primary production concurrent to

the expected strong variability during the growth season. This spatial heterogeneity is not fully captured by sampling at the standard low-resolution monitoring stations, showing the added value of our approach. Primary productivity was highest in April, and relatively large values were also observed offshore, indicating that a low phytoplankton biomass does not necessarily mean that primary production is low. Our GPP rates were based on the same electron requirement for C-fixation (Φ_e, C). However, this is a likely oversimplification as Φ_e, C is known to vary with abiotic conditions (Lawrenz et al., 2013) and the changes in nutrient conditions and temperature during the growth season are likely to affect GPP. This will be the topic of a future publication and we expect that the detection of several biogeographic regions will help us in predicting Φ_e, C .”

Reviewer: *It is not really clear whether the diurnal variability in the FRRF variables is a problem that needs to be solved.*

Response: It is not so much a problem that needs to be solved, but it does need to be taken into account when setting up a monitoring program including FRRF variables. It is important to realize that measurements taken at different times of the day, might not be comparable. To be able to include FRRF variables in a long-term monitoring program, the included sampling points should be sampled at the same time of the day.

Reviewer: *Are the clusters in the FCM analysis the relevant ones to provide 'useful' information to science & society? Should we / Can we move on to other clusters that are mentioned in the conclusions?*

We added the following text to the discussion:

“To understand the role of the phytoplankton in biogeochemical cycles, the FCM clusters would ideally reflect taxonomic or functional groups, as calcifiers, silicifiers, DMS producers (such as Phaeocystis) and nitrogen fixers (le Quéré et al., 2005). The lack of identification of distinct clusters makes this so far impossible. Other studies manually separate up to 10 phytoplankton groups with the same instrument (Marrec et al., 2018). These groups included Prochlorococcus, which is at the absolute limit of resolving capacity of the FCM because of their small size and low fluorescence. They furthermore distinguished the Pico-red in three groups based on FLO/FLR-ratio. Nano-cryptophytes group in high and low orange fluorescence and included a micro-eukaryotes group with a size from 10 to 20 μm . But these groups are still made up of many taxonomic genera and, apart from size, won't allow much for further interpretation of their role in the ecosystem or biogeochemical cycles. The same accounts for detection of nuisance phytoplankton; distinct clusters of toxic phytoplankton species are lacking. Although this will remain a challenge because toxicity in phytoplankton can differ within morphotypes and sometimes even differ per strain within a species (Tillman and Rick, 2003). But potentially, further research in flowcytometry can result in suspicious clusters to be flagged and further inspected by a specialist using microscopy. The potential is certainly there, as much of the information retrieved by the FCM is still unexplored; the clustering is performed on totals (area under the peak) instead of the pulse-shape. This in combination with more advanced camera options will need to further distinguish between groups in the future.”

Reviewer: *Do the FCM data help to better understand the FRRF data (and vice versa)? For example, do we see diatoms under light limited conditions (high F'/F_m , high α , low E_k) and picoplankton under nutrient limited conditions (low F'/F_m)? Other ecological niches that we know from literature? Different conditions promoting *Synechococcus* compared to other picoplankton?*

Response: We tried to incorporate the link between the methods better, we added the following sentences to the manuscript: “In this study a large part of the Dutch North Sea shifted from nutrient sufficiency to nutrient limitation between April and May, which was reflected in the low efficiency of PSII (F_v/F_m ; Fig. 4). The F_v/F_m recovered between May and June, which suggest that the phytoplankton adapted to nutrient limiting conditions (Kruskopf and Flynn, 2005). However, photophysiological parameters are also varying per taxonomic group; smaller taxa typically have lower F_v/F_m values and higher σPSII values (Kolber et al., 1988; Suggett et al., 2009b). Indeed, by flowcytometry we find that the biggest shift in community composition took place between May and June from a nanophytoplankton dominated community to a picophytoplankton dominated community. These findings demonstrate how flowcytometry and fast repetition rate fluorometry can supplementary improve ecosystem understanding.”

Technical comments

5 **Reviewer:**

- Collinear should be spelled with 2 ll's throughout the whole text.
- Page 9, line 4 & 5: I guess um means micrometers?
- Page 18, line 4: middle-right, please refer to the label C4 a-x.
- Figure 5: The figure would be easier to read if the colours per group are consistent between the cluster analysis on the right and the map on the left. Labels (A-D for April to August panels) would also help.
- Figure 9: Please add the hours of the day on the x-axis.
- Page 25, line 3: the word influenced is repeated too many times and therefor should get an e in the end.
- Page 28, line 11: estimates are.
- Line 13: parameter without s.
- Page 31, line 8: Jerico-next, without h.

15 **Response:** We adopted the suggested technical improvements.

References

20 Franck, F., Juneau, P., Popovic, R. (2002). Resolution of the Photosystem I and Photosystem II contributions to chlorophyll fluorescence of intact leaves at room temperature. *Biochimica et Biophysica Acta - Bioenergetics*, 1556(2–3), 239–246. [https://doi.org/10.1016/S0005-2728\(02\)00366-3](https://doi.org/10.1016/S0005-2728(02)00366-3)

25 Suggett, D. J., Moore, C. M., Hickman, A. E., & Geider, R. J. (2009). Interpretation of fast repetition rate (FRR) fluorescence: Signatures of phytoplankton community structure versus physiological state. *Marine Ecology Progress Series*, 376, 1–19. <https://doi.org/10.3354/meps07830>

30

35

Marked up manuscript

High resolution *in situ* measurements of phytoplankton photosynthesis and abundance in the Dutch North Sea

Hedy M. Aardema^{1,2}, Machteld Rijkeboer¹, Alain Lefebvre³, Arnold Veen¹, and Jacco C. Kromkamp³

¹Laboratory for Hydrobiological Analysis, Rijkswaterstaat (RWS), Zuiderwagenplein 2, 8224 AD Lelystad, The Netherlands
²~~Department of Climate Geochemistry, Max Planck Institute for Chemistry, Hahn-Meitner-Weg 1, 55128 Mainz, Germany~~

³~~IFREMER, Laboratoire Environnement et Ressources, BP 699, 62321 Boulogne sur Mer, France~~

³~~Department of Estuarine and Delta Systems, NIOZ Royal Netherlands Institute for Sea Research and Utrecht University, P.O. box 140, 4400 AC Yerseke, The Netherlands~~

Correspondence to: Hedy M. Aardema (hedy.aardema@mpic.de)

~~Present address: Department of Climate Geochemistry, Max Planck Institute for Chemistry, Hahn-Meitner-Weg 1, 55128 Mainz, Germany~~

Abstract. Marine waters can be highly heterogeneous both on a spatial and temporal scale, yet monitoring ~~is programs are~~ currently ~~mainly limited to relying primarily on~~ low-resolution methods. ~~This potentially leads to undersampling in time and space.~~ This study explores the ~~use potential~~ of two high-resolution *in situ* methods ~~to study for monitoring of~~ phytoplankton dynamics; Fast Repetition Rate fluorometry (FRRf) ~~to study for information on~~ phytoplankton photosynthesis and ~~productivity and scanning flow cytometry (FCM) to study for information on~~ phytoplankton ~~biomass abundance and community composition.~~ ~~Measurements These instruments were conducted deployed~~ during four cruises on the Dutch North Sea in April, May, June and August of 2017. ~~Both FRRf and FCM data show spatial heterogeneity with monthly variation. Automated unsupervised Hidden Markov Model (uHMM) spatial clustering The high-resolution methods were able to visualize both the spatial and seasonal variability of the phytoplankton community in the Dutch North Sea. Spectral cluster analysis was applied to objectively interpret the multitude of parameters and visualize potential spatial patterns. This resulted in identification of biogeographic regions with distinct phytoplankton communities. Manual adjustments were necessary to optimize visualization of some distinct phytoplankton communities. Stepwise multiple linear regression (n=61) revealed, which varied per cruise. Our results clearly show that photophysiology (alpha), phytoplankton biomass (total red fluorescence) and abiotic predictors (Turbidity, DIN, time of the day and temperature) determined integrated water column gross primary productivity. Apart from spatial heterogeneity, the diurnal trend is the sampling based on fixed stations do not give a significant predictor exposing clear trends with other good representation of the spatial patterns, showing the added value of our approach. Still, to fully exploit the~~

potential of the tested high-resolution measurement set-up, some major improvements are to be made. Among which the most important are: accounting for the diurnal cycle in photophysiological parameters. ~~Consequently, spatial patterns are difficult as temporal and spatial patterns occur simultaneously.~~ concurrent to the spatial variation, better predictions of the electron requirement for carbon fixation to estimate gross primary productivity, and the identification of more flowcytometer clusters with informative value. Nevertheless, ~~high resolution monitoring is a very useful supplement in addition to regular~~ already the richness of additional information provided by high-resolution methods such as the FCM and FRRf can improve existing low-resolution monitoring programs towards a more precise and ecosystemic ecological assessment of the phytoplankton community and productivity.

KEY WORDS: Fast Repetition Rate fluorometry, flow cytometry, phytoplankton photosynthesis, spatial variability, primary productivity

1 Introduction

~~Due to~~ The Dutch North Sea is of major socio-economic importance because of its close proximity to densely populated areas and the intensive utilization for shipping, fishing, sand extraction and development of offshore windmill farms. Due to this high anthropogenic pressure, the North Sea has undergone considerable biogeochemical and biological changes in the past decades (Burson et al., 2016; Capuzzo et al., 2015 and 2017). ~~Nutrient concentrations have shifted from a situation with increased input by agricultural run-off and wastewater to a large imbalance in the~~For example, nutrient load and stoichiometry were fluctuating substantially due to inflow of wastewater and agricultural run-off and subsequent mitigation efforts (Burson et al., 2016; Philippart et al., 2000). Additionally, water clarity decreased in large parts of the North Sea during the 20th century (Capuzzo et al., 2015). These abiotic changes affect biology resulting in primary productivity and community composition shifts throughout the trophic levels ~~and decrease of primary productivity~~, with large implications for ecosystem structure ~~functioning~~ and fisheries production (Capuzzo et al., 2017; Burson et al., 2016). Good biological monitoring of the North Sea is required for good management. A “robust North Sea” in which ecological processes and biodiversity can thrive will ensure sustainable use, which is of major socio-economic importance; the North Sea is in close proximity to densely populated areas with high recreational value, crossed with major shipping lanes, serving as intensive fishing ground, used for sand extraction and is used for the on-going energy transition involving the creation of many offshore windmill farms.

~~In the future, large~~Over time, further changes are expected due to ~~the planned energy transition and under the impact of~~ climate change ~~and coinciding~~. Anticipated climate change effects include ocean acidification, sea level rise, and increasing temperatures. Already, the North Sea is warming more rapid than most other seas (Philipart et al., 2011). These changing environmental conditions will have a big impact on marine biogeochemistry ~~and thereby on~~ phytoplankton community composition and primary productivity (Sarmiento et al., 2004; Behrenfeld et al., 2006; Marinov et al., 2010; ~~Schiebel et al., 2017~~). Changes in phytoplankton community composition and primary productivity ~~impacts~~affect the entire ecosystem and global biogeochemical cycles (Montes-Hugo et al., 2009; Falkowski et al., 1998; ~~Schiebel et al., 2017~~). Systematic and sufficient monitoring of these changes is of crucial importance to recognize threats, and, once identified as such, develop mitigation actions.

Although phytoplankton community composition and productivity can be highly variable on a spatial and temporal scale, governmental monitoring still consists mainly of low-resolution measurements (Baretta-Bekker et al., 2009; Kromkamp ~~&~~ van Engeland, 2010; Cloern, ~~1996~~; Cloern et al., 2014; Rantajarvi et al., 1998). ~~In spite~~Currently, biological monitoring of ~~this~~phytoplankton in the ~~amount~~Dutch North Sea is dictated by the requirements set by OSPAR and the EU Marine Strategy Framework Directive (MSFD 2008/56/EC). It consists of ~~low-resolution sampling arrays has been cut back considerably since~~HPLC analysis of Chl *a* concentration and microscopy counts of *Phaeocystis* cells and, at some stations, coccolithophores or toxic dinoflagellates. Sampling points were reduced from almost 70 in 1984 (Fig. 1; Baretta-Bekker et al., 2008).

~~to less than 20 today, while strong seasonal patterns, high riverine input, and tidal forces make the Dutch North Sea a region with high spatiotemporal variability.~~ Modern automated ~~flow-through~~flow systems ~~have the potential to be an effective addition to monitoring programs because they offer the opportunity to record phytoplankton composition, abundance and photosynthetic activity~~the surface ocean with high spatial and temporal resolution. ~~This could potentially be an effective addition to current monitoring programs. These~~Such high-resolution methods are well established in physical oceanography but for biological parameters, the implementation has been lacking. This is mostly due to the complicated interpretation of biological parameters, resulting in high uncertainties in the current global estimates of net primary productivity (Silsbe et al., 2016). Automated ~~flow-through~~ methods are not able to replace ~~some more detailed~~low-resolution measurements ~~such as species identification by microscope~~, but their higher spatial and temporal ~~resolution and potentially shorter analysis time make it easier~~resolutions provide the possibility to identify short-lived events and ~~serve~~act as an early warning system. Additionally, ~~they are able to give extra~~because the measurements are done *in situ*, it is possible to acquire information on ~~photophysiology, which can improve understanding of ecosystem dynamics, rates of living organisms and samples unaffected by transport, storage or conservation.~~ Two non-invasive, high-resolution ~~instruments that can~~methods with potential to be ~~used~~implemented in ~~marine ecosystem~~phytoplankton monitoring programs are scanning ~~flow cytometers~~flow cytometry (FCM) for information on phytoplankton abundance and community composition and Fast Repetition Rate ~~fluorometers~~fluorometry (FRRf) to give information on phytoplankton photophysiology. Scanning flow cytometry is a method for counting and pulse-shape recording

of phytoplankton cells resulting in a high number of parameters on size, fluorescence and scattering properties per algal cell. Based on these characteristics cluster analysis allows for division into groups of similar pigment characteristics and size classes (Thyssen et al., 2015; Rijkeboer, 2018). ~~The FRRF uses active fluorescence to gain insight into phytoplankton photophysiology. This technique is an alternative to the traditional production-light curves (PE-curves) by measuring the photosynthetic electron transport rate (or gross photosynthesis) at increasing ambient light levels (Suggett et al., 2009a; Silsbe and Kromkamp, 2012). Electron transport rate per unit volume is estimated by a series of single turnover light flashes that cumulatively close all photosystems (Kromkamp and Forster, 2003; Suggett et al., 2003). This single turnover technique allows for calculation of the effective absorption cross-section and, in combination with an instrument specific calibration coefficient, the absorption coefficient and amount of reaction centres per volume (Kolber et al., 1998; Kromkamp and Forster, 2003; Oxborough et al., 2012; Silsbe et al., 2015). Electron transport rate per unit volume is used to estimate gross primary productivity (Kromkamp et al., 2008; Smyth et al., 2004; Suggett et al., 2009a). These characteristics allow for division into groups based on pigment characteristics and size classes (Thyssen et al., 2015). Ideally these groups reflect functional groups, such as calcifiers, silicifiers, DMS producers (such as *Phaeocystis*) and nitrogen fixers to aid in better functional understanding of ecosystem dynamics (le Quéré et al., 2005; Beese 2009a). These two methods are supplementary, because the interaction of phytoplankton with their environment is always a sum of the community composition and their physiology, inclusion of phytoplankton physiology can improve understanding and interpretation of ecosystem dynamics.~~ For instance, if waters become more turbid, phytoplankton can acclimate by increasing their effective absorption cross section, but it could also lead to a shift in community composition toward species with higher light use efficiency (Moore et al., 2006). Combination of these two instruments therefore allows for a more in-depth analysis and understanding of ecosystem processes.

The aim of this study is to test two high resolution methods, a pulse shape recording flowcytometer and a FRR fluorometer, on their suitability to be developed into a novel phytoplankton monitoring method. The two instruments were deployed concurrently on four 4-day cruises in April, May, June and August to meet a wide range of environmental conditions and phytoplankton community states. These measurements allow for quantification of seasonal and mesoscale spatial patterns in phytoplankton abundance, photophysiology and gross primary production. In this paper we provide an overview of the acquired results, use a spectral cluster analysis to visualize spatial heterogeneity and we evaluate the potential of these methods to optimize current monitoring programs.

~~The FRRF uses active fluorescence to gain insight into phytoplankton photophysiology. This technique is an alternative to the traditional production-light curves (PE-curves) by measuring the electron transport rate (or gross photosynthesis) at increasing ambient light levels (Suggett et al., 2009; Silsbe et al., 2012). Electron transport rate per unit volume is estimated by a series of single turnover light flashes that cumulatively close all photosystems (Kromkamp et al., 2003; Suggett et al., 2003). This single turnover technique allows for calculation of the effective absorption cross-section and, in combination with an instrument specific calibration coefficient, the absorption coefficient and amount of reaction centres per volume (Kolber et~~

al., 1998; Kromkamp et al., 2003; Oxborough et al., 2012; Silsbe et al., 2015). Electron transport rate per unit volume is used to estimate gross primary productivity (Kromkamp et al., 2008; Smyth et al., 2004; Suggett et al., 2009).

In this study, we provide an example of how high-resolution methods can serve in biological monitoring. During four cruises in different seasons, aiming to find four different stages in the seasonal phytoplankton growth period, continuous measurements were conducted with an FCM, FRRf, and Ferrybox to retrieve a wide range of data. An overview will be given on the information acquired with these measurements. Additionally, we will use a model to visualize spatial heterogeneity and identify regions based on the photophysiological characteristics and presence of five phytoplankton groups separated based on pigment ratio and size. Lastly, gross primary productivity is calculated and compared to high-resolution data and low-resolution data to get a better understanding on the key drivers for gross primary productivity in the Dutch North Sea.

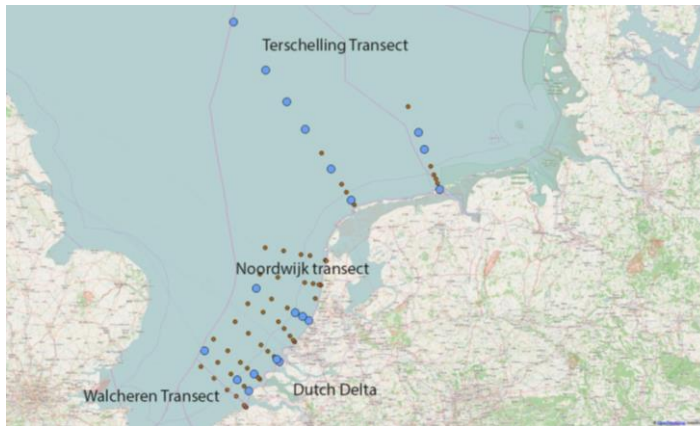
2 Methods

2.1 Study site and sampling

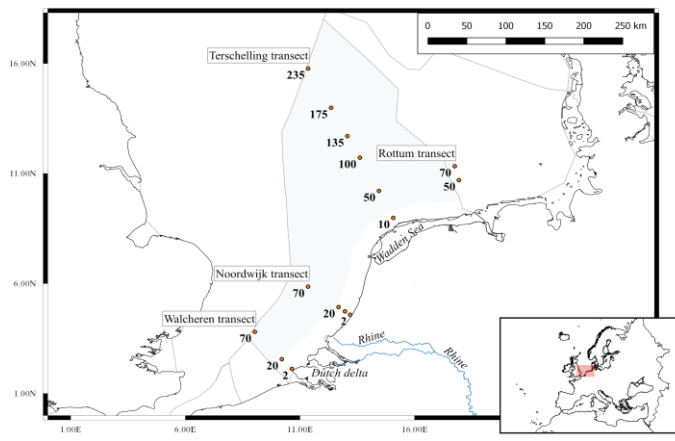
The Dutch North Sea is a shallow tidal shelf sea in the southern part of the North Sea. The main water flow is northward. Atlantic water enters the North Sea ~~in the south~~ from the south via the Channel ~~but~~ and from the majority of the Atlantic northeast where it curves around Scotland ~~and flows southwards and eastwards, where it meets the Channel water and the freshwater from the rivers.~~ Both currents meet north of the Dutch coast forming the Frisian Front. For a detailed description on the North Sea physical oceanography, see Sundermann ~~Sündermann~~ and Pohlman (2011). Along the Dutch coast, high river input from especially the Rhine River decrease the salinity and loads the coastal zone with high nutrient concentrations (Burson et al., 2016). Anthropogenic pressure is high in the Dutch North Sea resulting in a history of large shifts in nutrient concentrations and water clarity (Capuzzo et al., 2015; Burson et al., 2016).

The monitoring of the Dutch North Sea is performed by the Dutch government (Rijkswaterstaat) in a monitoring program called MWTL (Monitoring Waterstaatkundige Toestand des Lands, freely translated as ‘Monitoring of the status of the governmental waters of the country’). The location of the sampling stations of the program are organized along transects (Fig. 1). Notice the decrease in the number of sampling stations between 1983 (small brown dots) and 2014 (larger blue-filled circles). The stations are sampled between March and October with a frequency of every two or four weeks, dependent on the

transect.



5 **Figure 1: Sampling locations of the MWTL monitoring program in 1984 (small brown dots) and 2014 (larger blue filled circles). A few transect names are given.**



5 Figure 1: Sampling locations of the MWTL monitoring program referred to in this study. The stations are named according to the transect (Terschelling, Noordwijk and Walcheren), followed by the amount of kilometres from the coast (labels next to sampling points). The boundaries of the Exclusive Economic Zone (EEZ) are indicated by the grey dotted lines and the Dutch EEZ is coloured light blue. The locations of three major infows to the Dutch North Sea are named at the corresponding locations (Rhine river, Dutch Delta and the Wadden Sea). Insertion visualizes the location of the Dutch North Sea in a broader map of Europe.

10 In 2017, four 4-day sampling surveys (10-13 April, 15-18 May 12-15 June and 14-17 August), were conducted for the JERICO-NEXT project on board the RV *Zirfaea* during their regular monitoring cruises on the Dutch North Sea. To assess the heterogeneity of the Dutch North Sea and the benefits associated with high-resolution monitoring the four cruises were conducted in different months (April, May, June and August), thereby aiming to cover different seasons and stages of the phytoplankton bloom (Baretta-Bekker et al., 2009). ~~During these cruises the high-resolution methods (FRRf, FCM and Ferrybox) were combined with lower resolution methods on nutrient concentrations and vertical light extinction using vertical deployments of a rosette frame equipped with a CTD and Niskin bottles.~~2009).

15 On the RV *Zirfaea* the water inlet was situated approximately 3.5 m below sea surface level. From the water inlet the sample water, with a flow rate of approximately 24 ~~litres~~ litres per minute, was split towards 1) a flow-through 4H-JENA Ferrybox (4H-JENA engineering GmbH, Germany) equipped with an FSI Excell® Thermosalinograph (Sea-Bird Scientific, USA) to measure temperature and salinity and a SCUFA™ Submersible Fluorometer (Turner Designs Inc., USA), and 2) at a flow rate of 1 L per minute towards a 230 cm³ flow through sampling container where water was cleared from bubbles and sand. The time from water inlet to sampling chamber was approximately 2 minutes. A FastOcean Fast Repetition Rate fluorometer (FRRf) with Act2-based laboratory flow through system (Chelsea Technologies Group Ltd, UK) and a Cytosense scanning flowcytometer (Cytobuoy BV, the Netherlands) automatically sampled from the sampling unit every 30 minutes. Since the average speed of the ship was 8 knots, the average spatial resolution of FCM and FRRf measurements was on average 7.5 kilometres. The Ferrybox sensors stored data every minute. ~~At discrete stations (10 to 15 per cruise) water samples were collected for nutrient analysis with a rosette sampler. Simultaneously, the rosette sampler recorded the irradiance extinction in the water column with a QSP-200L Log Quantum Scalar Irradiance Sensor (Biospherical Instruments Inc., USA). The diffuse attenuation coefficient K_d (m⁻¹) was calculated as the linear regression of the natural logarithm of irradiance corrected for changes in surface irradiance (PAR, 400-700 nm) versus water depth.~~During the cruises the high-resolution methods (FRRf, FCM and Ferrybox) were combined with lower resolution methods, consisting of measurements at 13 to 19 stations. At these stations surface samples were taken for nutrient and chlorophyll *a* analyses (see 2.2 chemical analyses) using a rosette sampler equipped with a CTD and Niskin bottles.

2.2 Chemical analyses

Samples for nutrient ~~analysis~~analyses were filtered over Whatmann GF/F filters and kept frozen until analyses. The analyses of ammonium (NH₄⁺), nitrite (NO₂⁻), nitrate (NO₃⁻), ortho-phosphate (PO₄) and silicate (Si) concentrations were conducted by the Rijkswaterstaat laboratory (the Netherlands) according to ~~RWS internal analysis protocol A1.004~~ISO 13395, 15681, 16264 using a San-plus⁺⁺ Analyzer (Skalar Analytical B.V., the Netherlands). In the RWS internal protocol, nitrite+nitrate is measured by first reducing nitrate to nitrite using a cadmium/copper column and addition of ammoniumchloride as a buffer. Thereafter, sulphanilamide, α-naphthyl ethylenediamine dihydrochloride and phosphoric acid are added and the extinction at 540 nm compared to a NaNO₂ standard. For measurement of Ammonium concentrations first EDTA was added to bind Calcium and Magnesium. Then, sodium salicylate, sodium nitroprusside and sodium hypochlorite were added and the extinction at 630 nm compared to a NH₄Cl standard. Ortho-phosphate was measured by adding molybdate reagent and ascorbic acid to the sample and led through an oilbath at 37 ± 2 °C. Followed by measuring the extinction at 880 nm and comparing to a standard. Silicate concentration was measured by subsequent addition of molybdate reagent, oxalic acid and ascorbic acid. The silicate concentration was then determined by measuring the extinction at 810 nm and comparing to a silicate standard. The detection limits of the nutrient analyses were: NO₃NO₂: 0.7 μM, Si: 0.36 μM and PO₄³⁻: 0.03 μM.

Chlorophyll *a* concentration (hereafter Chl *a*) was ~~sampled~~determined by filtering over Whatmann GF/C filters and freezing the filter at -80 °C. ~~Thereafter the~~The Chl *a* was extracted in 20 ml 90% acetone and centrifuged for 15 minutes with glass pearls (1.00-1.05 mm) using a Bullet Blender Tissue homogenizer (Next Advance, Inc., Troy, USA) under cooling of solid CO₂. The extract was analysed in duplicates using Ultra High Performance Liquid Chromatography (UHPLC). The calibration of the UHPLC system is performed every analysis day by making a 12-point standards calibration curve calculated using quadratic regression with weighting method 1/A to better distinguish smaller peaks (R²>0.995). The injection volume was 20 μl, unless the concentration was below the lowest standard, in which case a second injection of 40 μl was reanalysed. The analysis was conducted by the MUMM laboratory (Belgium) using ~~High Performance Liquid Chromatography (HPLC)~~ according to RWS analysis protocol A200. Quality control was performed by the RWS laboratory (The Netherlands).

2.3 High frequency methods

2.3.1 Variable fluorescence

Variable fluorescence was measured with a FastOcean Fast Repetition Rate fluorometer (FRRf) and Act2-based laboratory system (Chelsea Technologies Group Ltd, UK). Temperature was controlled by connecting a Lauda ecoline cooler (LAUDA-Brinkmann, LP., USA) to the water jacket of the Act2 system.

The acquisition protocol consisted of 100 excitation flashes with a flash pitch of 2 μs and 40 relaxation flashes with a flash ~~duration~~pitch of 60 μs. Excitation flashes were performed with the blue LED (450 nm) and strength of the LEDs was

automatically adjusted to the phytoplankton concentration by the manufacturer' FAsPro software. A loop of simultaneous blue and green flashes (450 nm+530nm) was performed after the acquisition loop of only blue LEDs in case the blue LEDs were not able to reach saturation (for instance with high cyanobacteria concentrations), but as this was not the case, only the parameters measured by blue LEDs were used for further calculation. The sequence was repeated 20 times with a sequence interval of 100 ms. The sample was refreshed before each fluorescent light curve (FLC) by flushing for 60 seconds and kept well-mixed by "flushing" for 200 ms between acquisition loops.

The FLC protocol consisted of 14 light steps of 100 s, of which the light intensity was automatically adjusted to get the optimal FLC shape based on the previous light curve. A pre-illumination step (55 seconds on 12 $\mu\text{mol photons m}^{-2} \text{s}^{-1}$) was included before the FLC to low light acclimate the phytoplankton and to relax [non-photochemical quenching \(NPQ\)](#) of diatoms and other chlorophyll *a-c* algae as they stay in the light activated state in the dark. ([Goss et al., 2006](#)). After each light step, measurements were made in the dark for 18s to retain a value for F_0' : ([minimal fluorescence in light acclimated state](#)). The data [was/were](#) corrected for the background fluorescence by taking sample blanks multiple times per day by filtration over a 0.45 μm filter and subtracting the last determined background fluorescence from the sample fluorescence.

An overview of the derived photosynthetic parameters can be found in Table 1. To derive values for the maximum photosynthetic electron transport rate (P_{max}), minimum saturating irradiance (E_k) and the light utilisation efficiency (α) the relative electron transport rate (rETR) of the samples was fitted to the exponential model of (Webb et al. 1974), after normalizing the data to the irradiance as described by (Silsbe and Kromkamp, 2012):

$$F_q'/F_m' = \frac{P_{\text{max}} \left(1 - \exp\left(\frac{\alpha}{E_k}\right)\right)}{E} P_{\text{max}} \left(1 - \exp\left(\frac{-E}{E_k}\right)\right) \quad (1)$$

where E is the irradiance in $\mu\text{mol photons m}^{-2} \text{s}^{-1}$, F_q'/F_m' the effective PSII quantum efficiency, α is the initial slope of the rETR vs irradiance curve and E_k is the light saturation parameter (in $\mu\text{mol photons m}^{-2} \text{s}^{-1}$). The relative maximum rate of photosynthetic electron transport (P_{max}) was calculated as:

$$P_{\text{max}} = E_k \times \alpha \quad (2)$$

Table 1: The derived photosynthetic parameters used in the text (see [Oxborough et al. \(2012\)](#) and [Silsbe et al. \(2015\)](#) for more information). Variables used in equation 1-8 are not included but discussed in the text.

	Description	unit
Parameters derived from fluorescence induction curve		
F_0	Minimum fluorescence, measured at zero th flashlet of an FRRF single turnover measurement when all PSII reaction centers (RCII) are open. Estimate for chlorophyll <i>a</i> concentration.	Dimensionless
F_m	Maximum fluorescence, reached at n th flashlet of an FRRF single turnover measurement when all PSII reaction centers are closed.	Dimensionless

Formatted: Font: 9 pt, Bold, Font color: Black

Formatted Table

$1/\tau$	Rate of re-opening of a closed RCII	ms^{-1}
σ_{PSII}	Effective absorption cross section of PSII photochemistry	$\text{nm}^2 \text{PSII}^{-1}$
Parameters calculated from parameters derived from fluorescence induction curve		
JV_{PII}	PSII charge separation rate per unit volume (see eq. [3])	$\mu\text{mol electrons m}^{-3} \text{h}^{-1}$
F_q'/F_m'	Quantum efficiency of PSII under dark conditions (see eq. [4])	Dimensionless
a_{LHII}	Absorption coefficient of PSII light harvesting (see eq. [5])	m^{-1}
[RCII]	Functional PSII reaction centers per volume (see eq. [6])	nmol RCII m^{-3}
Parameters derived from Fluorescence light curve (FLC)		
α_{PSII}	Initial slope of the FLC, an estimate of affinity for light	$\mu\text{mol electrons } (\mu\text{mol photons})^{-1}$
E_k	Minimum saturating irradiance of fluorescence light curve	$\mu\text{mol photons m}^{-2} \text{s}^{-1}$
P_{max}	Maximum photosynthetic electron transport rate	$\mu\text{mol electrons m}^{-2} \text{s}^{-1}$
Parameters calculated from parameters derived from fluorescence light curve and irradiance		
Surface GPP	Surface Gross Primary Productivity (see eq. [3]) calculated based on the FLC-parameters and incoming irradiance.	$\mu\text{g C L}^{-1} \text{h}^{-1}$

The PSII flux in $\mu\text{mol electrons m}^{-3} \text{h}^{-1}$ was calculated as the product of the effective PSII efficiency (F_q'/F_m'), the optical absorption cross section of the light harvesting pigments of PSII (a_{LHII}) and the irradiance (E):

$$JV_{PII} = F_q'/F_m' \cdot (in \mu\text{mol electrons } (PSII \text{ m}^{-3}) \text{ h}^{-1}) = F_q'/F_m' * a_{LHII} * E \quad (3)$$

where

$$F_q'/F_m' = \frac{F_m' - F'}{F_m'} \quad (4)$$

and

$$a_{LHII} (in \text{m}^{-1}) = \frac{F_0 + F_m}{F_m - F_0} * K_a \quad (5)$$

K_a (m^{-1}) is an instrument specific factor necessary for obtaining absolutes rate of photosynthetic transport (see Oxborough et al. (2012) and Silsbe et al. (2015) for more information). The amount of reaction centres per cubic metre ([RCII]) was calculated as

$$[RCII] (in \text{nmol m}^{-3}) = K_a * \frac{F_0}{\sigma_{PSII}} \quad (6)$$

and the approximate number of reaction centres per Chl *a* (note that the Chl *a* concentration is estimated based on minimum fluorescence value (F_0), and is therefore a mere estimation). If [RCII] is known the number of PSII units per mole Chl *a* (n_{PSII}) can be calculated:

$$\tau_{PSII} = \frac{\{RCII\}}{\{CHT-a\}} \quad (7)$$

for more information on the calculation of [RCII] and $a_{L,IIII}$ see Oxborough et al. (2012) and Silsbe et al. (2015).

Q_A reoxidation or rate of re-opening of a closed RCII was calculated as 1 divided by the time constant of re-opening of a closed RCII with an empty Q_B site (τ_{ES}) in ms^{-1} .

Standardized daily anomalies (Z-scores) were calculated for the photophysiological parameters as:

$$Z - score = \frac{x - \text{daily mean}(x_0 \dots x_{24})}{\text{Daily standard deviation}(x_0 \dots x_{24})} \quad (7)$$

Partial days were excluded because this could potentially offset the daily mean and standard deviation.

Gross Primary Productivity (GPP) was estimated ~~by integrating surface productivity over water depth. Volumetric P_{max} and α were derived~~ by fitting JVPII in $\mu mol \text{ photons } m^{-3} h^{-1}$ to equation 1 (the exponential model of Webb et al., 1974) ~~to derive a volumetric P_{max} and these parameters used to integrate productivity over depth where the light extinction α GPP in the water column $\mu g C L^{-1} h^{-1}$ was estimated as~~

$$E(z) = E_{surface} * e^{-K_d * z} \quad (9)$$

~~with $E(z)$ being the irradiance at depth z . The value for α then calculated using equation 1 and incident surface irradiance. To avoid effects of changing incident surface irradiance ($E_{surface}$) was held constant over on the month spatial pattern and calculated as α to be able to compare GPP between regions we used monthly average light intensity over surface irradiances ($E_{surface}$) in our calculations of primary productivity. From 2010 to 2016 irradiance (400-700 nm) was measured at the roof of the NIOZ building in Yerseke using a LI-190 quantum PAR sensor. Hourly data were averaged and hourly averages stored using a LI1000 datalogger. The light extinction coefficient, K_d , $E_{surface}$ was then calculated based on a vertical irradiance profile obtained with a QSP-200L Log Quantum Scalar Irradiance Sensor (Biospherical Instruments Inc., USA) which was conducted approximately 10 times per cruise (see Methods-Study Site and sampling). In order to interpolate between these profiles a correlation with the turbidity (in NTU, as measured by the Ferrybox) as predictor was determined based on linear regression: $\ln(K_d) = 0.785 * \ln(\text{Turbidity}) - 1.324$ ($n=71$, $R^2=0.77$, $p<0.01$). The calculated water column by averaging all irradiance data from the years 2010-2016 for the respective month. The primary productivity in electrons units was converted to carbon units by assuming 6 moles of electrons were required to fix one mole of carbon, based on a study in the adjacent Oosterschelde and Westerschelde estuaries (Kromkamp et al., in prep.).~~

2.3.2 CytoSense scanning flowcytometry

Single cell measurements of the phytoplankton community were ~~carried out~~conducted using a bench-top scanning flowcytometer (CytoBuoy BV, the Netherlands) equipped with two lasers (488 nm and 552nm). ~~Both lasers (< 60mW each)). Both laser beams~~ were continuously ca. 5 µm high and 300 µm wide and were focussed on the same spot in the middle of the flow-through chamber ~~having a height of ca. 5 µm and a width of 300 µm.~~ The speed of the particles ~~is was~~ ca. 2.2 m s⁻¹. ~~With this configuration Forward light Scatter (FWS) and Sideward light Scatter (SWS) of all particles were measured.~~ The system contained 3 fluorescence ~~detector channels; FLY separating fluoresced wavelengths~~ of 550-600 nm (FLY: Phycoerythrin); ~~FLO of~~ 600-650 nm (Chlorophyll *b* and FLO: Phycocyanin) and ~~FLR >above 650 nm for~~(FLR: chlorophyll *a* and ~~e detection.~~). Additionally, the Forward light Scatter (FWS) and Sideward light Scatter (SWS) of all particles was measured. ~~The FCM was equipped with a double set of detectors (PMT's) for each of the three fluorescence channels to increase the dynamic range (Rutten, 2015).~~ Per cell the pulse shape recording and the parameters (FWS, SWS, FLR, FLO and FLY) plus their affiliates (length, total and maximum values) ~~are recorded and saved. The FCM was equipped with a double set of detectors (PMT's) for each of the three channels to increase the dynamic range (Rutten, 2015), were recorded and saved.~~ The instrument was checked daily for drift using 3 µm Cyto-Cal™ 488 nm alignments beads (Thermo Fisher Scientific Inc., USA). Additionally, the FCM was equipped with an Image-in-flow camera to take pictures of the nano- and micro-phytoplankton; ~~this.~~ This allows for linking pulse shape recordings to microscopy results and thereby identification of represented phytoplankton groups in respective clusters.

Phytoplankton cells were clustered based on the pulse shape recording of the individually scanned phytoplankton. In this paper we ~~mainly~~ discriminate the phytoplankton groups based on their size (pico, nano and micro) and Orange/Red fluorescence ratio (hereafter O/R ratio; Table 2). ~~The chosen cluster criteria were based on expert judgement (SeaDataNet, 2018) and corresponding to other studies (Sieburth et al., 1978; Vulot et al., 2008).~~ ~~The clustering was done by the software Easyclus software-1.26- (ThomasRuttenProjects, The Netherlands)- according to these criteria. Noise, air bubbles and other potential outliers were removed.~~ Size was calculated based on the length FWS. ~~Length FWS was found to be a good estimate of the length of the particles because due~~Due to the speed acceleration of the particles in the sheath fluid of the FCM the organisms will flow along their long axis, ~~which makes the FWS a good estimate of the length of the particles.~~ We obtained a linear relation between Length FWS and measured length of diverse phytoplankton species, having an angle of inclination of almost 1 and R²=0.99-98 (Rijkeboer, 2018). For organisms smaller than 5 µm there may be some deviation from this relationship due to the width of the laser beam (which is 5 µm).

Table 2: The phytoplankton groups distinguished in the current study.

Name	Cluster criteria		Main corresponding taxonomic group(s)
	Length FWS	O/R-ratio	
Pico-Red	<4 µm*	<1	Pico-eukaryotes

Formatted: Font: Times New Roman

Formatted: Font: 9 pt, Bold, Font color: Black

Formatted: Normal, Space After: 10 pt, Border: Top: border, Bottom: (No border), Left: (No border), Right: (No border), Between : (No border)

<u>Pico-Synecho</u>	<u><4 μm^*</u>	<u>≥ 1</u>	<u><i>Synechococcus</i></u>
<u>Nano-Crypto</u>	<u>4-20 μm</u>	<u>≥ 1</u>	<u><i>Cryptophyceae</i></u>
<u>Nano-Red</u>	<u>4-20 μm</u>	<u>≤ 1</u>	<u><i>Diatoms, Haptophytes, Dinoflagellates</i></u>
<u>Micro-Red</u>	<u>>20 μm</u>	<u>≤ 1</u>	<u><i>Diatoms, Haptophytes, Dinoflagellates</i></u>

*In June <6 μm

2.4 Data analysis

Outliers of the complete dataset were removed after visual inspection of pairplots made with the pairplot function of the HighstatLib HighstatLib.V4 script (Zuur et al., 2009) and. For the FRRf data, the fitted F_q^2/F_m^2 -EFLC curves were visually inspected for a good fit and removed based on expert judgement, which led to removing 1% to 7% of the FLC fits. Especially at low biomass FLCs became noisy, therefore a minimum fluorescence signal was set for calculations of photosynthetic parameters, below. Below this blank corrected instrument-specific fluorescence signal F_q^2/F_m^2 became noisy and often reached above the biologically unlikely limit of 0.65. (Kolber and Falkowski, 1993). The datasets of the high-resolution measurements (FRRf, FCM and Ferrybox) were linked using corresponding timestamps. When multiple measurements were performed within one FLC, the average was used.

Spatial clusters in the Dutch North Sea were defined To find regions with similar phytoplankton communities, data was spectrally clustered using R (version 3.4.1, R Core Team, 2017) with the additional the uHMM R package (Poisson-caillault and Ternynck, 2016) in the statistical software R (version 3.4.1, R Core Team, 2017). The package default settings normalize data before clustering, and automatically find the number of clusters based on spectral classification and the geometry of the data. This new methodology is more robust than the classical hierarchical and k-means technics (Rousseeuw et al., 2013, 2015). Datapoints were then per cluster labelled and plotted on a map to visually identify regions. Cruises were analysed separately and not as one continuous time series as the time gaps between the sampling cruises were large. All photophysiological colinear predictors were removed (VIF > 6; Zuur et al., 2009). The FCM phytoplankton groups based on total red fluorescence were included despite colinearity.

Separate stepwise multiple regressions were performed for all months combined by stepwise deletion of insignificant predictors. Predictors were Phytoplankton parameters were first tested for colinearity collinearity and all predictors with a variance inflation factor (VIF) over 6 were removed (Zuur et al., 2009). Interactions of the predictors were not included. Residuals were visually checked 2009; see supplementary material for pairplots). This left for normality by plotting a qqnorm plot of the residuals of the model and for homogeneity of the variances by plotting the residuals of the model against the fitted values and against each separate predictor.

the cluster analysis FCM-parameters Pico-red, Nano-red, Micro-red and *Synechococcus* and the FRRf-parameters σ_{PSII} , F_v/F_m , α_{LIII} , $1/\tau$, E_k . Datapoints were then per cluster labelled and plotted on a map to visually identify regions. Principal Component Analyses (PCA) were performed to find which variables contributed most to the cluster results The PCA's were based on correlation matrixes with scaled parameters to correct for unequal variances and was carried out with the prcomp() function in R (version 3.4.1, R Core Team, 2017). The PCA visualization was done using the supplemental R package factoextra

Formatted: English (United States)

(Kassambra and Mundt, 2017). Maps were made using QGIS v. 2.14.2 and other figures were made with ggplot2 in R (Wickham, 2009).

3 Results

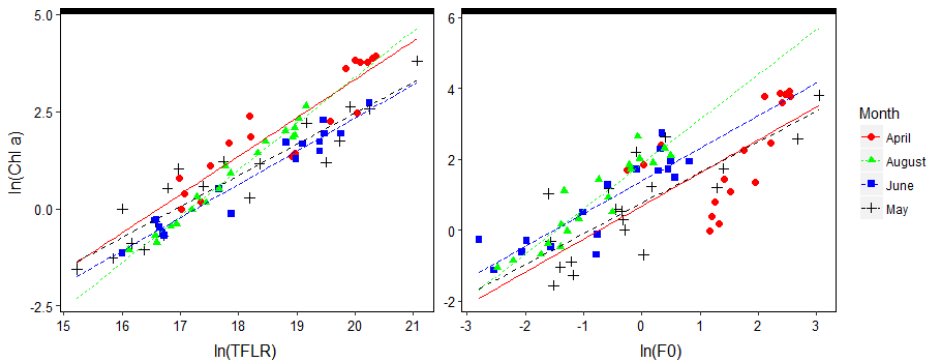
3.1 Environmental Abiotic conditions

Environmental conditions in the Dutch North Sea are spatially heterogeneous and strongly influenced by seasonal dynamics. Sea surface temperature increases from 9.5 ± 1.0 °C in April to 19.0 ± 0.6 °C in August (Table 3; supplementary table S1). Seasonal variations in salinity are small with highest monthly mean salinity was measured in April (34.1 ± 1.8), while spatial variability of salinity is higher with river influx decreasing the salinity down to 26 in the coastal zone. The monthly average of turbidity does show seasonal variation and was clearly higher in April (2.3 ± 3.0 NTU) in comparison to other months, which. This was reflected in the highest K_d values, which were also highest in April (0.39 ± 0.28 m⁻¹; supplementary table S1). It needs to be noted that monthly averages are not completely comparable, because of differences in sampling route and stations (Fig. 4).

The average nutrient concentrations of all stations sampled during the different cruises is shown in Table 4. To see if nutrient concentrations were potentially limiting we used threshold concentration for DIN and Si as $2 \mu\text{mol L}^{-1}$ and PO_4^{3-} as $0.2 \mu\text{mol L}^{-1}$ (Peperzak et al., 1991, Philippart et al., 2007) although Ly et al. (2014) showed that for Wadden Sea phytoplankton phosphate can become limiting when values become lower than 0.13 – $0.16 \mu\text{mol L}^{-1}$.

Nutrient concentrations show both high spatial and seasonal variability (supplementary Table 1). The general trend in all transects is an offshore moving gradient of decreasing nutrient concentrations. Offshore stations (>70 km offshore west of the Netherlands, >135 km North of the Netherlands) are DIN limited year round, while regions closer to freshwater influx are DIN sufficient in all sampled months except August. This clearly reflects the input of the Rhine and its waters remained relatively close to the coast; no influence seems present at waters further than 70 km offshore. In April nutrient concentrations are on average higher and only potentially limiting in the most southerly part of the Dutch North Sea (Walcheren transect) and further offshore (>70 km offshore west of the Netherlands, >135 km North of the Netherlands). In later months, nitrate

and silicate limitations gradually moves towards the coastal zone, with nutrient limitation at all sampled stations in August. Phosphate levels were generally quite low and possibly limiting, with exception in April north of the Wadden Islands up to 135 km offshore. Later in the year (June and August) phosphate concentrations recovered in the Southern part of the Dutch North Sea reaching up to $0.6 \mu\text{M}$. Silicate, an essential element for diatoms, seemed to be present in limiting concentrations at all sampled times at the Walcheren stations, suggesting that the cruise in April was already beyond the peak of the diatom bloom. Nutrient ratios (DIN:DIP, DSi:DIP and DIN:DSi) suggest P limitation, and for diatoms Si limitation in April and May, and N limitation in August, whereas in June values were closer (but below) to the Redfield Ratio. Apart from the seasonal trend of the nutrient limitation on the onshore-offshore gradient moving towards the coast, there also seems to be a south-to-north trend, with the southern Dutch North Sea being depleted earlier in the season in comparison to the more northerly area.



Dissolved Inorganic Nitrogen (DIN; Nitrate+Nitrite+Ammonium) and silicate (Si) concentrations show both spatial and seasonal variability (Table 3). Spatially, two trends are distinguishable: a coastal-offshore gradient and a longitudinal gradient. The seasonal variability determines the strength and position of these spatial gradients. The coastal to offshore gradient moves shoreward from April to August and the southern stations are depleted earlier in the season in comparison to the more northerly stations. In April DIN and Si concentrations are on average higher and only potentially limiting ($\text{Si} < 1.8 \mu\text{mol L}^{-1}$, $\text{DIN} < 2 \mu\text{mol L}^{-1}$; Peeters and Peperzak et al. (1990) and references therein) in the most Southern part of the Dutch North Sea (Walcheren transect) and at offshore stations ($>70 \text{ km}$ offshore west of the Netherlands, $>135 \text{ km}$ North of the Netherlands). In later months, DIN and Si limitations gradually moves towards the coastal zone. Stations closest to freshwater influx (Noordwijk 2

and 10) become DIN and Si-limited later in the year (Table 3). The increased DIN concentration at the transect close to the Rhine outflow is absent seventy kilometers offshore (Noordwijk 70), suggesting that the Rhine water remained close to the coast.

5 Phosphate concentrations were generally quite low and possibly limiting (ortho-phosphate $\text{PO}_4^{3-} < 0.5 \mu\text{mol L}^{-1}$; Peeters and Peperzak et al, 1990). With exceptions in April north of Terschelling between 50 and 100 km offshore and in May at Noordwijk 2, a region with high freshwater influx. In August phosphate concentrations recovered in the Southern part of the Dutch North Sea reaching up to $0.6 \mu\text{M}$. For a table on the N:P ratios see the supplementary table S2.

10

15 **Table 3: nutrient concentrations (μM) separated per month (April, May, June and August) and station. The stations are named according to name of the transects and the distance in kilometres from the coast (Fig. 1). Potentially limiting nutrient concentrations are shown in red ($\text{DIN} < 2 \mu\text{mol L}^{-1}$, $\text{Si} < 1.8 \mu\text{mol L}^{-1}$, $\text{PO}_4^{3-} < 0.5 \mu\text{mol L}^{-1}$; Peeters and Peperzak et al, 1990). B.d: below detection limit.**

Station	DIN (μM)					PO_4^{3-} (μM)					Si (μM)			
	April	May	June	August		April	May	June	August		April	May	June	August
Walcheren 2	1.0	2.4	3.4	1.0	-	0.2	0.2	0.4	0.6	-	0.6	0.7	1.4	1.9
Walcheren 20	1.2	3.1	1.1	b.d	-	0.1	0.1	0.3	0.3	-	b.d	2.7	0.5	2.0
Walcheren 70	1.1	1.2	1.1	b.d	-	0.2	0.2	0.2	0.1	-	b.d	0.6	0.4	0.9
Noordwijk 2	37.5	21.7	4.9	b.d	-	0.3	0.6	0.2	0.2	-	6.7	3.5	0.8	1.2
Noordwijk 10	28.5	15.0	3.1	b.d	-	0.2	0.1	0.4	0.1	-	2.9	3.2	0.7	1.4
Noordwijk 20	21.6	4.9	0.9	b.d	-	0.2	0.1	0.2	0.1	-	1.3	0.7	0.8	0.6
Noordwijk 70	b.d	1.0	0.9	b.d	-	0.2	0.2	0.3	0.2	-	b.d	1.1	1.7	0.1
-	-	-	-	-	-	-	-	-	-	-	-	-	-	-
Terschelling 10	10.1	1.9	0.9	b.d	-	0.3	0.2	0.2	0.2	-	3.0	2.4	0.5	0.7
Terschelling 50	8.9	b.d	3.4	2.8	-	0.5	0.2	0.2	0.3	-	4.6	1.7	2.4	5.0
Terschelling 100	12.6	b.d	1.9	b.d	-	0.5	0.2	0.3	0.2	-	3.9	0.5	1.1	1.7
Terschelling 135	1.6	0.8	0.9	b.d	-	0.4	0.1	0.1	0.3	-	2.0	0.8	0.9	1.8
Terschelling 175	0.9	NA	1.0	b.d	-	0.2	NA	0.2	0.2	-	0.6	NA	0.5	b.d
Terschelling 235	1.0	NA	0.9	b.d	-	0.2	NA	0.3	0.3	-	b.d	NA	1.1	0.5

5

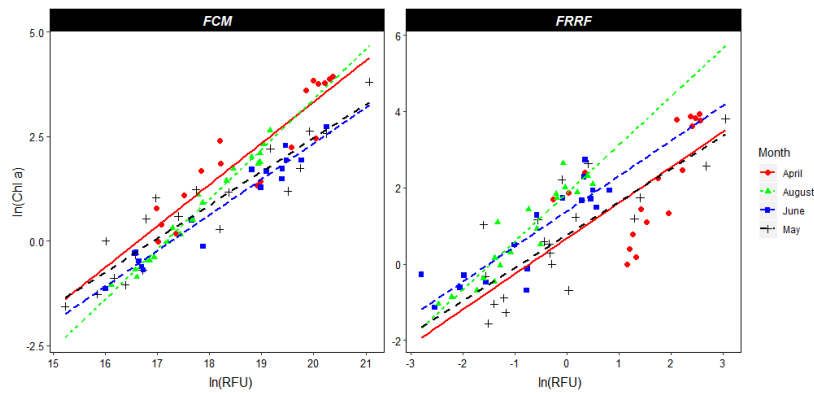


Figure 2: linear regression of the natural logarithms of Chl *a* concentration in $\mu\text{g L}^{-1}$ as determined by HPLC (y-axis) and on the x-axis: the natural logarithm of; FCM-derived total red fluorescence (TFLR-in relative fluorescence units (RFU), left panel) and FRRF-derived minimum fluorescence (F_0 in RFU, right panel). Both FCM red fluorescence ($p < 0.01$, adjusted $R^2 = 0.90$) and the FRRF F_0 ($p < 0.01$, adjusted $R^2 = 0.66$) are significant predictors for Chl *a* concentrations. The months (April, May, June and August) were a significant predictor of Chl *a* concentration for both the FRRF ($p < 0.05$) and the FCM ($p < 0.01$). The interaction between the x and y axis was only significant for the FCM data ($p < 0.05$).

10

15

3.2 Phytoplankton parameters

Information on total phytoplankton abundance can be obtained from both FRRF and FCM (Fig. 2). The FCM provides data on abundance in the amount of cells per millilitre of seawater and gives an estimate of Chl *a* concentration based on the cumulative red fluorescence of all cells (hereafter TFLR). The FRRF also provides an estimate of Chl *a* based on the minimum fluorescence (F_0). Using cell count or fluorescence as predictor of phytoplankton presence yields contrasting results (Fig. 3), because of the wide range of phytoplankton cell sizes; microplankton have a substantially higher biomass, and thus fluorescence, per cell in comparison to picoplankton. So while the phytoplankton cell count is higher in June and August in comparison with April, the community in the former months consists of mainly picoplankton which contribute little to total fluorescence resulting in a considerably lower fluorescence in June and August (Fig. 3). Fluorescence is therefore a better predictor of biomass or of Chl *a* concentration than cell counts, although Chl

20

25

Formatted: Heading 2

~~***α concentration is a limited predictor of biomass because the Chl *a* concentration per cell is species-specific and is subject to phenotypic acclimation to abiotic conditions (Flynn, 1991, 2005; Geider et al., 1997).***~~

High-resolution measurements of phytoplankton presence are based on either cell numbers (flowcytometers) or fluorescence (fluorometers, such as the “standard” chlorophyll sensors, FRRf, and some flowcytometers). Both parameters can yield
5 contrasting results due to the wide range of phytoplankton cell sizes and species-specific Chl *a* content per cell (Falkowski and Kiefer, 1985; Kruskopf and Flynn, 2005). In this study this is clearly demonstrated by the higher phytoplankton average cell count in June in comparison to April, while the average fluorescence is higher in the latter (supplementary material; Fig. S1). This can be explained by the high relative abundance of pico-phytoplankton, which contributes little to total fluorescence.

10 Both the FRRf and FCM provide significant predictors of HPLC-derived Chl *a* concentration (Fig. 2). When performing an ANCOVA with month as factorial predictor, natural logarithm transformations were necessary because of the highly unequal variances between months. The ANCOVA with the FRRf-derived F_0 as Chl *a* predictor revealed that Chl *a* concentrations significantly differed per month ($p < 0.01$) but not the slope, and that F_0 was a significant predictor ($p < 0.01$) of Chl *a* concentration (adjusted $R^2 = 0.66$). Yet, the FCM estimate of Chl *a* concentration (TFLR) was a better predictor ($p < 0.01$) with
15 an adjusted R^2 of 0.90. The ANCOVA with the FCM-derived TFLR as Chl *a* predictor resulted not only in a significant difference of the Chl *a* concentration per month ($p < 0.01$) but also in a significantly different slope ($p < 0.05$), suggesting that ~~abiotic factors and phytoplankton community composition are influencing the amount of fluorescence per Chl *a* molecule (Fig. 2). In April and August the slope is steeper in comparison to May and June. An explanation could be the package effect (Dubinsky et al., 1986), where stacking of Chl *a* at low light intensities causes a shading effect within the cells and a steeper slope of Chl *a* concentration with *in vivo* fluorescence. Because there is a lack of agreement in photophysiological parameters between April and August, it is likely that the months do not have the same drivers for the steeper slope. In April the high σ_{PSII} coincides with high n_{PSII} , suggesting that although the chlorophyll self-shades it does not result in a lower absorption cross section because of the high amount of RCII in relation to Chl *a* molecules. In contrast, in August the phytoplankton community is nutrient limited and has a higher σ_{PSII} , in correspondence with results obtained by Kolber et al. (1988) who observed that
20 nutrient limitation increases σ_{PSII} . Self shading in this month is more likely a result of smaller cell size as indicated by the higher abundance of picoplankton (Table 3; Geider et al., 1986) other predictors that differ per month are influencing the amount of fluorescence per Chl *a* molecule (Fig. 2).~~

~~The~~ Chl *a* concentration is a limited predictor of biomass because the Chl *a* concentration per cell is species-specific and subject
30 ~~to phenotypic acclimation to abiotic conditions (Falkowski and Kiefer, 1985; Kruskopf and Flynn, 2005). Therefore, the FRRf yields other biomass related proxies next to the minimum fluorescence; that allow for circumvention of the use of chlorophyll *a* to estimate primary productivity (Oxborough et al., 2012). These parameters are~~ the total absorption coefficient in the water (a_{LIII} in m^{-1}) based on the absorption of the photosynthetic pigments associated with PSII and the amount of PSII reaction centres per volume ($[RCII]$ in $nmol RCII m^{-3}$). Both are very strongly correlated to F_0 . ~~The, although the~~ ratio of RCII

to a_{LIII} can vary by nature, affecting n_{PSII} . However, these three biomass-related proxies show a perfect relationship to each other (Supplementary material). The minimum fluorescence measured with the FRRf (F_0) is related to the red fluorescence measured with the FCM (TFLR; $r=0.7$). Interestingly, TFLR and F_0 are not correlated to total orange fluorescence, which indicates that the cyanobacterial picoplankton is not a fixed proportion of the total phytoplankton biomass (Supplementary material); Fig. S3).

A pairplot analysis of the combined data of all cruises shows that some photosynthetic parameters are highly correlated (Supplementary material). The correlation of α and F_v/F_m , indicators for photosynthetic affinity and photosynthetic efficiency, are perfectly correlated ($r=1$). The parameters derived from the PE curve also show high correlation, being dependent on the light acclimation state of the phytoplankton trends in the maximum electron transport rate (P_{max}) and the light saturation parameter (E_k) are similar. Surprisingly, α does not show any correlation with E_k , suggesting that the light affinity is not dependent on the level of irradiance where the PSII reaction centres become saturated, or that its value is also affected by nutrient limitation, obscuring a relationship with E_k . The effective absorption cross-section per photosystem, σ_{PSII} , is very strongly negatively related to n_{PSII} ($r=-0.9$). This is to be expected; the larger n_{PSII} , the smaller the number of pigment molecules associated with it.

Community composition is variable over the months with the biggest shift in community composition between May and June (Fig. 3). In May mean F_v/F_m is low (0.26 ± 0.09), suggesting physiological stress (Table 3). This coincides with a shift of nutrient sufficiency in the largest part of the sample region (with only potentially limiting conditions in the most southerly part of the Dutch North Sea and further offshore) in April to a larger region of nutrient limitation in May. In June the mean F_v/F_m recovers and community composition changes. Both groups of picophytoplankton (*Synechococcus* and total) increase in relative abundance between May and June, while the nanophytoplankton shows a strong decrease (Fig. 3). Because the picophytoplankton fraction makes up for only a small part of the biomass, the microphytoplankton is the largest contributor to red fluorescence in June, although this group does not increase in relative abundance in comparison to May. After June the microplankton disappears, leaving 80% of the average community composition to picoplankton. The shift to smaller cell sizes at nutrient limiting conditions is not surprising because of the higher nutrient affinity of smaller cells.

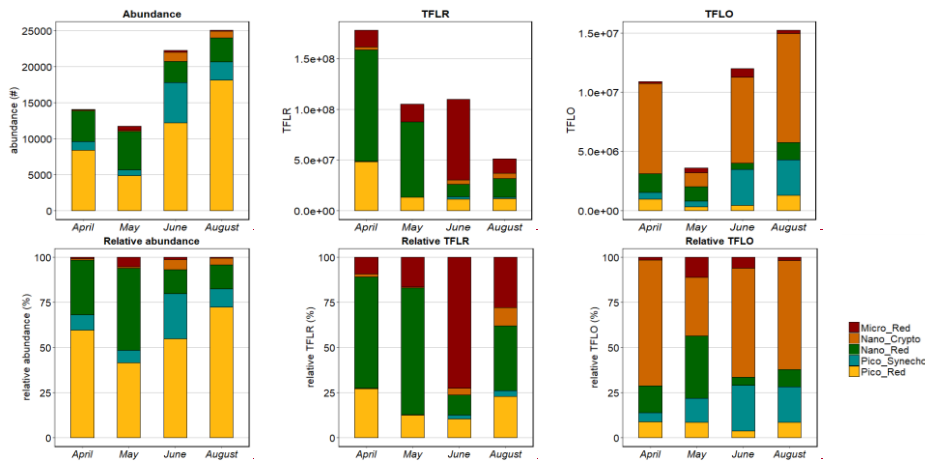


Figure 3: Phytoplankton abundance per phytoplankton group distinguished with the flowcytometer, shown as average (relative) abundance per month (left), total red fluorescence (middle) and total orange fluorescence (TFLO; right). The upper graphs are absolute and lower graphs relative.

5

3.3 Spatial distributions

Both the biomass concentration and the phytoplankton community composition, expressed as percentage of the total cell numbers, showed a dynamic picture (Fig. 4). In all cases, microphytoplankton < 10% of the total cell counts, although in terms of biomass they sometimes dominate (Fig. 3).

10

In April, high biomass concentrations (using TFLR) are observed close to the Dutch Delta in the South of the Dutch EEZ and west to the island of Texel and Vlieland. Very low concentrations are found offshore, especially in the more central part towards the Doggersbank area. The north-western wedge of the Dutch North Sea was
3.3 Phytoplankton community composition

15

Both cell numbers and the phytoplankton community composition showed high spatial heterogeneity in the Dutch North Sea in the sampled months (Fig. 3). In cell numbers, the pico-red group was always present as the dominating group. Because of their low total biovolume, they were contributing less to total red fluorescence. The relative abundance of picophytoplankton was generally higher offshore and in the northern part of the Dutch North Sea. The pico-Synechococcus group showed a strong numerical presence offshore in April and in most of the Dutch North Sea in June. The nano-red group was often a dominant group, both in sense of cell numbers as contribution to total red fluorescence. The nano-cryptophytes were never abundant in cell numbers, but contributed to the total red fluorescence in the northern offshore regions. The microphytoplankton group had

20

a low numerical abundance and represented always less than 10% of the total cell counts. Yet in terms of red fluorescence they sometimes dominate, which occurred most frequently in coastal regions (Fig. 3).

In April the northern part of the Dutch North Sea was numerically dominated by picoplankton whereas the southern part and the north coastal area of the Dutch EEZ were numerically dominated by nanophytoplankton. Orange fluorescent dominating species (like The taxons with high phycoerythrin content (*Synechococcus* and Cryptophyceae) were made up only a small proportion of the total phytoplankton community in April (generally less than 10%), however about 100 km% and were most abundant in the norther part of the Dutch North of the island of Vlieland there was a patch of water where they seem to dominate the phytoplankton Sea (Fig. 4e). Microphytoplankton abundance < 3%, and highest numbers were found close to the Dutch Delta and along the Noordwijk transect. In April, the lowest F_w/F_m values (0.4-0.5) were found in the southern part of the Dutch EEZ. Highest values were found offshore on and towards the Terschelling transect, and at the coastal stations of the Noordwijk transect.

The situation in May is different from April (Fig. 4, second column). The higher biomass near the Texel and Delta area has mainly disappeared, and is much more homogeneously distributed while the community composition is very heterogeneous. The biomass concentration is about 50% lower than in April (Table 2, Fig. 3). Unfortunately, the RV *Zirfaea* did not sail to the NW edge of the Dutch coastal zone (Dogger Bank), but the higher dominance of Orange fluorescent dominated species on the Terschelling transect observed in April is still visible in May (Fig. 4f). The phytoplankton community in May is different from April and occurs very patchy (Fig. 3, second column). Offshore Along the Walcheren transect and at a section of the Terschelling transect (~60-135 km off the coast) the highest percentages of picophytoplankton were observed (60-80%), whereas the highest percentage of nanophytoplankton was observed north of Terschelling 100 and closer to the Frisian coast. Notice that this coast was visited twice in 2 days, and that abundance varied between those occasions (40-60% vs. 60-80%), yet the difference between visits was only 6%; the first time around 64% and the second time around 58%. The two visits did fall into different diurnal time periods, the first time was at the end of the day (around 18:00h) while the second time was early morning (around 7:00h), but both of these time periods were in the flood tide. In May, F_w/F_m was in general much lower than in April (0.1-0.3) across most of the Dutch EEZ. Higher values were found in the southern coastal stations, a possible consequence of the outflow of the Scheldt River, and 70 km offshore Noordwijk. At both of these regions low values for F_w/F_m were found in April so possibly these phytoplankton communities have already acclimated to low nutrient conditions. The range in σ_{PSII} was larger in May in comparison to April. A small area near the coast of Noordwijk showed low σ_{PSII} values. This might reflect Rhine River waters, but the effect was not noticeable further north in the coastal zone. Between May and June the community composition shifted and phytoplankton cell numbers increased. Both groups of pico-phytoplankton (*Synechococcus* and Pico-red) increase in relative abundance between May and June, while the nano-phytoplankton shows a strong decrease (Fig. 3). Highest abundance of pico-phytoplankton was observed offshore. The microphytoplankton is the largest contributor to red fluorescence in the coastal region, although this group does not increase in relative abundance in

comparison to May (Fig. 3). In August the pico-phytoplankton was dominating the phytoplankton communities with an average contribution to total cell numbers of over 80% and only slightly lower values were observed (but still > 70%) along the southern Dutch coast, where the abundance of nano-phytoplankton was higher. Micro-phytoplankton was hardly observed, but because of their high red fluorescence they contributed to total red fluorescence in coastal regions.

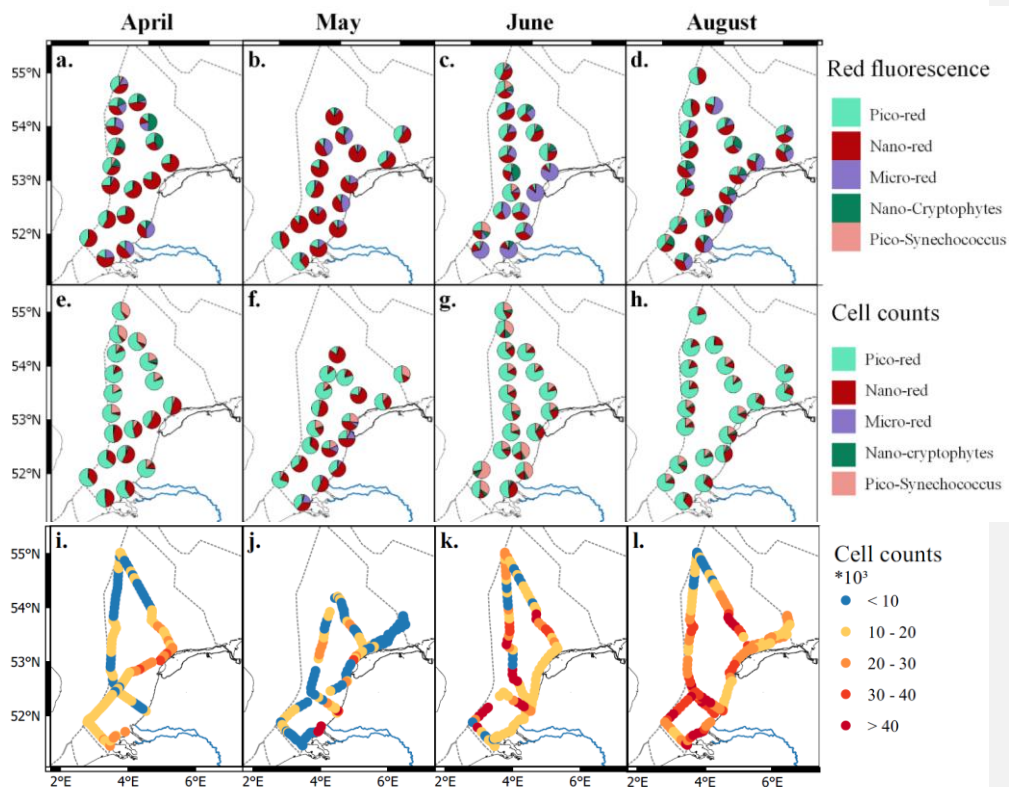


Figure 3: Relative phytoplankton community composition using FCM-derived total red fluorescence (first row: a-d) and cell numbers (second row, e-h) in April, May, June and August (from left to right). The groups are clustered according to table 2.

3.4 Photophysiology

Photosynthetic parameters are sometimes highly correlated (Supplementary material; Fig. S3). The correlation of α and F_v/F_m , indicators for photosynthetic affinity and photosynthetic efficiency, were, as expected, perfectly correlated ($r=1$). The parameters derived from the PE-curve, P_{max} and E_k , show high correlation. But surprisingly, α does not show any correlation with E_k . This suggests that the light affinity is not dependent on the level of irradiance where the PSII reaction centres become saturated, or that its value is obscured by nutrient limitation. As expected σ_{PSII} is very strongly negatively related to n_{PSII} ($r=-0.9$); the larger n_{PSII} , the smaller the number of pigment molecules associated with it.

In April, the photophysiology of the phytoplankton communities in the Dutch North Sea showed low variability. The F_v/F_m values stayed above 0.5 in northern regions and above 0.4 in southern regions (Fig. 4a). The σ_{PSII} stayed in a narrow range between 2.5-4 $\text{nm}^2 \text{PSII}^{-1}$ (Fig. 4e). E_k in April showed more variability in comparison to the F_v/F_m and σ_{PSII} , without clear spatial patterns in offshore regions. In the coastal zone, the E_k is lower off the coast from Walcheren and higher off the coast from Noordwijk (Fig. 4i).

In May photophysiological parameters of the phytoplankton communities in the Dutch North Sea were strongly heterogeneous with only smaller scale spatial patterns (Fig. 4b,f,j). F_v/F_m was in general much lower in May (0.1-0.5) than in April (>0.4) across most of the Dutch EEZ (Fig. 4b). The range in σ_{PSII} was larger in May in comparison to April (Fig. 4f). The σ_{PSII} was also higher across the Dutch North Sea, except from a small area near the coast of Noordwijk. A possible consequence of the outflow of the Rhine River. In the same region the E_k is high ($> 450 \mu\text{mol photons m}^{-2} \text{s}^{-1}$), but in other regions where E_k is high this does not coincide with an increased σ_{PSII} . The E_k across the Dutch North Sea in May is heterogeneous without large-scale spatial patterns.

In June the photophysiology of the phytoplankton in the Dutch North Sea is still as heterogeneous as in May, but larger scale spatial patterns seem to occur. The F_v/F_m values recovered to above 0.4 in the coastal zone, but not in offshore regions in the Southern North Sea. The F_v/F_m of the southern offshore phytoplankton, between Walcheren 70 and Noordwijk 70 (Fig. 1), remained lowest (<0.2 ; Fig. 4c). The σ_{PSII} was lower than in May, apart from the southern offshore region that remained higher (Fig. 4g). In a small region around Noordwijk 70 the phytoplankton community had a particularly low σ_{PSII} ($<2.5 \text{ nm}^2 \text{PSII}^{-1}$) which did not present itself in anomalies in the other photophysiological parameters. The E_k in May was low in the Northern coastal zone and higher in offshore regions (Fig. 4k).

In August the F_v/F_m recovered across the Dutch North Sea (Fig. 4d). The σ_{PSII} was high in northern offshore region, and comparable to June in the rest of the Dutch North Sea (Fig. 4h). The E_k shows some interesting variability in August. The regions off the Noordwijk coast and the of the Wadden Island coast were sampled twice, on two different times. These double

measurements resulted in strongly different E_k , suggesting that time is a more important predictor in comparison to spatial variability.

To further investigate possible daily patterns we calculated standardized daily anomalies (z-scores). These show a clear diurnal trend in photosynthetic activity (Fig. 5). F_v/F_m is lowest during the middle of the day, while E_k , σ_{PSII} and $1/\tau$ peak during the day. As E_k is strongly correlated to P_{max} (Fig. S3); a clear diurnal pattern is also present in the photosynthetic electron transport rate.

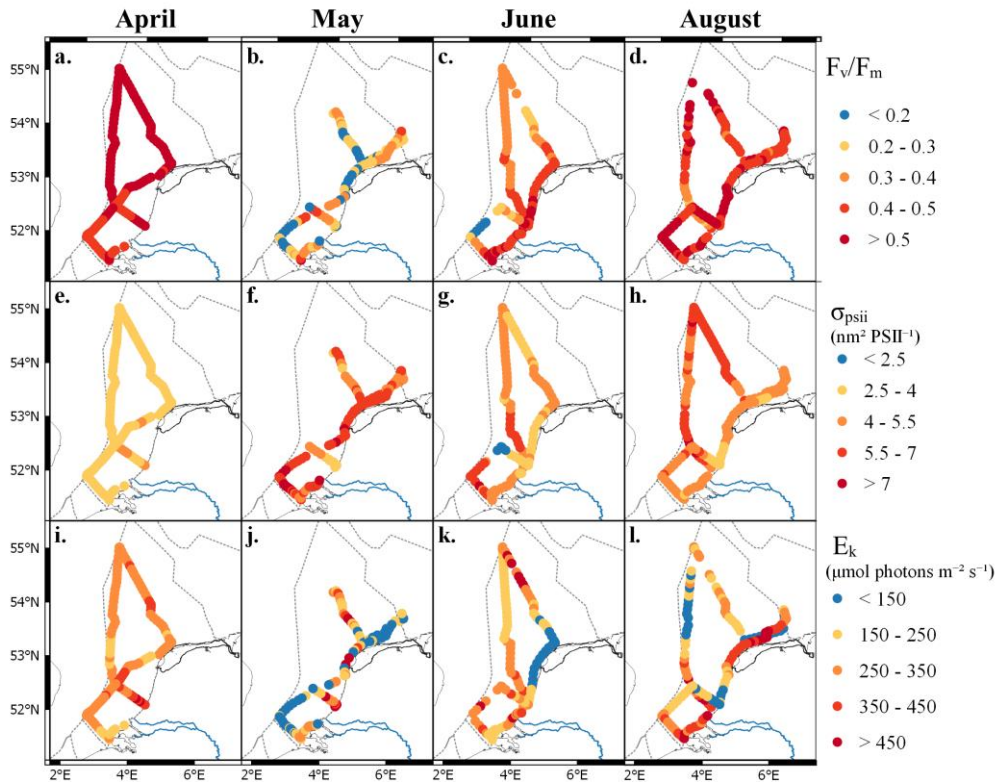


Figure 4: Maps of the photophysiological parameters F_v/F_m (a-d), σ_{PSII} (e-h; in $\text{nm}^2 \text{PSII}^{-1}$) and E_k (i-l; in $\mu\text{mol photons m}^{-2} \text{s}^{-1}$) per month (from left to right: April, May, June and August). For more details on the location see Fig. 1.

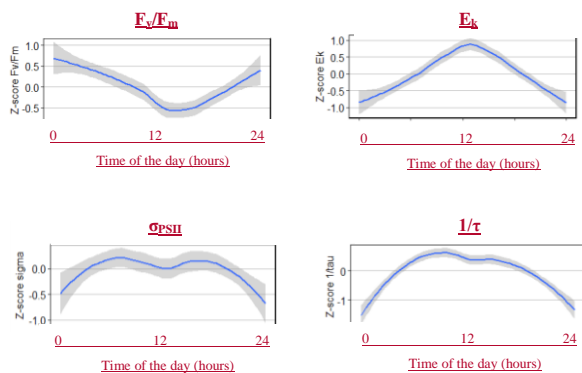


Figure 5: Standardized daily anomalies (z-scores) of F_v/F_m , E_k , σ_{PI} and $1/\tau$ showing the diurnal trends in photophysiological data. On the x-axis the time of the day and on the y-axis the z-score.

3.5 Gross primary productivity

Gross primary productivity ranged from minimum $0.35 \mu\text{g C L}^{-1} \text{h}^{-1}$ in June to peak productivities of $602 \mu\text{g C L}^{-1} \text{h}^{-1}$ in the coastal zone in May (Fig. 6). The average GPP was highest in April and lowest in August. Monthly averages ranged from $116 \pm 59 \mu\text{g C L}^{-1} \text{h}^{-1}$ in April and $8.7 \pm 8.3 \mu\text{g C L}^{-1} \text{h}^{-1}$ in August, although these averages are not completely comparable due to different ship routes per month (Fig. 6). In April spatial heterogeneity in GPP was low. Highest rates in April were measured offshore ($> 250 \mu\text{g C L}^{-1} \text{h}^{-1}$) and in the coastal regions close to the Wadden Islands (Terschelling 10 in Fig. 1). In May, the GPP is heterogeneous without clear spatial pattern. Most production rates stay below $30 \mu\text{g C L}^{-1} \text{h}^{-1}$, with local GPP peak rates over $600 \mu\text{g C L}^{-1} \text{h}^{-1}$ in the southern coastal zone. In June the Dutch North Sea was on average lower than in May, and showed slightly more large-scale spatial patterning. Highest values in June were observed ($30\text{-}40 \mu\text{g C L}^{-1} \text{h}^{-1}$) northwest of Noordwijk. In August GPP was low throughout the Dutch North Sea with the majority of water-column productivity rates staying below $10 \mu\text{g C L}^{-1} \text{h}^{-1}$. In the southern coastal zone slightly higher rates were found, reaching up to $50 \mu\text{g C L}^{-1} \text{h}^{-1}$.

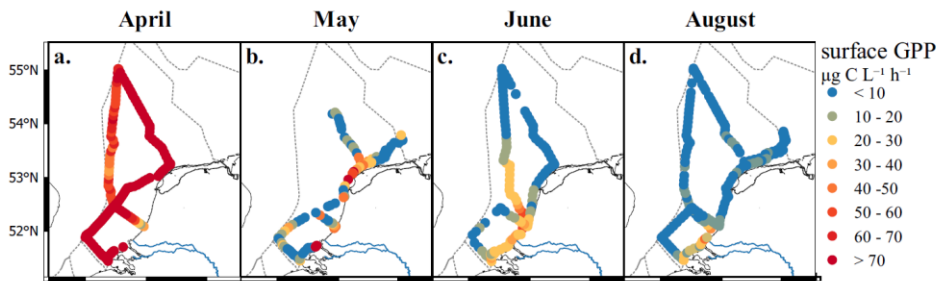
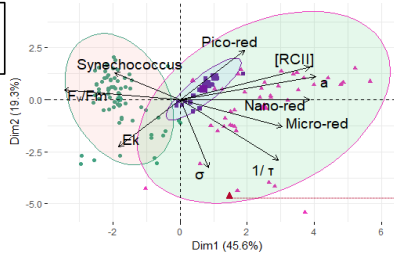
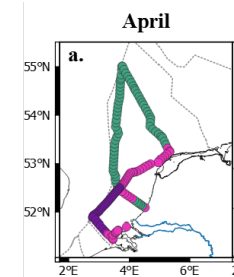
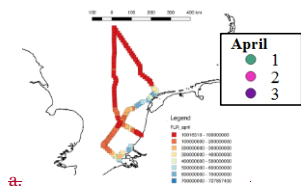


Figure 6: Gross primary productivity of the surface (a-d; in $\mu\text{g C L}^{-1} \text{h}^{-1}$) per month (from left to right: April, May, June and August). Colors represent rates, where blue is low and red is high (see legend).

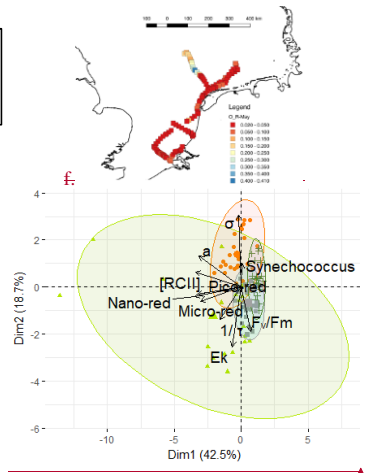
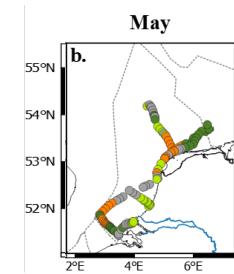
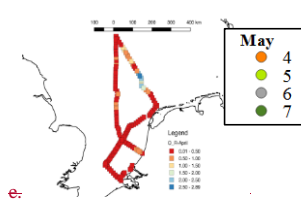
5 **3.5 Spatial clustering**

Strong collinearity between measured parameters was present. For spatial clustering these were removed based on the variable inflation factor ($\text{VIF} > 6$; see supplementary material for pairplots), which resulted in removal of the photophysiological parameters P_{max} , α , a_{LHII} , n_{PSII} , the FCM-parameter of the total red fluorescence and the GPP. From the five defined phytoplankton groups (Table 2), the nano-crypto group was not used in the clustering because of collinearity ($\text{VIF} > 6$). The remaining variables were the abundance of the remaining four FCM-defined phytoplankton groups (Pico-Red, Pico-Synecho, Nano-Red and Micro-Red), the total O/R ratio and five photophysiological parameters (F_v/F_m , σ_{PSII} , $1/\tau$, $[\text{RCII}]$, and E_k). For an overview of the collinearity between variables see the pairplots in the supplementary material.

Spectral cluster analysis resulted in identification of two to four clusters in each cruise. Most of these clusters were spatially separated and can therefore be seen as regions with distinct phytoplankton communities (Fig. 7). In April the clustering resulted in three clusters with a clear spatial pattern. In the PCA the variables that contributed most to the first principal component were all biomass related: $[\text{RCII}]$ and a_{LHII} , related to the photosynthetic capacity per reaction center and per volume, and the abundance of the Nano-red group. The second principal component has photosynthetic parameters as two main contributors



	PC1	PC2
σ_{psII}	0.8	28.8
F_w/F_m	13.7	0.6
a_{440}	18.7	3.4
[RCII]	17.1	6.6
$1/\tau$	9.8	22.7
E_k	3.9	13.8
Pico-red	4.2	15.1
Nano-red	16.9	0.0
Micro-red	10.5	4.5
Synechococcus	4.3	4.4
Variance explained (%)	45.6	19.3



	PC1	PC2
σ_{psII}	0.1	36.7
F_w/F_m	0.8	14.5
a_{440}	17.5	6.7
[RCII]	20.4	1.6
$1/\tau$	4.4	7.5
E_k	0.7	26.3
Pico-red	18.5	0.4
Nano-red	21.1	0.6
Micro-red	16.4	1.4
Synechococcus	0.0	4.3
Variance explained (%)	42.5	18.9

Formatted Table

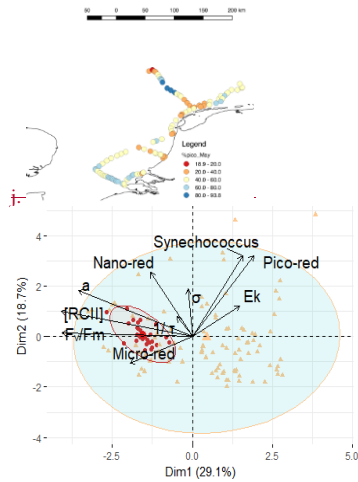
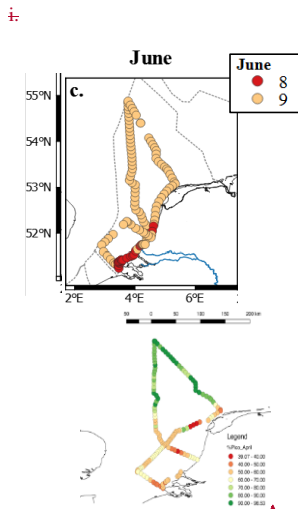
Formatted: Font: 9 pt, Font color: Black, German (Germany)

Formatted: Centered, Tab stops: 6,86 cm, Left

Formatted: Centered

Formatted: Font: 9 pt, Font color: Black, German (Germany)

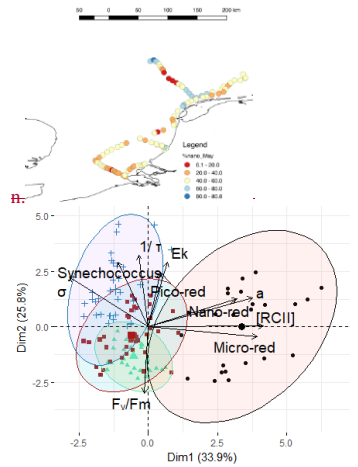
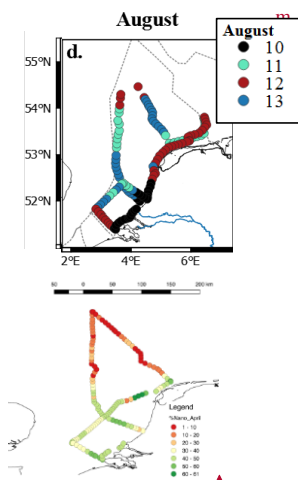
Formatted: English (United Kingdom)



	PC1	PC2
σ_{psII}	0.0	9.3
F_v/F_m	27.6	0.1
α_{III}	20.9	8.7
[RCII]	28.0	2.6
I/τ	0.4	1.7
E_k	3.7	3.9
Pico-red	6.1	26.9
Nano-red	2.9	16.9
Micro-red	6.3	2.9
Synechococcus	4.2	27.0
Variance explained (%)	29.1	18.7

Formatted: Font: 9 pt, German (Germany)

Formatted: English (United Kingdom)



	PC1	PC2
σ_{psII}	12.1	9.9
F_v/F_m	0.0	17.5
α_{III}	21.0	3.3
[RCII]	25.8	0.0
I/τ	0.2	20.6
E_k	0.7	16.8
Pico-red	0.3	11.8
Nano-red	15.3	3.1
Micro-red	22.9	0.4
Synechococcus	1.8	16.7
Variance explained (%)	33.9	25.7

Formatted: Font: 9 pt, German (Germany)

Formatted: English (United Kingdom)

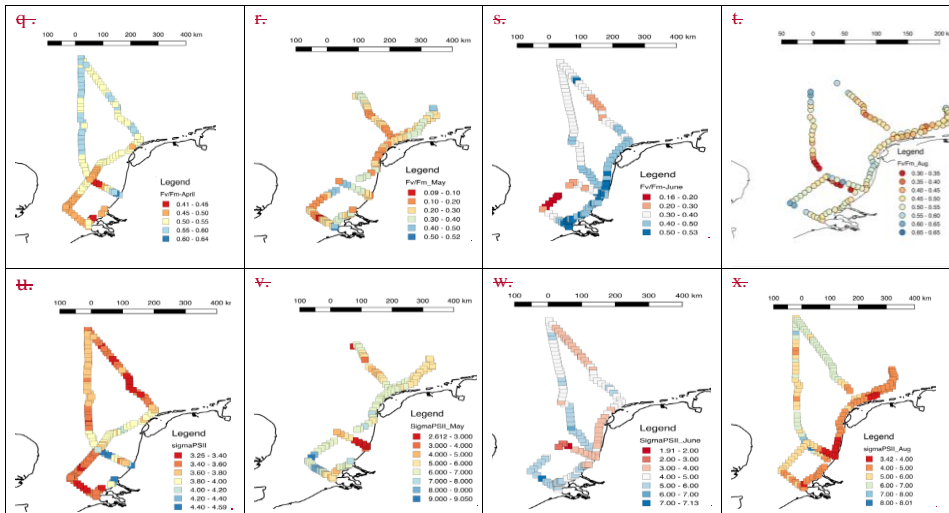


Figure 4: Phytoplankton biomass using FCM-derived total red fluorescence (first row, a-d), O/R ratio (second row, e-h), percentage pico (third row, i-l) and percentage nano (fourth row, m-p), F_v/F_m (fifth row, q-t) and σ_{PSII} (sixth row, u-x) in April 2017 (left panels), May 2017 (middle left panels), June 2017 (middle right panels) and August 2017 (right panels). Please note the different scaling, which was necessary to optimally visualize spatial heterogeneity.

5

June showed an increase in phytoplankton abundance, although the community changed toward less nanoplankton (Fig. 3). Highest biomass concentrations were found along the coast, along with highest nanophytoplankton proportional presence (Fig. 4, middle right panels). Highest abundance of picophytoplankton was observed more offshore, although near the Dogger Bank there was a decrease in picophytoplankton abundance. The total O/R ratio showed an increased abundance of Orange fluorescent dominating species in most of the offshore waters between 50 and 150 km, and a decrease in relative abundance near the Dogger bank area (Fig. 4, middle right panels). Microphytoplankton abundance was less than 8%, yet they represented the largest contributors to red fluorescence (Fig. 3). They show a somewhat patchy distribution along the coast and near the Dogger Bank. The F_v/F_m increased in comparison to May in the coastal region, but not in offshore regions in the Southern North-Sea (Fig. 4). **Figure 7: Overview of the spectral cluster analysis based on the non-collinear phytoplankton parameters (FCM: Pico-red, Nano-red, Micro-red, *Synechococcus*, FRRF: σ_{PSII} , F_v/F_m , chl_{III} , $1/\tau$, E_k) separated per month (top to bottom: April, May, June and August). With on the left clusters visualized on maps and in the middle the bi-plots of the PCA of the data with confidence ellipses per cluster (confidence 95%). In all graphics clusters are visualized by different colors as shown in the legend inset. Of the confidence ellipses the border lines (and not the fill) correspond to the clusters. In the bi-plot overlapping confidence ellipses suggest a high similarity between groups while the size of the ellipse is a measure of variability within the group. On the right the table of the PCA analysis with contribution in % of the different variables, in bold the three variables that contribute most to the principal component.**

10

15

20

(σ_{PSII} and $1/\tau$; 51.5%). Cluster one covers most of the Northern part of the Dutch North Sea, and a small part of the Noordwijk transect to the coast. The bi-plot of the PCA shows that the first cluster is negatively correlated to the main contributors of PC1

25

([RCII] and a_{LHH} ; Fig. 7), so this region consists a phytoplankton community with lower photosynthetic capacity per bulk and per volume. The coastal region is separated in two clusters, 2 and 3, with overlapping confidences ellipses (Fig. 7). The confidence interval of cluster 2 is larger than cluster 3, suggesting that the phytoplankton community in cluster 2 is more heterogeneous. Both clusters are positively correlated to the main contributors to PC1 ([RCII] and a_{LHH}), meaning this clusters consists of a community with higher photosynthetic capacity per volume.

In May the cluster analysis resulted in four different clusters, but without well-defined spatial pattern. The PCA biplots show that the confidence interval of cluster 5 overlaps most of the other clusters, indicating that this clusters has a weak support. E_k is negatively correlated with cluster 4 and σ_{PSII} , suggesting that cluster 4 contains low light acclimated algae. In contrast, in June only two clusters were found with a \Rightarrow

~~In August the increase in phytoplankton abundance observed in front of the Dutch Delta in June was still visible, but more northerly, the biomass seemed to decrease again (Fig. 4e). Unfortunately no data are available for July to check whether this community displaced northward over time. The picophytoplankton was present at highest abundance (>80%) and only slightly lower values were observed (but still >70%) along the southern Dutch coast, where the abundance of nanophytoplankton was higher. Microphytoplankton was hardly observed, only a small patch (2-3.5%) was observed near the coast of the province of North Holland. The effective absorption cross section was low in the coastal zone in comparison with offshore regions (Fig. 4x).~~

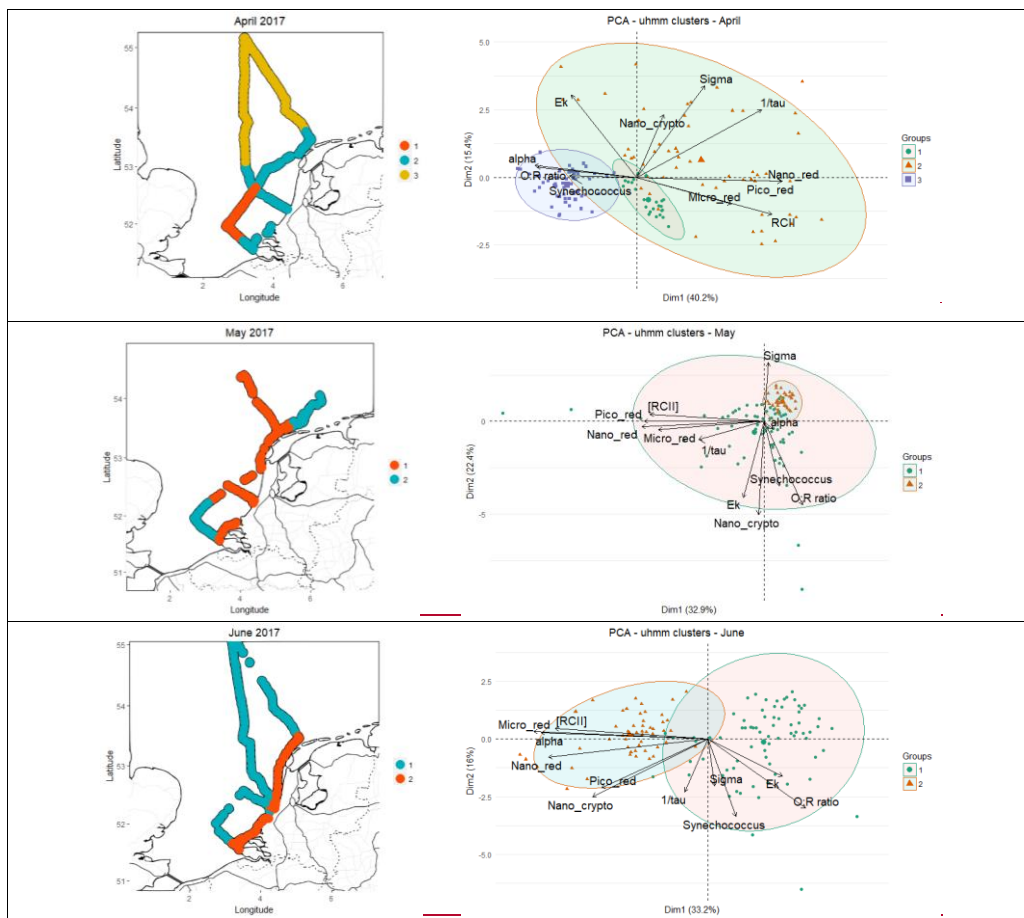
3.4 Spatial clustering

Spatial clustering (uHMM) of photophysiological characteristics and phytoplankton community composition was performed to get an overview of spatial heterogeneity and the variability over the season (Fig. 5). Colinear variables were removed based on the variable inflation factors (VIF>6), which resulted in removal of the photophysiological parameters P_{max} , F_v/F_m , a_{LHH} , α_{PSII} , and the FCM parameter of the total red fluorescence. The five defined phytoplankton groups (Table 2) had a higher VIF than 6 (maximum 9.6), but were retained for the sake of completeness. The remaining variables were the five FCM defined phytoplankton groups (Table 2), the total O/R ratio and five photophysiological parameters ($1/\tau$, [RCII], σ_{PSII} , α and E_k). PCA analysis was performed to get an overview of the variables that explained most of the variation of the identified spatial clusters and to understand main drivers per region. The first two components of the PCA analyses explained 49.2% (June) to 59.7% (August) of the variance.

UHMM analysis resulted in identification of two to four spatial clusters, which were not uniform over the months. In April the most distinct phytoplankton community is found in the Northern part of the Dutch North Sea (Fig. 5). The biomass concentration in this region is low and the phytoplankton community characterized by a high O/R ratio and high photosynthetic

5 affinity (α). In April the whole coastal region is identified as the same spatial cluster, with high biomass concentration and a
variable phytoplankton community. A small region offshore (~70 km) in the Southern North Sea has a very uniform
phytoplankton community, which seems mainly consisting of microphytoplankton with a low light saturation level (E_k) and
low effective absorption cross section (σ_{psII}). In May and June, the phytoplankton community in the Dutch North Sea seems
quite uniform with only two distinct spatial clusters. In June these clusters are clearly divided in a coastal and an offshore
zone, while in May the clusters are spatially less well defined. The uniform phytoplankton community found in April in a
small region offshore (~70 km) in the Southern North Sea remains present but in May a similar community is found in the
eastern coastal region. Unfortunately, this region was not sampled in April. This spatial cluster is still very uniform, but not
with distinct drivers in comparison with the other spatial cluster. It seems mainly typified by a high effective absorption cross
10 section and low biomass and low O/R ratio. In June a distinct separation between coastal and offshore phytoplankton
communities is present. The PCA shows that the offshore phytoplankton community is consisting of a diverse phytoplankton
community while the coastal phytoplankton community is consisting of mainly micro phytoplankton with low light saturation
level high F_v/F_m and high photosynthetic affinity (α).

15 at III and RCII. The four clusters identified in August was the most heterogeneous month are spatially separated, but with four
different phytoplankton communities some complications (Fig. 5). The first phytoplankton community, which covers the most
Northern most part of the Dutch North Sea and the coastal region of the Northern part of the Netherlands and the offshore
region of Noordwijk, were characterized by high effective absorption cross section and rate of reopening of closed RCII's ($1/\tau$).
The second phytoplankton community is corresponding to the southern coastal regions, a region with high freshwater influx,
20 and is positively associated with most phytoplankton groups and the amount of RCII's per volume. The third phytoplankton
community is characterized by low light saturation level and high photosynthetic efficiency and low rate of reopening of closed
RCII's ($1/\tau$). Finally, the fourth spatial cluster was also found in April and May; in August it is a more a variable group of
phytoplankton and the northern coastal region expands more to the south. Different spatial clusters were appointed to the
same region visited within a two-day time span twice; in the north-eastern northeastern coastal region and at the transect of
25 Noordwijk. Both times, the third cluster 11 is one of the overlapping spatial clusters. The third cluster Cluster 11 corresponds
to only night time sampling periods and is defined by low light saturation level E_k and low $1/\tau$, suggesting indicative
of a low light acclimated phytoplankton community. This suggests that this cluster 11 is more a temporal than cluster instead
of a spatial cluster.



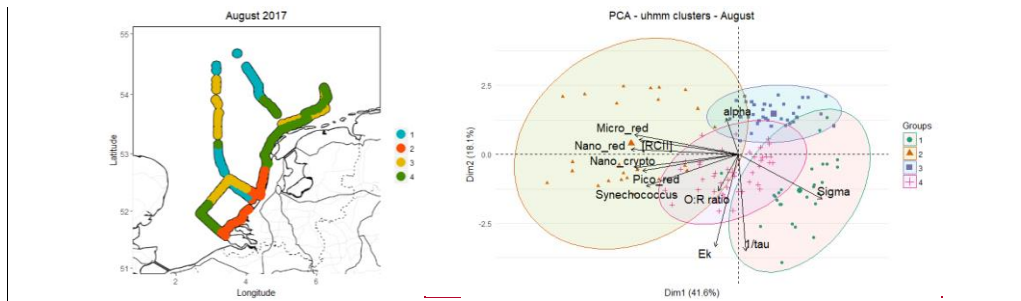


Figure 5: Maps separated per month of spatial clusters as August but only including the measurements performed within an 8 hour timeframe around noon (12:00±4h; see supplementary material Fig. S4). In this timeframe the southern coastal zone is distinct from the rest of the Dutch North Sea and corresponds to cluster 10 in the analysis of the complete dataset (Fig. 7d), so this cluster is defined by uHMM clustering (left) and a bi-plot of the PCA of the data (right) with as variables the FCM-based parameters O/R ratio and the total red fluorescence of the five described phytoplankton groups (Table 2) and non-colinear FRRF-parameters on photophysiology ($1/\tau$, [RCH], σ_{PSII} , α , E_k). In the bi-plot of the PCA colors represent assigned spatial clusters with confidence ellipses (confidence 95%). Overlapping confidence ellipses suggest a high similarity between groups while the size of the ellipse is a measure of spatial variability within the group.

In April the uHMM did not visualize the phytoplankton community with distinct O/R ratio north of Terschelling (Fig. 4e). Manual increase of the number of states in the spectral classification to four did not result. Cluster 12 and 13 are grouped together in a different spatial cluster at the aforementioned location (Fig. 6), but instead split up the coastal spatial cluster with a distinct community off the coast of Noordwijk and a small patch to the north-west. Forcing another spatial the 12±4h timeframe as cluster did result in a visualisation of the community with high O/R ratio north of Terschelling (Fig. 6), but Cluster 11 is not recognized as cluster this region with a more northern part of the transect and the coastal region of Noordwijk. These regions do also show a higher O/R ratio in the spatial map (Fig. 4e).

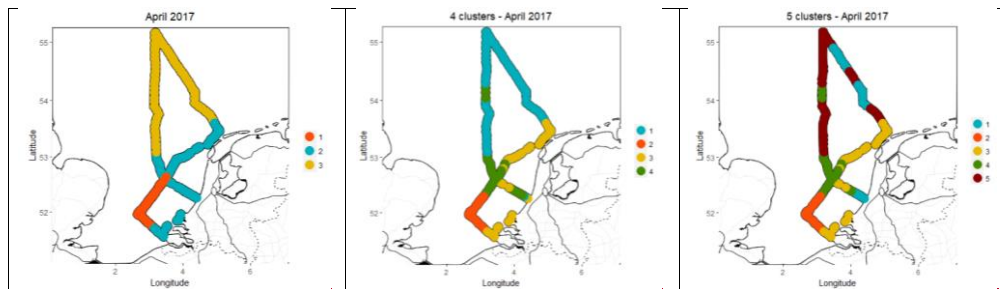


Figure 6: Maps of the cruise in April of spatial clusters as defined within the 12±4h timeframe, so seems indeed controlled by uHMM clustering, with automatic set number of states (left) and manually increasing the number of clusters to four (middle) and five (right).

Formatted: English (United States)

Cluster variables consisted of the FCM-based parameters O/R ratio and the total red fluorescence of the five described phytoplankton groups (Table 2) and non-colinear FRRF parameters on photophysiology ($1/\tau$, [RCH], σ_{PSII} , α , E_k).

5 3.5 PCA of the standard MWTL measuring points

The bi-plot of the PCA of the low resolution data combined for all months, shows that despite large differences in absolute values of abiotic and biological parameters (Table 3), the confidence ellipses are largely overlapping, suggesting the drivers of the different months are similar. The bi-plot further visualizes a negative relation between the nutrient concentrations (DIN, PO₄ and Si) and σ_{PSII} (Fig. 8) and, although σ_{PSII} can also depend on the species (Kolber et al., 1988; Suggett et al. 2009), it does not seem to associate with any of the floweytometer clusters. Furthermore, the TFLR of the picophytoplankton is negatively associated with the total and with the microphytoplankton part of the TFLR.

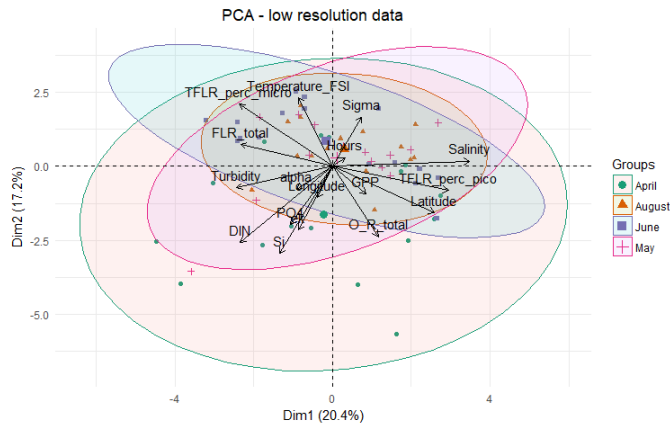


Figure 8: biplot of the PCA of the combined high and low resolution data (n=61) with as variables the FCM-based parameters (O/R ratio, TFLR and percentage of microphytoplankton and picophytoplankton to the TFLR), the non-colinear FRRF parameters ($1/\tau$, [RCH], σ_{PSII} , α , E_k), and abiotic data (DIN, PO₄, Si, salinity, Temperature, Turbidity) spatial data (Longitude, Latitude), time of the day (Hours) and the gross primary productivity (GPP). Colors represent different months with confidence ellipses (confidence 95%).

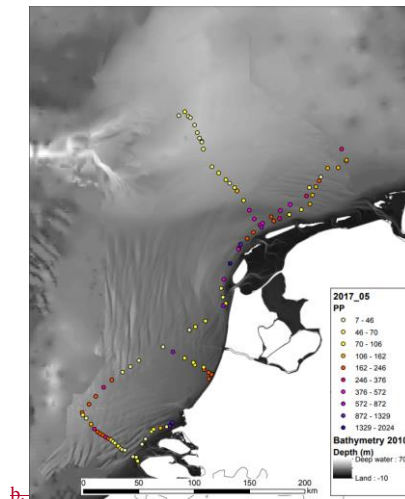
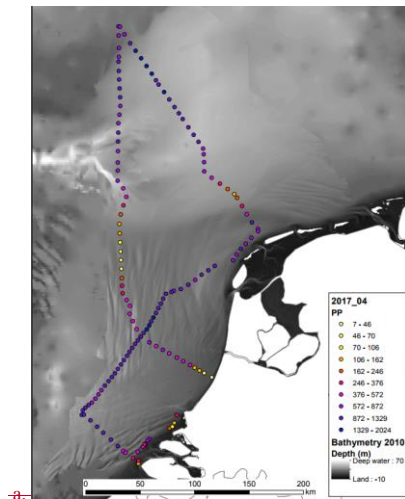
3.6 Water column integrated primary productivity

Water column integrated gross primary productivity (GPP) over the water column was calculated with high spatial and temporal resolution. Productivity ranged from minimum 7.5 mg C m⁻³ h⁻¹ (June) to maxima of 2024 mg C m⁻³ h⁻¹ in May. The

monthly average was highest in April ($781 \pm 409 \text{ mg C m}^{-2} \text{ h}^{-1}$) and lowest in August ($68 \pm 39 \text{ mg C m}^{-2} \text{ h}^{-1}$), although these averages are not completely comparable due to different ship routes per month (Fig. 4).

Figure 7 shows the spatial heterogeneity of gross primary productivity per month. April corresponds to the month with the highest biomass concentration and higher nutrient concentration in comparison to the other months, resulting in higher GPP.

In the coastal zone nutrients concentrations and turbidity are higher due to river water influx, but GPP in this region is lower. In April, phytoplankton populations were not nutrient limited in most areas which makes light availability a better predictor for primary productivity. In April offshore water column productivity shows quite some rather than spatial variability and it is higher in comparison to the coastal zone, likely due to a lower light attenuation in the offshore water column, while in the other months the opposite appears, confirming this hypothesis. GPP is highest offshore ($> 800 \text{ mg C m}^{-2} \text{ h}^{-1}$) along the 70 km line to west of Den Helder and high near the coastal Wadden Sea. In May spatial variability is limited with some very local high GPP values ($> 600 \text{ mg C m}^{-2} \text{ h}^{-1}$), but most values show production rates below $213 \text{ mg C m}^{-2} \text{ h}^{-1}$. In June the Dutch North Sea showed slightly more spatial variability, but GPP was lower than in May. Highest values in June were observed ($300\text{--}400 \text{ mg C m}^{-2} \text{ h}^{-1}$) northwest of Noordwijk, where in April the values were low. In August, a similar spatial distribution with low GPP is visible as in June with the majority of values below $100 \text{ mg C m}^{-2} \text{ h}^{-1}$. Yet, the GPP rates on the Terschelling transect were about twice as high as in June.



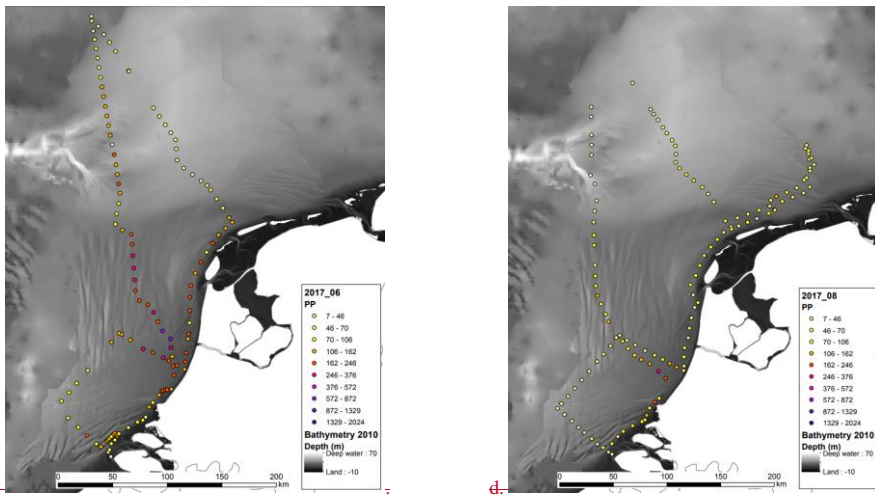


Figure 7: Water column integrated gross primary productivity ($\text{mg C m}^{-2} \text{h}^{-1}$) per month (a, April, b, May, c, June, d, August).

5 A stepwise multiple linear regression ($n=61$) for all months combined revealed that significant interactions included photophysiology (α), phytoplankton biomass (T) and abiotic predictors (Turbidity, DIN, time of the day and temperature). A log transformation of the GPP was necessary to correct for the heteroscedasticity of the data. Colinear predictors were removed before analysis ($VIF > 6$), which included F_v/F_m (collinear with α), E_k (collinear with P_{max}), σ_{PSII} (collinear with σ_{PSII}), $[RCH]$ and α_{LIII} (collinear with total red fluorescence). Statistically non-significant predictors included the percentage of micro or picoplankton, maximum rate of photosynthesis, silicate and phosphate concentration, effective absorption cross-section, salinity, the mean O/R ratio, and spatial predictors (latitude, longitude). Significant abiotic predictors included the quadratic of the time of the day (hours), turbidity, temperature and DIN (Table 4). Surprisingly, temperature and DIN concentrations are negatively correlated with the GPP, which could be a biased effect of not separating different months.

15 As shown above, variability in the data is related to the month (i.e. seasonal patterns) of sampling and the area sampled (i.e. to different abiotic and biotic factors). However, physiological activity can also be influenced by diurnal patterns, and we therefore investigated if our data show might be influenced by diurnal patterns in photosynthetic activity. This was done by calculating the z scores per day and plot these as a function of the diurnal time. The results show clear diurnal trends in photosynthetic activity (Fig. 9). P_{max} , E_k , σ_{PSII} and $1/\tau$ are all higher during the day than at night, while F_v/F_m and α are lowest in the early afternoon (Fig. 9).

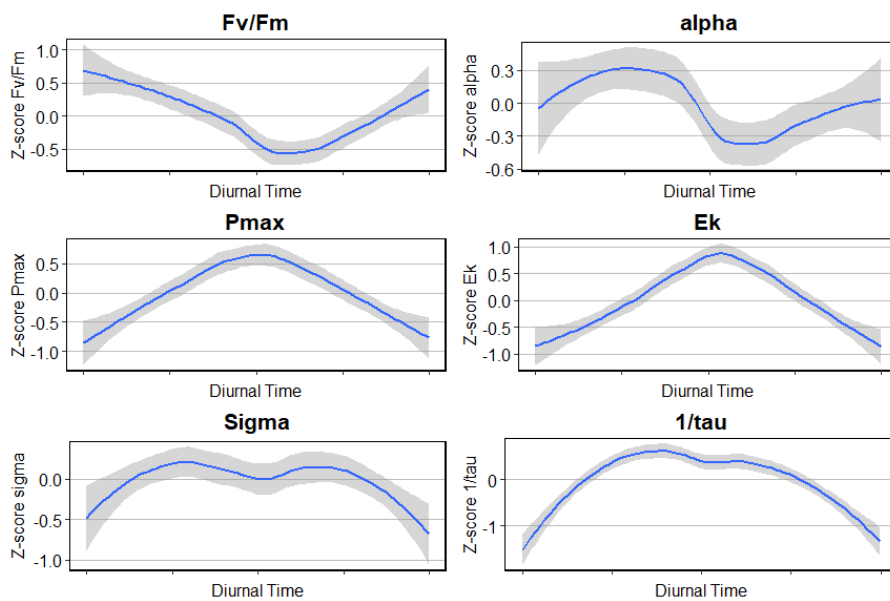


Figure 9: Diurnal trends in photophysiological data. Z-scores were calculated by subtracting the daily mean from the value and dividing by the standard deviation of that day. Partial days were excluded because this could potentially offset the daily mean and standard deviation and would therefore not give reliable results.

4 Discussion

This study examines the use of high resolution measurements to supplement low resolution monitoring. Multiple investigate spatial and seasonal patterns in photophysiological parameters and phytoplankton community composition with high spatial resolution. If successful, the method employed here can be further developed as novel monitoring method to improve existing monitoring programmes towards a more precise and ecosystemic ecological assessment (OSPAR, MSFD).

Previous studies found that the strong seasonal dynamics in the Dutch North Sea affect the spatial distribution and community composition of the phytoplankton community (Baretta-Bekker et al., 2009; Brandsma et al., 2011). The high resolution methods used in this study, the FRRf and FCM, were able to visualize this spatial and seasonal variability of the phytoplankton community in the Dutch North Sea in a supplementary way. The typical spring bloom was partly captured by the cruise of April: photophysiology was uniform and primary productivity high. Between April and May, the efficiency of PSII (F_v/F_m ; Fig. 4) decreased throughout the Dutch North Sea. A decreasing F_v/F_m is generally associated with limiting nutrient conditions. Spatial clustering may serve as an example of how to use multiple high-resolution or other abiotic stressors (Suggett et al., 2009b; Kolber et al. 1988; Kolber and Falkowski, 1993; Beardall et al. 2001; Ly et al. 2014), but can also reflect a change in community composition. Photophysiological parameters in a monitoring program. Lastly, the water column-integrated gross primary productivity of the Dutch North Sea is estimated and its main forcing factors are vary per taxonomic group: smaller taxa typically have lower F_v/F_m values and higher σ_{PSII} values (Kolber et al., 1988; Suggett et al., 2009b). No major shift in community composition was identified by flowcytometry between April and May. This suggests that an abiotic stressor, such as the nutrient limiting conditions in a large part of the Dutch North Sea, instead of the community composition was driving the decrease in efficiency of PSII. In contrast, the recovery of the F_v/F_m between May and June did coincide with a shift in community composition. In May the phytoplankton communities were mostly nanophytoplankton-dominated, while in June the communities were dominated by picophytoplankton (offshore) and microphytoplankton (coastal). So, although a recovery of the F_v/F_m can also occur as adaptation of the phytoplankton to nutrient limiting conditions (Kruskopf and Flynn, 2005), it seems that the shift in community composition was the major driver for the recovery of the F_v/F_m between May and June. These findings are a good example of how concurrent measurements by flowcytometry and fast repetition rate fluorometry can supplementary improve ecosystem understanding.

Environmental conditions in the Dutch North Sea are spatially heterogeneous and strongly influenced by seasonal dynamics. The timing of the phytoplankton bloom period corresponds well to the study of Baretta-Bekker et al. (2009) on phytoplankton dynamics in the Dutch North Sea from 1991 to 2005. In April we covered a phytoplankton bloom period, typified by high biomass concentrations, high quantum efficiencies and electron transport rates of PSII. The May cruise covered the collapse of the phytoplankton bloom period, as shown by the lower average quantum efficiency of PSII and high variability in biomass concentrations (Table 3). The cruises in June and August covered a low Chl- a period and a second late summer bloom period was not detected. Although a second bloom period is known to occur in some regions of the Dutch North Sea, an onset later than August is not unusual (Baretta-Bekker). The identification of only 5 distinct phytoplankton groups by flowcytometry has limited informative value. Yet, size distribution does affect the carrying capacity of the ecosystem, microphytoplankton are a food source for higher trophic levels than picophytoplankton. Picophytoplankton is part of the microbial food web, with less trophic efficiency and low contribution to carbon export (Azam et al., 1983; Finkel et al., 2010). The shift from nanophytoplankton-dominated communities in April to picophytoplankton-

Formatted: Font: Times New Roman

dominated communities in August, therefore implicates that over the season the trophic efficiency and carbon export decrease. To increase the informational value of the flowcytometry data beyond size, the FCM clusters would need to reflect taxonomic or functionally relevant groups. Interesting groups include calcifiers, silicifiers, DMS producers (such as *Phaeocystis*) or nitrogen fixers (le Quéré et al., 2005). The lack of identification of distinct clusters makes this so far impossible. Marrec et al. (2018) manually separate up to 10 phytoplankton groups from the data of the Cytosense flowcytometer. Yet, most of these groups still comprise many taxonomic genera and, apart from size, do not allow much for further interpretation of their role in the ecosystem or biogeochemical cycles. Also for detection of nuisance phytoplankton, distinct clusters of toxic species are lacking. Yet, toxicity in phytoplankton can differ even between strains within one species, so finding a distinct cluster by flowcytometry is problematic (Tillman and Rick, 2003). However, much of the information retrieved by the FCM is still unexplored; the clustering is performed on totals (area under the peak) instead of the entire pulse-shape. Identification of 'suspicious' clusters with potential toxic species could be helpful. These suspicious clusters can flag sampling points to be further inspected by a specialist using microscopy. Combination of flowcytometry with an Image-in-flow camera may open up the possibility to identify groups with more informative value.

Biomass might be one of the most important parameters to understand phytoplankton dynamics, but its direct measurement is not possible using high-resolution methods. Chlorophyll *a* concentration is often used as an estimate for biomass, although the Carbon:Chl *a* ratio is dependent on abiotic conditions and species-specific phenotypic plasticity (Flynn, 1991, 2005; Geider et al., 1997; Alvarez-Fernandez and Riegman, 2014; Halsey and Jones, 2015). In this study, chlorophyll concentrations were estimated by red fluorescence, which resulted in a good fit both using the FRRf (adjusted $R^2=0.66$) and FCM (adjusted $R^2=0.90$). Both the FRRf and the flowcytometer estimate the chlorophyll *a* concentration based upon the fluorescence in the red spectrum after excitation in the blue spectrum. There are some slight differences in the optics, the FRRf excites with a 450 nm LED and measures the fluorescence at 682 ± 30 nm, while the FCM excites at 488 nm and filters the red fluorescence over a longpass 650 nm filter towards the red fluorescence detector. The smaller detection range of the FRRf detector is optimized around the maximum emission of PSII and limits contamination by PSI (Franck et al., 2002; Oxborough et al., 2012). The second difference is the fluorescent state of the photosystems, the strong laser of the flowcytometer can only measure the maximum fluorescence (F_m), which is a parameter more prone to quenching than the minimum fluorescence measured by the FRRf. Yet, the biggest difference concerns the method; where the flowcytometer measures the fluorescence per particle, the FRRf does only a bulk measurement. In a bulk measurement other particles in solution scatter the excitation and emission photons, plus the emitted fluorescence of the phytoplankton is subject to reabsorption, especially at higher biomass densities. The latter seems to have the most impact on chlorophyll *a* concentrations, as the fit of the flowcytometer derived red fluorescence is a better fit than the FRRf minimum fluorescence. Other studies that use the FCM to estimate chlorophyll *a* concentrations also showed good relationships, but find better fits using the bulk measurements using a fluorimeter (Thyssen et al., 2015; Marrec et al., 2018). An alternative to the controversial use of chlorophyll *a* as estimation for biomass is the biomass estimation from cell abundances. Although this requires assumptions on cell shape and a constant C content per

biovolume (Tarran et al., 2006). Yet another alternative to explore is to estimate biovolume based on scattering properties of the cell using a pulse shape recording flowcytometer. This relationship appears to be taxon specific (Rijkeboer, pers. comm.) and needs to be further explored by comparison of calculated biovolume (based on the Image in Flow pictures) and the flowcytometric properties of the cell.

5 Phytoplankton biomass does not necessarily reflect primary productivity, as high grazing pressure can keep biomass low while production is high. This is clearly visualized by the lack of resemblance between patterns in cell numbers (Fig. 3 a-d) and gross primary productivity (Fig. 6). The reliability of variable fluorescence as estimate of ~~et al., 2008~~. Generally, pico-autotrophs contributed considerably to cell numbers but covered only a small fraction of the total biomass (Fig. 3). As nutrient limitation progressed from April to August, the relative abundance of picoplankton reached over 80%, which corresponded to less than 30% of the relative fluorescence. In June and August the molar nutrient N:P ratios were generally below the Redfield ratio and concentrations were in the limiting range, suggesting that phytoplankton populations were N-limited in a large part of the Dutch North Sea. This impacts the community composition: generally it is assumed that nutrient limitation favours small cell size, because of the higher surface to volume ratio of smaller cells, and that fluctuating nutrient concentrations favour larger cells due to their greater maximum uptake rate and storage capacity (Stolte and Riegman, 1995; Giannini and Ciotti, 2016; Philippart et al., 2000), and the shift towards smaller species observed by us using FCM is thus in accordance with this theory. The change in community composition over the season has implications for the whole ecosystem, because microphytoplankton is a better food source for higher trophic levels than picophytoplankton, which is more involved in the microbial food web, with less trophic efficiency and low contribution to carbon export (Quere et al., 2005). Nutrient limitation does not only affect community cell size but also low values of F_v/F_m are often related to nutrient limitation (Kolber et al. 1988, Kolber and Falkowski 1993, Beardall et al. 2001, Ly et al. 2014), although this is not always the case, and it seems likely that after acclimation to limiting nutrient conditions F_v/F_m can recover again as was seen in the current study in June (see also Kruskopf and Flynn, 2006). The σ_{psII} was negatively associated with DIN and turbidity in the PCA on the low resolution data (Fig. 8), and although this value is assumed to vary per taxonomic group, it is not associated with any floweytometer group (Kolber et al., 1988; Suggett et al., 2009), hence most of the variability seems to be driven by light and nutrient conditions. The values for the effective absorption cross section are slightly lower but in similar range to other studies (Suggett et al., 2009).

30 The gross primary productivity as found in the current study was both spatially and temporally variable. Average surface productivity of $44 \pm 64 \mu\text{g C L}^{-1}\text{h}^{-1}$ and peak primary productivity in April and lower values the rest of the year is in agreement with earlier studies in the North Sea coastal zone (is depending on many cell processes from the photon absorbance to carbon assimilation. The variable fluorescence reflects the first step of photosynthesis; the efficiency of which photons are captured and electrons produced and transferred. However, to ~~Brandema et al., 2011~~). To interpret water column integrated gross primary productivity in an ecological or biogeochemical meaningful way, the FRR units of electrons per unit

Formatted: Font: Times New Roman

Formatted: Font: Times New Roman

Formatted: Font: Times New Roman

time ~~were~~ need to be converted to carbon units. Gross photosynthesis correlates well with photosynthetic oxygen evolution (Suggett et al., 2003), and multiple studies have shown good correlation between ¹⁴C-derived estimates of primary productivity and FRRF-derived estimates using a constant conversion factor (Melrose et al., 2006; Kromkamp et al., ~~2005~~, 2008). ~~In~~ However, in reality this ~~study~~ parameter is not a constant, as along ~~the estimate of 6 moles electrons per mole pathway~~ from electron to carbon atom ~~was used, based on a study in the same biogeographic region by Kromkamp et al. (in prep.)~~. This ~~a simplified assumption because the conversion from electron transport rate to gross primary productivity is complicated and depends on the consumption of electrons~~ are consumed by other cell processes (Flameling and Kromkamp, 1998; ~~Schuback et al., Halsey and Jones, 2015; Schuback et al., 2016~~). Therefore, a reliable GPP estimate in carbon units from FRR fluorometry requires more research and estimates provide relative rather than qualitative values. Despite its limitations the fact that the method can measure *in situ*, with relatively little phytoplankton manipulation before measurement, makes the method promising. Calibration with other methods, such as concurrent C14 of C13 incubations, could help to better understand the processes from electron excitation to carbon fixation. However, it should be recognized that these methods introduce other uncertainties; they measure something in between net and gross primary productivity, depending on the incubation time and growth rate of the phytoplankton (Halsey and Jones, 2015). Thus, which method is measuring the 'true' primary productivity remains controversial and should be interpreted with care.

When including photophysiology (or photophysiology based GPP estimates) in a monitoring program, it is critical to consider diurnal variability. Diurnal trends make extrapolation of rates obtained at a specific timepoint to daily rates difficult. Most photophysiological parameters we measured showed diurnal trends (Fig. 5). The diurnal trend is dictated by the phytoplankton cell cycle, a circadian oscillator and photophysiological response to varying irradiance (Suzuki and Johnson, 2001; Cohen and Golden, 2015; Schuback et al., 2016). Phytoplankton use photophysiological plasticity to minimize photodamage and optimize growth under fluctuating irradiance (Schuback et al., ~~2016~~; Behrenfeld et al., 2002). ~~The conversion factor from The electron flux to requirement for carbon fixation depends on biogeographic region and taxonomy, but~~ is also subject to diurnal variation (Schuback et al., 2016; Lawrenz et al., ~~2012~~2013; Raateoja, 2004). ~~As we passed several "biogeochemical" provinces, indicated by the cluster analysis, it is difficult to separate diurnal variability from variability introduced by phytoplankton in different biogeochemical areas. However, as we observed this diurnal variability also in the same clusters on a number of occasions, it is clear that diurnal variability is inherent in our analysis. For future studies it is advised to include Langragian based approach where the same phytoplankton community can be followed during a complete light-dark cycle. The diurnal trend in coupling of electron flux and carbon fixation is dictated by cell cycle, a circadian oscillator and irradiance, and photophysiological plasticity minimizes photodamage and optimizes growth under fluctuating light and nutrient concentrations (Claquin et al., 2014; Cohen and Golden, 2015; Schuback et al., 2016).~~ To interpret spatial variability separately from temporal variability and to provide a reliable estimate of gross primary productivity, Schuback et al. (2016) suggest a correction with NPQ_{NISV}, which needs further research in order to get a

Formatted: Font: Times New Roman, English (United States)

Formatted: Font: Times New Roman

more reliable GPP value. The presence of non photochemical quenching (NPQ) makes the interpretation of most photophysiological parameters complicated in our study because the lack of dark acclimation time decreases the comparability between samples. Most photophysiological parameters we measured showed diurnal trends, although, but as said, this is likely not only due to NPQ but also to phytoplankton cell cycle (Claquin et al., 2014; Schuback et al., 2016) and rhythms driven by a circadian oscillator (Cohen and Golden, 2015). But although the presence of NPQ compromises the use of fluorescence as estimate for chlorophyll concentrations, the good relationship between the HPLC-derived Chl *a* concentration and fluorescence of the FRRF and FCM suggest that most of the NPQ is dissipated during the time in the tubing and low light acclimation. The clear diurnal trends we observed are in agreement with previous studies and is usually explained by photophysiological plasticity to minimize photodamage (Schuback et al., 2016). more reliable estimate of gross primary productivity, Schuback et al. (2016) suggest a correction with normalized Stern-Volmer quenching (NPQ_{NSV}). This approach needs further research, for example by using a Lagrangian approach where the photosynthetic activity of the same population is followed during the day. Until a reliable correction method has been established, a monitoring program including photophysiology should account for diurnal variability, for instance by using only measurements collected in a certain timeframe. Despite the limitations of GPP estimates by variable fluorescence, our results clearly show large spatial variability in gross primary production that is not explained by diurnal variability. This spatial heterogeneity is not fully captured by sampling at the standard low-resolution monitoring stations, showing the added value of our approach. ~~2016; Behrenfeld et al., 2002).~~ This makes interpreting spatial patterns difficult as temporal and spatial patterns occur simultaneously, yet, spatial patterns were generally more prominent than the diurnal oscillations.

Primary productivity is an important but difficult to estimate parameter. Its importance is evident, being at the base of the marine food web. In recent decades primary productivity in the North Sea seem to decline, with implications for the ecosystem structure and fisheries productivity. Capuzzo et al. (2017) and Cloern et al. (2014) see a global declining trend in primary production measurements. This is worrying as marine ecosystems face many changes and possible threats caused by global warming and increased use of marine resources by man. Remote sensing methods and models are used to estimate primary productivity, but despite improvements in satellite capabilities and ocean colour analyses, the current global annual NPP estimates are uncertain (Silsbe et al., 2016). One of the reasons is that for satellite estimates or modelling purposes variation in phytoplankton community composition or physiology are usually not included. Primary productivity is then estimated solely based on abiotic factors in combination with Chl *a* estimates (Cole and Cloern, 1987; Behrenfeld and Falkowski, 1997; Westberry et al., 2008; Westberry and Behrenfeld, 2013), although some models include P^{max} as parameters, which is parameterized from temperature only. Yet, Chl *a* and abiotic conditions alone are limited predictors of biological processes, because the Carbon:Chl *a* ratio is not only dependent on abiotic conditions but also to species-specific phenotypic plasticity needed to acclimate to those abiotic conditions (Flynn, 1991, 2005; Geider et al., 1997; Alvarez-Fernandez and Riegman, 2014) and Chl *a* is still difficult to

Formatted: Font: Times New Roman, English (United States)

measure in turbid case-2 waters. Therefore, *in vivo* measurements are required to calibrate remote sensing based models while *in vivo* high resolution methods require remote sensing methods to extrapolate over a wider spatial and temporal scale and we suggest that automated production measurements based on FRRf methodology can fulfil this role.

5 Depth integration of high resolution measurements is a complicated estimate, depending on light penetration through the water column and assuming vertical homogeneity. For most part of the year, the assumption that the mixed layer depth (MLD) reaches below the euphotic zone and causes vertical homogeneity in photoacclimation and community composition, is a safe assumption for the Dutch North Sea, yet short-lived thermal stratification is a regional phenomenon in summer (Van Leeuwen et al., 2015). This short-lived thermal stratification can result in subsurface chlorophyll maximum layers, which, when MLD is shallower than the euphotic zone, will result in a phytoplankton community with distinctly different photophysiological characteristics. Additionally, to calculate water column productivity, an assumption on light penetration through the water column is needed. In this study, light extinction was actively measured approximately ten times per cruise and based on the correlation with turbidity these figures are spatially interpolated using linear regression. Although the light attenuation in the water column is strongly influenced by turbidity, the situation is more complex involving not only underwater processes (absorption and scattering) but also surface processes like reflection and refraction (Brown et al., 1984). Additionally, turbidity is measured in the near-infrared (880 nm), but different substances in the water have characteristically shaped light absorption spectra and photosynthetic active radiation spans a wide range of wavelengths (400-700 nm), this nonlinearity can make the light attenuation coefficient based on turbidity a rough estimate (Kirk, 1994), but as we observed a good correlation between turbidity and K_d ($r^2=0.77$), we assume our K_d estimates are reliable.

The use of automated cluster analyses to interpret spatial heterogeneity is a necessity when dealing with the high amount of data collected by high resolution methods. The unsupervised Hidden Markov Model

(uHMM) Biogeographic regions

25 Our GPP rates were based on the same electron requirement for C-fixation ($\Phi_{e,C}$). However, this is an oversimplification as $\Phi_{e,C}$ is known to vary with abiotic conditions (Lawrenz et al., 2013). Therefore, the changes in nutrient conditions and temperature during the growth season are likely to affect GPP. This will be the topic of a future publication and we expect that the detection of several biogeographic regions will help us in predicting $\Phi_{e,C}$. The in this study applied automated cluster methods allowed for identification of distinct phytoplankton communities or biogeographic regions. The spectral clustering method used in this study was originally designed to detect phytoplankton blooms and understanding the involved dynamics, but here used (Rousseeuw et al., 2015; Lefebvre and Poisson-Caillault, in press). In this study this method was applied to identify different phytoplankton communities and observe spatial patterns. In some months, like April and June, it was indeed possible to identify regions with distinct phytoplankton communities. In other months, such as May, the clustering was not clearly regional scale (Rousseeuw et al., 2015). In general, we see in all months about heterogeneous over the whole Dutch North Sea. A clear distinction between phytoplankton communities of the coastal zone and off-coast regions. A further

separation between the Dutch south coast and the coast off the northern Wadden Islands can usually be made. A separate off-coast area seems to be the southernmost study area, i.e. the northern corner of the Walcheren transect. August is the most heterogeneous month, while both biomass and nutrient concentrations are low, suggesting that niche differentiation is more strongly present than in other months. Broadly, August conditions correspond to the hydrographical regions formerly identified in the Dutch North Sea (Fig. 10; Van Leeuwen et al., 2015; Capuzzo et al., 2015). However, shore regions could be made in all months, except May. Unfortunately, the model was not able to automatically visualize all spatial heterogeneity.

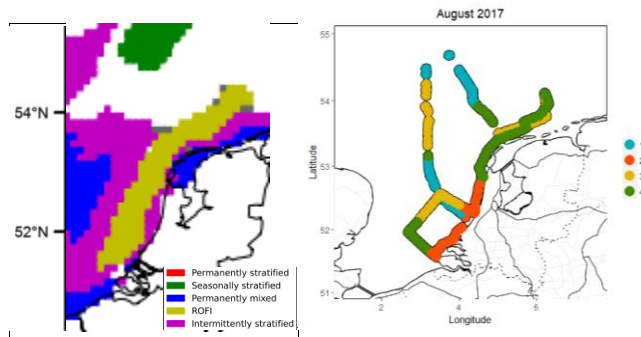


Figure 10: hydrographical regions as defined by Van Leeuwen (2015; left) and spatial clusters by uHMM-clustering in August (right).

In April a distinct phytoplankton community was present. For instance, in April off the coast from Terschelling, only we found a distinct community with high cryptophyte abundance not resulting in a distinct separate cluster when manually increasing the number of spatial clusters from three to five. Additionally, temporal variation (i.e. day-night differences) was interfering with the spatial clustering in August. Although such models are useful for visualization and following changes in spatial heterogeneity, input and output need to be critically evaluated before implementation in monitoring programs. To test whether the differences between months result from seasonal variation or other factors, results over multiple years and additional seasonal cruises need to be made to better characterize heterogeneity of the phytoplankton community structure.

Currently, biological monitoring of phytoplankton in the Dutch North Sea is dictated by the requirements set by OSPAR and the EU Marine Strategy Directive and limited to HPLC analysis of Chl *a* concentration, microscopy counts of *Phaeocystis* cells, and at a few stations, coccolithophores or toxic dinoflagellates. Unfortunately, sampling points were reduced from almost 70 in 1984 to less than 20 today, while strong seasonal patterns, high riverine input, and tidal forces make the Dutch North Sea

a region with high spatiotemporal variability. At the same time, the Dutch North Sea is an area under high anthropogenic pressure, which has led to substantial biogeochemical changes over the past decades (Burson et al., 2016; Capuzzo et al., 2015 and 2017). These abiotic changes affect biology, with potential large implications for ecosystem function and services (Prins et al., 2012; Capuzzo et al., 2017; Burson et al., 2016).

5 Designing 'smart' phytoplankton monitoring

A smart monitoring program combines high and low resolution methods in a supplementary way. No method or parameters will offer clear-cut answers, low-resolution nor high-resolution methods alone. Low resolution methods remain a necessity to support the proposed measurements set-up for three reasons: the practical requirement for calibration and blank correction, to retrieve more detailed taxonomical information and to capture the variability in the water column. Firstly, FRRf measurements are affected by interference of colored dissolved matter which can lead to under or overestimation of some parameters (like F_v/F_m ; Cullen and Davis, 2003). The blank correction is still manual and should be done at least when abiotic conditions change. Secondly, regular measurements of the whole water column remain a necessity to retrieve information on the vertical heterogeneity and the light extinction in the water column. Surface water measurements are only a good reflection of the water column when mixed layer depth is deeper than the euphotic zone. Stratification or mixed layer depth shallower than the euphotic zone can result in subsurface chlorophyll maximum layers and significantly different phytoplankton community (Latasa et al., 2017). Extrapolation of surface measurements to water column estimates is required to assess the carrying capacity of the ecosystem and the contributions to biogeochemical cycles. Only frequent CTD casts equipped with PAR sensor can determine the mixed layer depth and the light extinction in the water column. Thirdly, the level of detail required to identify harmful, keystone or invasive species is only achieved by microscopy analysis. But once identified, flowcytometry is much more suitable for counting the organisms. Another potential combination of high and low resolution methods would be to use high-resolution methods to identify extra sampling points based on real-time projections, opening up early warning methodologies. For example, in the April cruise both Noordwijk 70 and Terschelling 235 km show high gross primary productivity, but in between both high and low productivity rates occur which are not detected with the current sampling program (Fig. 6). The combination of high-resolution *in situ* methods with remote sensing has potential to further increase the spatial and temporal scale. Estimating biological parameters using remote sensing is still difficult, especially in turbid, coastal, case-2 waters (Gohin et al., 2005; van der Woerd et al., 2008). Therefore, *in vivo* measurements are required to calibrate remote sensing based models and we suggest that automated flowcytometry and production measurements based on FRRf methodology can fulfil this role.

Systematic and sufficient monitoring of these changes is of crucial importance to recognize threats, and, once identified as such, develop mitigation actions. The current low-resolution monitoring program is clearly not able to cover the entire biological variability. For instance in April, both Noordwijk 70 and Terschelling 235 km show high gross primary productivity, suggesting that production of the entire area between these points is similar, but both high and low productivity rates occur (Fig. 7). Although extra sampling points in clearly deviating areas would be very useful, because only low resolution offer the level of detail which is required to identify toxic, keystone or invasive species, adding high resolution methods to the current

monitoring program will already allow for obtaining sensible information between sampling points. A smart monitoring system should use high-resolution methods as it delivers information which is difficult to obtain otherwise, can be used to calibrate and validate remote sensing model and can also be used to identify extra sampling points, possibly even based on real-time projections, opening up early warning methodologies.

5 Conclusions

The combination of FRR fluorometry and flowcytometry offers an elaborate view of the phytoplankton community. Accounting for diurnal patterns and identification of FCM clusters for functional types such as nitrogen fixers, calcifiers or DMS-producers are steps needed to increase the value for interpretation ecosystem dynamics and biogeochemical fluxes.

Data interpretation may be supported by automated cluster analyses, such as the uHMM used in the current study, to interpret spatial heterogeneity and to deal with the high amount of data collected by high-resolution methods. However, our model needs to be improved to capture more of the spatial heterogeneity present in ecology of the Dutch North Sea. Overall, the addition of high-resolution monitoring is a very useful supplement to current monitoring to improve.

A good monitoring program monitors the presence of functional types of phytoplankton, including the harmful taxons, the carrying capacity of the ecosystem and changes in biogeochemical cycling. The objective of this study was to evaluate the use of FRR fluorometry and flowcytometry for such monitoring purposes. The four conducted cruises spread over 5 months offered a wide variety of environmental conditions and phytoplankton community states, which the utilized methods were able to visualize. Inclusion of high-resolution methods in monitoring programs allows for analysis of finer scale events. Furthermore, it allows for analysis of living phytoplankton and is thereby able to measure rates and avoid effects of preservation and storage of samples. Another advantage is that high-resolution methods allows for easier comparison between countries, once common protocols have been established. Nevertheless, low resolution methods remain a necessity for more detailed taxonomic analysis, information on vertical heterogeneity, to calibrate and to correct for blanks. Data analysis might be the biggest bottleneck of the implementation of these high-resolution methods. The cluster analysis of flowcytometric data has high potential for improvement to increase the informative value of the method. Especially identification of phytoplankton clusters with a functional quality, such as nitrogen fixers, calcifiers or DMS-producers, would be helpful for interpretation of ecosystem dynamics and biogeochemical fluxes. Regarding the FRRf, the main challenge is converting electron transport rate to gross primary productivity in carbon units. Further research in these topics would benefit implementation of these methods into monitoring protocols. Furthermore, it is important to account for diurnal patterns in monitoring set-up to be able to distinguish between diurnal and spatial variability. Possibly the diurnal variability could be modelled, but more studies with a Langragian based approach are needed for a better understanding of the impact

of diurnal variability in the data. Overall, the in this study presented high-resolution measurement set-up has high potential to improve phytoplankton monitoring by supplementing existing low-resolution monitoring programs.

Acknowledgements

We want to thank the captain and crew of the RV *Zirfaea* and the shipboard Eurofins employees for their hospitality and great help during the cruises. We thank Annette Wielemaker for assistance with the GIS maps of primary production, René Geertsema for assistance with the flowcytometry data analysis and Ralf Schiebel for useful comments on the manuscript. Furthermore, we would like to thank the Rijkswaterstaat laboratory for conducting the nutrients and chlorophyll measurements and Rijkswaterstaat for the opportunity to perform measurements alongside the regular monitoring program. This project has received funding from the European Union's Horizon 2020 research and innovation programme under grant agreement No 654410 (JerichoJerico-Next).

References

Alvarez-Fernandez, S., &and Riegman, R. (2014). Chlorophyll in North Sea coastal and offshore waters does not reflect long term trends of phytoplankton biomass. *Journal of Sea Research*, 91, 35–44. <https://doi.org/10.1016/j.seares.2014.04.005><https://doi.org/10.1016/j.seares.2014.04.005>

Azam, F., Fenchel, T., Field, J., Gray, J., Meyer-Reil, L., & Thingstad, F. (1983). The Ecological Role of Water-Column Microbes in the Sea. *Marine Ecology Progress Series*, 10(3), 257-263. Retrieved from <http://www.jstor.org/stable/24814647>

Baretta-Bekker, J.-G., Baretta, J.-W., Latuhihin, M.-J., Desmit, X., &and Prins, T.-C. (2009). Description of the long-term (1991-2005) temporal and spatial distribution of phytoplankton carbon biomass in the Dutch North Sea. *Journal of Sea Research*, 61(1–2), 50–59. <https://doi.org/10.1016/j.seares.2008.10.007><https://doi.org/10.1016/j.seares.2008.10.007>

Beardall, J., T. Berman, P. Heraud, M. O. Kadiri, B. R. Light, G. Patterson, S. Roberts, B. Sulzberger, E. Sahan, U. Uehlinger, and B. Wood. (2001-). A comparison of methods for detection of phosphate limitation in microalgae. *Aquatic Sciences* 63:107-121.

Behrenfeld, M.J., Maranon, E., Siegel, D.A., Hooker, S.B. (2002). Photoacclimation and nutrient-based model of light-saturated photosynthesis for quantifying oceanic primary production. *Mar. Ecol. Prog. Ser.*, 228:103-117

Formatted: Spanish (Spain)

Formatted: Font color: Text 1

Formatted: Font color: Text 1

Formatted: Font color: Text 1

Behrenfeld, M. J., O'Malley, R. T., Siegel, D. A., McClain, C. R., Sarmiento, J. L., Feldman, G. C., Milligan, A.J., Falkowski, P.G., Letelier, R.M., Boss, E. S. (2006). Climate-driven trends in contemporary ocean productivity. *Nature*, 444(7120), 752–755. <https://doi.org/10.1038/nature05317>

5 Brandsma, J., Hopmans, E. C., Philippart, C. J. M., Veldhuis, M. J. W., Schouten, S., & Sinninghe Damsté, J. S. (2012). Low temporal variation in the intact polar lipid composition of North Sea coastal marine water reveals limited chemotaxonomic value. *Biogeosciences*, 9(3), 1073–1084. <https://doi.org/10.5194/bg-9-1073-2012>

10 Burson, A., Stomp, M., Akil, L., Brussaard, C. P. D., & Huisman, J. (2016). Unbalanced reduction of nutrient loads has created an offshore gradient from phosphorus to nitrogen limitation in the North Sea, 869–888. <https://doi.org/10.1002/lno.10257>

15 Capuzzo, E., Stephens, D., Silva, T., Barry, J., Forster, R. M. (2015). Decrease in water clarity of the southern and central North Sea during the 20th century. *Global Change Biology*, 21(6), 2206–2214. <https://doi.org/10.1111/gcb.12854>

20 Capuzzo, E., Lynam, C. P., Barry, J., Stephens, D., Forster, R. M., Greenwood, N., ~~McQuatters-Gollop, A., Silva, T., van Leeuwen, S.M.~~, Engelhard, G. H. (2017). A decline in primary production in the North Sea over 25 years, associated with reductions in zooplankton abundance and fish stock recruitment. *Global Change Biology*, (May), 1–13. <https://doi.org/10.1111/gcb.13916>

25 Cloern, J.-E., Foster, S.-Q., & Kleckner, A.-E. (2014). Phytoplankton primary production in the world's estuarine-coastal ecosystems. *Biogeosciences*, 11(9), 2477–2501. <https://doi.org/10.5194/bg-11-2477-2014>

[Dubinsky, Z., P. G. Cohen, S.E. and Golden, S.S. \(2015\). Circadian Rhythms in Cyanobacteria. *Microbiol Mol Biol Rev.* 79\(4\):373-85. 10.1128/MMBR.00036-15.](https://doi.org/10.1128/MMBR.00036-15)

30 [Cullen, J.J., and Davis, R.F. \(2001\). The blank can make a big difference in oceanographic measurements. *Limnol. Oceanogr. Bulletin*, 12\(2\), 29–35.](https://doi.org/10.1002/limn.1001)

~~Falkowski, and K. Wyman. 1986. Light harvesting and utilization by P. and Kiefer, D.A. (1985). Chlorophyll a fluorescence in phytoplankton. *Plant Cell Physiology*, 27:1335-1349; relationship to photosynthesis and biomass. *Journal of Plankton Research*, 7(5), 715–731.~~

Formatted: Default Paragraph Font, Underline, Font color: Black

Field Code Changed

Formatted: Underline, Font color: Black

Formatted: Font color: Text 1

Field Code Changed

Formatted: Default Paragraph Font

Falkowski, P.-G. (1998). Biogeochemical Controls and Feedbacks on Ocean Primary Production. *Science*, 281(5374), 200–206. <https://doi.org/10.1126/science.281.5374.200>

Field Code Changed

Formatted: Default Paragraph Font

5 [Finkel, Z. V., Beardall, J., Flynn, K. J., Quigg, A., Rees, T. A. V., & Raven, J. A. \(2010\). Phytoplankton in a changing world: cell size and elemental stoichiometry. *Journal of Plankton Research*, 32\(1\), 119–137. <https://doi.org/10.1093/plankt/fbp098>](#)

Flameling, I.-A. and J. Kromkamp (1998). Light dependence of quantum yields for PSII charge separation and oxygen evolution in eukaryotic algae. *Limnology and Oceanography*. 43:284-297

10

Flynn, K.-J. 1991. Algal carbon-nitrogen metabolism: a biochemical basis for modelling the interactions between nitrate and ammonium uptake. *Journal of Plankton Research*. 13:373-387.

Flynn, K.-J. 2005. Modelling marine phytoplankton growth under eutrophic conditions. *Journal of Sea Research* 54:92-103.

15

[Geider, R. J., Platt, T., & Raven, J., 1986. Size dependence of growth and photosynthesis in diatoms: a synthesis. *Marine Ecology Progress Series*, 30, 93–104. <https://doi.org/10.3354/meps030093>](#)

[Franck, F., Juneau, P., and Popovic, R. \(2002\). Resolution of the Photosystem I and Photosystem II contributions to chlorophyll fluorescence of intact leaves at room temperature. *Biochimica et Biophysica Acta - Bioenergetics*, 1556\(2–3\), 239–246. \[https://doi.org/10.1016/S0005-2728\\(02\\)00366-3\]\(https://doi.org/10.1016/S0005-2728\(02\)00366-3\)](#)

20

Geider, R.J., ~~H.L.~~ MacIntyre, ~~H.L.~~ and ~~Kana, T. M. Kana-~~(1997-). Dynamic model of phytoplankton growth and acclimation: responses of the balanced growth rate and the chlorophyll a:carbon ratio to light, nutrient-limitation and temperature. *Marine Ecology Progress Series* 148:187-200.

25

[Giannini, M.F.C., Ciotti, Á M. \(2016\). Parameterization of natural phytoplankton photo-physiology: Effects of cell size and nutrient concentration. *Limnology and Oceanography*, 61\(4\), 1495–1512. <https://doi.org/10.1002/lno.10317>](#)

[Gohin, F., Loyer, S., Lunven, M., Labry, Froidefond, C.J.M., Delmas, D., Huret M. and Herbland, A. 2005. Satellite-derived parameters for biological modelling in coastal waters: Illustration over the eastern continental shelf of the Bay of Biscay. *Remote Sensing of Environment* 95: 29-46.](#)

30

Goss, R., Ann Pinto, E., Wilhelm, C., Richter, M. (2006). The importance of a highly active and Δ pH-regulated diatoxanthin epoxidase for the regulation of the PS II antenna function in diadinoxanthin cycle containing algae. *Journal of Plant Physiology*, 163(10), 1008–1021. <https://doi.org/10.1016/j.jplph.2005.09.008>

5 Halsey, K. H., & Jones, B. M. (2015). Phytoplankton Strategies for Photosynthetic Energy Allocation. *Annu. Rev. Mar. Sci.* 2015. 7:265–97. <https://doi.org/10.1146/annurev-marine-010814-015813>

Kassambara, A. and Mundt, F., 2017. factoextra: Extract and Visualize the Results of Multivariate Data Analyses. R package version 1.0.5. <https://CRAN.R-project.org/package=factoextra>

10 [Kirk, J.T.O., 1983. Light and Photosynthesis in Aquatic Ecosystems. Cambridge University Press](#)

Kolber, Z., J. Zehr, and P. G. Falkowski. (1988). Effects of growth irradiance and nitrogen limitation on photosynthetic energy conversion in photosystem II. *Plant Physiology*. 88:923-929.

15 Kolber, Z. and P. G. Falkowski. (1993). Use of active fluorescence to estimate phytoplankton photosynthesis in situ. *Limnology and Oceanography*. 38:1646-1665.

20 ~~Kolber, Z., J. Zehr, and P. G. Falkowski. 1988. Effects of growth irradiance and nitrogen limitation on photosynthetic energy conversion in photosystem II. *Plant Physiology*. 88:923-929.~~

25 [Kolber, Z.S., Prášil, O., Falkowski, P.G. \(1998\). Measurements of variable chlorophyll fluorescence using fast repetition rate techniques: Defining methodology and experimental protocols. *Biochimica et Biophysica Acta - Bioenergetics*, 1367\(1–3\), 88–106. \[https://doi.org/10.1016/S0005-2728\\(98\\)00135-2\]\(https://doi.org/10.1016/S0005-2728\(98\)00135-2\)](#)

30 ~~Kromkamp, J.-C., & Forster, R.-M. (2003). The use of variable fluorescence measurements in aquatic ecosystems: differences between multiple and single turnover measuring protocols and suggested terminology. *European Journal of Phycology*, 38(2), 103–112. <https://doi.org/10.1080/0967026031000094094><https://doi.org/10.1080/0967026031000094094>.~~

Kromkamp, J. C., Dijkman, N. A., Peene, J., Simis, S. G. H., Gons, H. J., Kromkamp, J. C., ... Simis, S. G. H. (2008). Estimating phytoplankton primary production in Lake IJsselmeer (-The Netherlands-) using variable fluorescence (-PAM-FRRF) and C-uptake techniques Estimating phytoplankton primary production in Lake IJsselmeer (-The Netherlands-) using variable fluoresce. 262. [Doi:https://doi.org/10.1080/09670260802080895](https://doi.org/10.1080/09670260802080895)<https://doi.org/10.1080/09670260802080895>

Formatted: Font color: Text 1, English (United Kingdom)

Formatted: Font color: Text 1, English (United States)

Formatted: Font color: Text 1, English (United States)

Formatted: Font color: Text 1, English (United States)

Formatted: Font color: Text 1, English (United States)

Formatted: Font color: Text 1

Formatted: Font color: Text 1

Kromkamp, J.-C., & Van Engeland, T. (2010). Changes in phytoplankton biomass in the western ~~seh~~~~eldt~~~~Scheldt~~ estuary during the period 1978-2006. *Estuaries and Coasts*, 33(2), 270–285. <https://doi.org/10.1007/s12237-009-9215-3>

Formatted: Font color: Text 1

5 Kruskopf, M. and ~~K. J.~~ Flynn, ~~2006.~~ K.J. (2005). Chlorophyll content and fluorescence responses cannot be used to gauge reliably phytoplankton biomass, nutrient status or growth rate. *New Phytologist* 169:525-536.

[Latasa, M., Cabello, A.M., Morán, X.A.G., Massana, R. and Scharek, R. \(2017\). Distribution of phytoplankton groups within the deep chlorophyll maximum. *Limnol. Oceanogr.*, 62: 665-685.](#)

10 [Lawrenz, E., Silsbe, G., Capuzzo, E., Ylöstalo, P., Forster, R.M., Simis, S.G.H., Prášil, O., Kromkamp, J.C., Hickman, A.E., Moore, C.M., Forget, M.H., Geider, R.J., Suggett, D.J. \(2013\). Predicting the Electron Requirement for Carbon Fixation in Seas and Oceans. *PLoS ONE*, 8\(3\). <https://doi.org/10.1371/journal.pone.0058137>](#)

15 [Lefebvre A., Poisson-Caillault E., In press. High resolution overview of phytoplankton spectral groups and hydrological conditions in the eastern English Channel using unsupervised clustering. *Marine Ecology Progress Series*. <https://doi.org/10.3354/meps12781>.](#)

20 [Ly, J., C. J. M. Philippart, and J. C. Kromkamp. 2014. Phosphorus limitation during a phytoplankton spring bloom in the western Dutch Wadden Sea. *Journal of Sea Research* 88:109-120.](#)

Formatted: Font color: Text 1

25 [Marinov, I., Doney, S.-C., & Lima, I.-D. \(2010\). Response of ocean phytoplankton community structure to climate change over the 21st century: partitioning the effects of nutrients, temperature and light. *Biogeosciences*, 7\(12\), 3941–3959. <https://doi.org/10.5194/bg-7-3941-2010>](#)

Formatted: Default Paragraph Font, Underline

Field Code Changed

[Marrec, P., Doglioli, A.M., Grégori, G., Dugenne, M., Della Penna, A., Bhairy, N., Cariou, T., Hélias Nunige, S., Lahbib, S., Rougier, G., Wagener, T., Thyssen, M. \(2017\). Coupling physics and biogeochemistry thanks to high resolution observations of the phytoplankton community structure in the North-Western Mediterranean Sea. *Biogeosciences Discussions*, \(August\), 1–54. <https://doi.org/10.5194/bg-2017-343>](#)

30 Melrose, D.-C., Oviatt, C.-A., O'Reilly, J.-E., & Berman, M.-S. (2006). Comparisons of fast repetition rate fluorescence estimated primary production and 14C uptake by phytoplankton. *Marine Ecology Progress Series*, 311, 37–46. <https://doi.org/10.3354/meps311037>

Morris, E. P. and J. C. Kromkamp. 2003. Influence of temperature on the relationship between oxygen and fluorescence-based estimates of photosynthetic parameters in a marine benthic diatom (Cylindrotheca closterium). European Journal of Phycology 38:133-142.

5 Oxborough, K., Montes-Hugo, M., Doney, S. C., Ducklow, H. W., Fraser, W., Martinson, D., Stammerjohn, S. E., and Schofield, O. (2009). Recent Changes in Phytoplankton Communities Associated with Rapid Regional Climate Change Along the Western Antarctic Peninsula. Science, 323(5920), 1470–1473. <https://doi.org/10.1126/science.1164533>

10 Moore, C. M., Suggett, D. J., Hickman, a. E., Kim, Y.-N., Tweddle, J. F., Sharples, J., Geider, R.J., Holligan, P.M. (2006). Phytoplankton photoacclimation and photoadaptation in response to environmental gradients in a shelf sea. Limnol. Oceanogr. 44(0), 1–46. <https://doi.org/10.4319/lm.2006.51.2.0936>

15 Oxborough, K., Moore, C.M., Suggett, D.J., Lawson, T., Chan, H.-G., & Geider, R.-J. (2012). Direct estimation of functional PSII reaction center concentration and PSII electron flux on a volume basis : a new approach to the analysis of Fast Repetition Rate fluorometry (FRRf) data, OCEANOGRAPHY: METHODS, 142–154. <https://doi.org/10.4319/lom.2012.10.142><https://doi.org/10.4319/lom.2012.10.142>

20 Peeters, J. and Peperzak, L. (1990). Nutrient limitation in the North Sea: a bioassay approach. Netherlands Journal of Sea Research, 26(1), 61–73. [https://doi.org/10.1016/0077-7579\(90\)90056-M](https://doi.org/10.1016/0077-7579(90)90056-M)

25 Philippart, C. J. M., Cade, G. C., Raaphorst, W. Van, & Riegman, R. (2000). Long-term phytoplankton – nutrient interactions in a shallow coastal sea: Algal community structure, nutrient budgets, and denitrification potential. Limnol. Oceanogr., 45(1), 131–144.

Philippart, C. J. M., Beukema, J. J., Cadée, G. C., Dekker, R., Goedhart, P. W., Van Iperen, J. M., Leopold, M.F. Herman, P. M. J. (2007). Impacts of nutrient reduction on coastal communities. Ecosystems, 10(1), 95–118. <https://doi.org/10.1007/s10021-006-9006-7>

30 Philippart, C. J. M., Anadón, R., Danovaro, R., Dippner, J. W., Drinkwater, K. F., Hawkins, S. J., Oguz, T., O’Sullivan, G., Reid, P. C. (2011). Impacts of climate change on European marine ecosystems: Observations, expectations and indicators. Journal of Experimental Marine Biology and Ecology, 400(1–2), 52–69. <https://doi.org/10.1016/j.jembe.2011.02.023>

Formatted: Default Paragraph Font, Underline, Font color: Text 1, English (United Kingdom)

Poisson-caillault, E. and Ternynck, P (2016). uHMM: Construct an Unsupervised Hidden Markov Model. R Package version 1.0, <https://cran.r-project.org/package=uHMM><https://cran.r-project.org/package=uHMM>

Formatted: Default Paragraph Font, Underline, Font color: Text 1, German (Germany)

Prins, T., Quéré, C., Desmit, X., & Baretta-Bekker, J. G. (2012). Phytoplankton composition in Dutch coastal waters responds to changes in riverine nutrient loads. *Journal of Sea Research*, 73, 49–62. <https://doi.org/10.1016/j.seares.2012.06.009>

Quere, C. Le, Harrison, S. P., Colin Prentice, I., Buitenhuis, E. T., Aumont, O., Bopp, L., ---, ~~Claustre, H., Cotrim Da Cunha, L., Geider, R.J., Giraud, X., Klaas, C., Kohfeld, K.E., Legendre, L., Manizza, M., Platt, T., Rivkin, R.B., Sathyendranath, S., Uitz, J., Watson, A.J.~~ Wolf-Gladrow, D. (2005). Ecosystem dynamics based on plankton functional types for global ocean biogeochemistry models. *Global Change Biology*, 11(11), 2016–2040. <https://doi.org/10.1111/j.1365-2486.2005.01004.x><https://doi.org/10.1111/j.1365-2486.2005.01004.x>

Formatted: Default Paragraph Font, Underline, Font color: Text 1

Raateoja, M. P. (2004). Fast repetition rate fluorometry (FRRF) measuring phytoplankton productivity: A case study at the entrance to the Gulf of Finland, Baltic Sea. *Boreal Env. Res.* 9: 263–276.

Rantjärv, E., Olsonen, R., Hällfors, S., Leppänen, J. M., & Raateoja, M. (1998). Effect of sampling frequency on detection of natural variability in phytoplankton: Unattended high-frequency measurements on board ferries in the Baltic Sea. *ICES Journal of Marine Science*, 55(4), 697–704. <https://doi.org/10.1006/jmsc.1998.0384><https://doi.org/10.1006/jmsc.1998.0384>

Formatted: Default Paragraph Font, Font color: Text 1

Rijkeboer, M. (2018). Automated characterization of phytoplankton community into size and pigment groups based on flow cytometry. MEM 2018-20. RWS Information pp.18

Rousseuw, K., Poisson Caillault, E., Lefebvre, A., & Hamad, D. (2015). Achimer Hybrid hidden Markov model for marine environment monitoring. *IEEE Journal Of Selected Topics In Applied Earth Observations And Remote Sensing*, 8(1), 204–213. <https://doi.org/http://dx.doi.org/10.1109/JSTARS.2014.2341219><https://doi.org/http://dx.doi.org/10.1109/JSTARS.2014.2341219>

Rutten, T. (2015). Evaluatie testen van diverse CytoSense configuraties. TRP2015.001, 32 pp (in Dutch)

Sarmiento, J.-L., Slater, R., Barber, R., Bopp, L., Doney, S.-C., Hirst, A.-A., ---, ~~Kleypas, J., Matear, R., Mikolajewicz, U., Monfray, P., Soldatov, V., Spall, S. a.~~ Stouffer, R. (2004). Response of ocean ecosystems to climate warming. *Global Biogeochem. Cycles*, 18(3), GB3003. <https://doi.org/10.1029/2003GB002134><https://doi.org/10.1029/2003GB002134>

Formatted: Font color: Text 1

Formatted: Font color: Text 1

Formatted: Font color: Text 1

Formatted: Font color: Text 1

Formatted: Font color: Text 1, English (United States)

Formatted: Underline, Font color: Text 1

Schiebel, R., Spielhagen, R. F., Garnier, J., Hagemann, J., Howa, H., Jentzen, A., Martínez-García, A., Meiland, J., Michel, E., Repschläger, J., Salter, I., Yamasaki, M., Haug, G. (2017). Modern planktic foraminifers in the high-latitude ocean. *Marine Micropaleontology*, 136, 1–13. <https://doi.org/10.1016/j.marmicro.2017.08.004>

5 [Seadatanet \(2018\). SeaDataCloud Flow Cytometry Standardised Cluster Names. Natural Environment Research Council. Version 3. http://vocab.nerc.ac.uk/collection/F02/current/F0200007/](http://vocab.nerc.ac.uk/collection/F02/current/F0200007/)

Sieburth J.M., Smetacek, V., Lenz, J. (1978). Pelagic ecosystem structure: heterotrophic compartments of the plankton and their relationship to plankton size fractions. *Limnol Oceanogr* 23:1256–1263

10

Schuback, N., Flecken, M., Maldonado, M. T., Tortell, P. D. (2016). Diurnal variation in the coupling of photosynthetic electron transport and carbon fixation in iron-limited phytoplankton in the NE subarctic Pacific. *Biogeosciences*, 13(4), 1019–1035. <https://doi.org/10.5194/bg-13-1019-2016>

15

Sündermann, J., & Pohlmann, T. (2011). A brief analysis of North Sea physics. *Oceanologia*, 53(3), 663–689. <https://doi.org/10.5697/oc.53-3.663>

Formatted: Font color: Text 1

Silsbe, G.-M., & Kromkamp, J.-C. (2012). Modeling the irradiance dependency of the quantum efficiency of photosynthesis. *Limnology and Oceanography: Methods*, 10(9), 645–652.

20

<https://doi.org/10.4319/lom.2012.10.645>

Formatted: Font color: Text 1

Silsbe, G.-M., Oxborough, K., Suggett, D.-J., Forster, R.-M., Ihnken, S., Komárek, O., Lawrenz E., Prášil, O., Röttgers, R., Šicner, M., Simis, S.G.H., Van Dijk, M., Kromkamp, J.-C. (2015). Toward autonomous measurements of photosynthetic electron transport rates: An evaluation of active fluorescence-based measurements of photochemistry. *Limnology and Oceanography: Methods*, 13(3), 138–155. <https://doi.org/10.1002/lom3.10014>

25

Formatted: Font color: Text 1

Silsbe, G.M., Behrenfeld, M.J., Halsey, K.H., Milligan, A.J., Westberry, T.K. (2016). The CAFE model: A net production model for global ocean phytoplankton. *Global Biogeochemical Cycles*, 30(12), 1756–1777. <https://doi.org/10.1002/2016GB005521>

30

Smyth, T.-J., Pemberton, K.-L., Aiken, J., & Geider, R.-J. (2004). A methodology to determine primary production and phytoplankton photosynthetic parameters from Fast Repetition Rate Fluorometry. *Journal of Plankton Research*, 26(11), 1337–1350. <https://doi.org/10.1093/plankt/fbh124>

Field Code Changed

Formatted: Default Paragraph Font, Font color: Text

Formatted: Font color: Text 1

Suggett, D.-J., Oxborough, K., Baker, N.-R., MacIntyre, H.-L., Kana, T. M., & Geider, R.-J. (2003). Fluorescence Measurements for Assessment of Photosynthetic Electron Transport in Marine Phytoplankton. *European Journal of Phycology*, 38(4), 371–384. <https://doi.org/10.1080/09670260310001612655>

5 Suggett, D.-J., MacIntyre, H.-L., Kana, T. M., & Geider, R.-J. (20092009a). Comparing electron transport with gas exchange: Parameterising exchange rates between alternative photosynthetic currencies for eukaryotic phytoplankton. *Aquatic Microbial Ecology*, 56(2–3), 147–162. <https://doi.org/10.3354/ame01303>

10 Suggett, D.-J., C.-M. Moore, A. E. Hickman, and R.-J. Geider. (20092009b). Interpretation of fast repetition rate (FRR) fluorescence: signatures of phytoplankton community structure versus physiological state. *Marine Ecology-Progress Series* 376:1-19.

[Suzuki, L., and Johnson, C. H. \(2001\). Minireview Algae Know the Time of Day: Circadian and Photoperiodic Programs 1, 942\(May\), 933–942.](#)

15 Stolte, W., and Riegman, R. (1995). Effect of phytoplankton cell size on transient- state nitrate and ammonium uptake kinetics. *Microbiology*, 141(1995), 1221–1229.

20 Sündermann, J., and Pohlmann, T. (2011). A brief analysis of North Sea physics. *Oceanologia*, 53(3), 663–689. <https://doi.org/10.5697/oc.53-3.663>

[Tarran, G.A., Heywood, J.L., and Zubkov, M.V. \(2006\). Latitudinal changes in the standing stocks of nano- and picoeukaryotic phytoplankton in the Atlantic Ocean. Deep-Sea Research Part II: Topical Studies in Oceanography, 53\(14–16\), 1516–1529. https://doi.org/10.1016/j.dsr2.2006.05.004](#)

25 Thyssen, M., Alvain, S., Dessailly, D., Rijkeboer, M., Guiselin, N., & Creach, V. (2015). High-resolution analysis of a North Sea phytoplankton community structure based on in situ flow cytometry observations and potential implication for remote sensing. *Biogeosciences*, 12, 4051–4066. <https://doi.org/10.5194/bg-12-4051-2015>

30 [Van Leeuwen, S., Tett, P., Mills, D., and Van-Der Molen, J.-Tillmann, U., and Rick, H.J. \(2003\). North Sea phytoplankton: A review. Senckenbergiana Maritima, 33\(1–2\), 1–69. https://doi.org/10.1007/BF03043047](#)

[Van der Woerd, H. J. and R. Pasterkamp. 2008. HYDROPT: A fast and flexible method to retrieve chlorophyll-a from multispectral satellite observations of optically complex coastal waters, Remote Sensing of Environment, 112: 1795-1807.](#)

Field Code Changed

Formatted: Default Paragraph Font, Underline, Font color: Text 1

Formatted: Underline, Font color: Text 1

Vaulot, D., Eikrem W., Viprey, M., Moreau, H. (2008). The diversity of small eukaryotic phytoplankton (< or =3 micron) in marine ecosystems. *FEMS Microbiol Rev* 32:795–820

~~(2015). Stratified and nonstratified areas in the North Sea: Long term variability and biological and policy implications. J. Geophys. Res. Oceans, 120, 4670–4686. <https://doi.org/10.1002/2014JC010485>.~~

Webb, W.-L., M.-Newton, and D.M., Starr-, D. (1974-). Carbon dioxide exchange of *Alnus rubra*: a mathematical model. *Oecologia*. 17:281-291.

Wickham, H., 2009. ggplot2: Elegant Graphics for Data Analysis. Springer-Verlag New York

Zuur, A.F., Ieno, E.N., Walker, N., Saveliev, A.A., and Smith, G.M., ~~Springer-, (2009-).~~ Mixed effects models and extensions in ecology with R. [Springer](#)

Formatted: Font color: Text 1, English (United Kingdom)

Table 1: The derived photosynthetic parameters used in this study (see Oxborough et al. (2012) and Silsbe et al. (2015) for more information).

	Description	unit
C	Fraction of RCIIIs in the open state	Dimensionless
$F_0^{(s)}$	Fluorescence at zero th -flashlet of an ST measurement when $C \rightarrow 0$ (under ambient light)	Dimensionless
$F_m^{(s)}$	Fluorescence when $C = 1$ (under ambient light)	Dimensionless
$F_v^{(s)}$ or F_v	$\Delta F^{(s)}$, variable fluorescence	Dimensionless
$F_v^{(s)}/F_m^{(s)}$	Fluorescence parameter providing an estimate of PSII efficiency under ambient light (under ambient light)	Dimensionless
F_v/F_m	Quantum efficiency of PSII	Dimensionless
σ_{PSII}	Absorption cross section of PSII photochemistry	$\text{nm}^2 \text{PSII}^{-1}$
$[RCII]$	Concentration of functional RCII	nmol RCII m^{-3}
a_{LIII}	Absorption coefficient of PSII light harvesting	m^{-1}
α	Light utilisation efficiency	$\mu\text{mol electrons } (\mu\text{mol photons})^{-1}$
E_k	Minimum saturating irradiance of fluorescence light curve	$\mu\text{mol photons m}^{-2} \text{s}^{-1}$
P_{max}	Maximum photosynthetic electron-transport rate	$\mu\text{mol electrons m}^{-2} \text{s}^{-1}$
JV_{PH}	PSII flux per unit volume	$\text{mol electrons (PSII m}^{-2}) \text{d}^{-1}$
GPP	Gross Primary Productivity	$\text{mg C m}^{-2} \text{h}^{-1}$
n_{PSII}	Number of [RCII] per mole Chl a	$\text{mol RCII mol}^{-1} \text{chl} a$
$1/\tau$	Rate of re-opening of a closed RCII with an empty Q_B site	ms^{-1}
K_a	Instrument type specific constant allowing for direct calculation of [RCII] and JV_{PH} from FRR data	m^{-1}

Formatted: Font color: Black

Formatted Table

5

10

15

Table 2: The phytoplankton groups distinguished in the current study.

	Length FWS	Main corresponding taxonomic group
Pico-Red	<4 μm^*	Pico-eukaryotes
Pico-Synecho	<4 μm^*	e.g. <i>Synechococcus</i>
Nano-Crypto	4-20 μm	Cryptophyceae
Nano-Red	4-20 μm	Diatoms, Haptophytes
Micro-Red	>20 μm	Diatoms, Haptophytes

*In June <6 μm

Formatted: Font: 9 pt, Bold, Font color: Black

Formatted: Normal, Space After: 10 pt, Border: Top: (No border), Bottom: (No border), Left: (No border), Right: (No border), Between : (No border)

5

10

15

20

25

Table 3: Monthly averages \pm SD of abiotic conditions and biological parameters. Due to differences in sampling route and stations, the monthly averages are not completely comparable. Large standard deviations are due to spatial heterogeneity, for a more detailed description of the spatial heterogeneity, see figure 4 and the supplementary material. P_{max} and alpha are based on relative electron transport rates.

	April	May	June	August
Abiotics				
Salinity (‰)	34.1 \pm 1.8	33.5 \pm 2.3	33.6 \pm 1.8	34.0 \pm 1.3
SST (°C)	9.5 \pm 1.0	12.1 \pm 1.1	15.5 \pm 1.8	19.0 \pm 0.6
Turbidity (NTU)	2.3 \pm 3.0	1.1 \pm 0.8	1.3 \pm 1.3	1.2 \pm 0.7
PO ₄ (μM)	0.3 \pm 0.1	0.2 \pm 0.1	0.3 \pm 0.1	0.1 \pm 0.1
Si (μM)	2.1 \pm 2.2	1.6 \pm 1.1	1 \pm 0.6	1.3 \pm 1.1
NH ₄ (μM)	0.7 \pm 0.7	1.3 \pm 0.9	1.5 \pm 1.2	0.4 \pm 0.4
NO ₃ (μM)	9.3 \pm 11.4	3.5 \pm 5.6	0 \pm 0	0.2
DIN:DIP	43.8 \pm 53.2	25.5 \pm 36.7	9.0 \pm 6.9	2.4 \pm 1.9
DSi:DIP	7.9 \pm 9.3	9.2 \pm 8.5	4.0 \pm 2.5	5.3 \pm 3.7
K _a (m ⁻¹)	0.39 \pm 0.28	0.33 \pm 0.12	0.30 \pm 0.20	0.25 \pm 0.14
Biotics				
Chlorophyll <i>a</i> (μg L ⁻¹)	18.32 \pm 19.71	5.67 \pm 10.39	4.08 \pm 4.11	3.98 \pm 3.91
F _v /F _m	0.52 \pm 0.04	0.26 \pm 0.09	0.40 \pm 0.09	0.48 \pm 0.07
σ_{PSII} (nm ² PSII ⁻¹)	3.66 \pm 0.27	5.92 \pm 1.35	4.59 \pm 0.88	5.26 \pm 1.07
[RCH] (*10 ⁻⁹ nmol RCH m ⁻²)	31.3 \pm 17.1	6.94 \pm 10.5	4.13 \pm 2.78	2.21 \pm 1.84
α_{PSII} (*10 ⁻⁴ RCH (Chl <i>a</i>) ⁻¹)	8.02 \pm 0.55	8.94 \pm 6.05	6.65 \pm 1.68	5.95 \pm 1.15
1/ τ (ms ⁻¹)	0.24 \pm 0.06	0.52 \pm 0.10	0.49 \pm 0.07	0.62 \pm 0.12
α	0.53 \pm 0.03	0.25 \pm 0.09	0.39 \pm 0.08	0.48 \pm 0.08
E _k	300 \pm 52.5	223 \pm 147	253 \pm 124	277 \pm 137
P _{max}	158 \pm 30	56.5 \pm 42.4	97.5 \pm 47.7	130 \pm 60.4
GPP water column (mg C m ⁻² h ⁻¹)	781 \pm 409	207 \pm 277	136 \pm 101	68.4 \pm 39.1
GPP surface (μg C L ⁻¹ h ⁻¹)	115.7 \pm 58	27.5 \pm 72	16.5 \pm 13	8.7 \pm 8.3
O:R ratio	0.31 \pm 0.51	0.06 \pm 0.07	0.19 \pm 0.20	0.28 \pm 0.16
Relative abundance microplankton (%)	1 \pm 1	4 \pm 4	2 \pm 2	1 \pm 1
Relative abundance Nanoplankton (%)	32 \pm 17	44 \pm 16	23 \pm 8	18 \pm 6
Relative abundance Picoplankton (%)	68 \pm 17	52 \pm 52	75 \pm 9	82 \pm 6

Table 4: Coefficients of the stepwise multiple linear regression (n=61) for ln(GPP) with p<0.05 and VIF<6

	coefficients
Intercept	5.613
alpha	2.916
Turbidity	-9.929*10 ⁻²
DIN	-3.567*10 ⁻²
Temperature	-1.887*10 ⁻²
Total red fluorescence (biomass)	2.833*10 ⁻⁹

Hours	$4.141 \cdot 10^{-2}$
-------	-----------------------

Formatted: Font color: Red